Climate change and the variability in the risk of single and compound climate extremes

by

Ameneh Tavakol

B.S., University of Tehran, 2005
M.S., University of Tehran, 2010

AN ABSTRACT OF A DISSERTATION

submitted in partial fulfillment of the requirements for the degree

DOCTOR OF PHILOSOPHY

Department of Biological and Agricultural Engineering
Carl R. Ice College of Engineering

KANSAS STATE UNIVERSITY
Manhattan, Kansas

2020

Abstract

Extreme weather and climate events have significantly influenced society and the environment. As the world has warmed, the warmer temperatures have triggered the frequency, severity, and duration of other extremes. In this study, the spatial and temporal patterns of heatwave frequency and duration were analyzed in the Mississippi River Basin (MRB) using the validated reanalysis (NCEP-NCAR) data for 1948–2018. The heatwave was defined as at least two consecutive days when maximum temperature was higher than the 90^{th} percentile. Over the 70-year period of study, the highest frequency of heatwaves was recorded in the west and north-west of the MRB with no significant increase over time. The results of the study confirmed the "warming hole" in the eastern-central United States with a significant decrease in the frequency of heatwaves. The longest heatwaves were found in southern and central MRB. Applying change-point analysis, an abrupt increase was found in the MRB in the percentage of area with heatwaves longer than 10 consecutive days since 1966. Impacts of heatwaves increase when multiple hazards occur simultaneously (e.g. heatwaves and high humidity) and lead to a compound extreme outcome. Heat-index was used to analyze the variability of compound high temperature and high humidity over time and space. Extreme daytime and nighttime hot-humid conditions were defined using the National Weather Services fixed thresholds. Spatially, southern MRB showed a higher frequency of extreme hot-humid events during both days and nights. There were no extreme nighttime hot-humid events in the east, west, and north-west MRB. Trend analysis discovered 16% and 8% significant upward trends in the daytime and nighttime extreme hot-humid events, respectively.

In addition to single and bivariate extremes of the heatwave and hot-humid events, the trivariate extreme of hot, dry, and windy events (HDWs) was studied. Copula families, with the

flexibility of modeling joint behavior of more than one variable, were applied to discover the probability of compound HDWs in the central United States. The empirical method (i.e., counting the frequency of events) was used to test the accuracy of the copula. Results discovered south-west Kansas and North Texas as hotspots, where most of the HDWs are expected. A combination of drought and heatwave, in 1980 and 2011, showed an accelerating influence on the frequency of HDWs. The dependence structure between variables (temperature, relative humidity, and wind) showed no influence on the compound HDWs in the warm season (May through September). Results suggested an increase in the risk of HDWs despite the wind speed drop in a majority of the central United States. The results of this study are useful for a better understanding of the nature and variability of single and compound extreme events in the central United States that would influence water resources, irrigation, crops, wildfire, and human, plant, and livestock health. Findings suggest a need for more effective risk management in discovered hotspots considering a changing climate.

Climate change and the variability in the risk of single and compound climate extremes

by

Ameneh Tavakol

B.S., University of Tehran, 2005
M.S., University of Tehran, 2010

A DISSERTATION

submitted in partial fulfillment of the requirements for the degree

DOCTOR OF PHILOSOPHY

Department of Biological and Agricultural Engineering
Carl R. Ice College of Engineering

KANSAS STATE UNIVERSITY
Manhattan, Kansas

2020

Approved by:

Major Professor
Vahid Rahmani

Copyright

Abstract

Extreme weather and climate events have significantly influenced society and the environment. As the world has warmed, the warmer temperatures have triggered the frequency, severity, and duration of other extremes. In this study, the spatial and temporal patterns of heatwave frequency and duration were analyzed in the Mississippi River Basin (MRB) using the validated reanalysis (NCEP-NCAR) data for 1948–2018. The heatwave was defined as at least two consecutive days when maximum temperature was higher than the 90^{th} percentile. Over the 70-year period of study, the highest frequency of heatwaves was recorded in the west and north-west of the MRB with no significant increase over time. The results of the study confirmed the "warming hole" in the eastern-central United States with a significant decrease in the frequency of heatwaves. The longest heatwaves were found in southern and central MRB. Applying change-point analysis, an abrupt increase was found in the MRB in the percentage of area with heatwaves longer than 10 consecutive days since 1966. Impacts of heatwaves increase when multiple hazards occur simultaneously (e.g. heatwaves and high humidity) and lead to a compound extreme outcome. Heat-index was used to analyze the variability of compound high temperature and high humidity over time and space. Extreme daytime and nighttime hot-humid conditions were defined using the National Weather Services fixed thresholds. Spatially, southern MRB showed a higher frequency of extreme hot-humid events during both days and nights. There were no extreme nighttime hot-humid events in the east, west, and north-west MRB. Trend analysis discovered 16% and 8% significant upward trends in the daytime and nighttime extreme hot-humid events, respectively.

In addition to single and bivariate extremes of the heatwave and hot-humid events, the trivariate extreme of hot, dry, and windy events (HDWs) was studied. Copula families, with the

flexibility of modeling joint behavior of more than one variable, were applied to discover the probability of compound HDWs in the central United States. The empirical method (i.e., counting the frequency of events) was used to test the accuracy of the copula. Results discovered south-west Kansas and North Texas as hotspots, where most of the HDWs are expected. A combination of drought and heatwave, in 1980 and 2011, showed an accelerating influence on the frequency of HDWs. The dependence structure between variables (temperature, relative humidity, and wind) showed no influence on the compound HDWs in the warm season (May through September). Results suggested an increase in the risk of HDWs despite the wind speed drop in a majority of the central United States. The results of this study are useful for a better understanding of the nature and variability of single and compound extreme events in the central United States that would influence water resources, irrigation, crops, wildfire, and human, plant, and livestock health. Findings suggest a need for more effective risk management in discovered hotspots considering a changing climate.

Table of Contents

List of Figures xi
List of Tables xvi
Acknowledgements xvii
Dedication xviii
Chapter 1 - Introduction and Literature Review 1
Introduction 1
Climate change and changes in temperature, humidity and wind speed 1
Climate extreme events; single and compound events 4
Research Objectives 11
References 12
Chapter 2 - Evaluation of hot temperature extremes and heatwaves in the Mississippi River Basin 20
Chapter 3 - in the Mississippi River Basin 20
Introduction 20
Materials and Methods 23
Data 23
Study area 24
Methods 26
Temperature Indices 26
Trend Analysis 28
Change-point Analysis 29
Results 31
Daily maximum temperature (TX) 31
Annual frequency of HW (HWf) 35
Annual maximum length of HW (HWDI) 40
Impact of teleconnections on HWs 43
Discussion 45
Summary and Conclusion 48
References 49

Chapter 4 - Changes in the frequency of hot, humid days and nights in the Mississippi River Basin 58
Introduction 58
Materials and Methods 63
Data 63
Study area 64
Methods 64
Indices 64
Statistical tests 66
Results 67
Discussion 76
Conclusion 80
References 82
Chapter 5 - Temporal and spatial variation in the frequency of compound hot, dry winds in the central United States 91
Introduction 91
Definitions, Materials, and Methods 94
Hot, Dry, windy events (HDWs) Definition 94
Study Area 97
Data 97
Results and Discussion 98
Frequency of HDWs 98
Monthly and Diurnal Changes 100
Temporal Trend 103
Summary and Conclusions 107
References 109
Chapter 6 - The Probability of compound climate extremes in a changing climate: A copula-based study of hot, dry, and windy events in the central United States 114
Introduction 114
Materials and methods 117
Data 117

Methods 119
Copula Families 120
Fitting the copula 121
Results 124
Empirical vs copula 124
Variability of percentiles corresponding to the fixed thresholds 126
Dependence among variables 128
Pairwise probability between variables 130
Temporal changes of HDWs 132
Discussion 136
References 138
Chapter 7 - Summary and Conclusion 144
Recommendations and limitations 150
References 151

List of Figures

Figure 1-1. The worldwide annual average surface temperature anomalies relative to 1961–1990 retrieved from IPCC based on three combined air temperature and sea surface temperature data sets (Hartmann et al., 2013)..... 2

Figure 1-2. (a) Trends in surface specific humidity (g of moisture per kg of air) using different sets of data over 1973–2012. (b) Global annual average anomalies in land surface specific humidity. Anomalies are relative to the 1979–2003 climatology. The figure has been retrieved from IPCC (Hartmann et al., 2013). 5

Figure 2-1. Location of the Mississippi River Basin (MRB) in North America. 25

Figure 2-2. The 70-year (1948–2017) five month average of TX for the warm season (a), May (b), June (c), July (d), August (e) and September (f). Values on the bottom left of the plots show the range of monthly values..... 32

Figure 2-3. Annual frequency of hot days (TX90) in MRB for 1948 to 2017 (bars). Dotted black lines indicate the trend lines before and after the change-point (1997); and dashed red lines show the average of TX90 before and after change-point. 33

Figure 2-4. The spatial distribution of average annual TX90 for 1948–2017 (whole period) (a). The spatial pattern of TX_X90 for every grid cell (b) and the spatial distribution of annual average TX90 in the first 35-year period (1948–1982) (c) and the second 35-year period (1983–2017) (d). 34

Figure 2-5. Change-point and trend analysis of TX90 for the MRB. Spatial and temporal distribution of significant change-points by decade (a), trends of TX90 for the entire period (1948–2017) (b), and for before (c) and after (d) the change-point for the grid cells that had a significant change-point. The upward (red) and downward (blue) triangles show positive and negative trends, respectively. Shaded areas indicate significant trends. The regions with no triangle in (c) and (d) had no significant change-point. 36

Figure 2-6. Temporal changes in HW_f for the MRB from 1948 to 2017. Bars indicate annual values of HW_f. Dotted black lines are trend lines and the dashed red lines show the average of HW_f before and after change-point in 1997. 37

Figure 2-7. Spatial distribution of HW_f for 1948–2017 (a), the spatial distribution of HW_X90 for 1948-2017 (b), the spatial distribution of HW_f in the first 35-year period (1948–1982) (c) and the second 35-year period (1983–2017) (d). 39
Figure 2-8. Change-point and trend analysis of HW_f in the MRB. Decade of occurrence for significant change-points (a), trend of HW_f for the entire period (1948–2017) (b), and for before (c) and after (d) the change-point for the grid cells that had a significant change-point. The upward (red) and downward (blue) triangles show positive and negative trends, respectively. The shaded areas indicate cells with significant trends. The regions with no triangle in plots (c) and (d) did not have a significant change-point. 40
Figure 2-9. Spatial and temporal distribution of significant change-points (a), trends of HWDI for the entire period (1948–2017) (b) and for before (c) and after (d) the change-point for the grid cells that had a significant change-point. The upward (red) and downward (blue) triangles show positive and negative trends, respectively. The shaded areas show significant trends. The regions with no triangle in plots (c) and (d) did not have a significant change-point. 42
Figure 2-10. The percentage of the MRB covered by TX90 (a), HW_f (b), and HWDI (c) during normal and EL Niño years. The percentage of the MRB represents the fraction of the grid cells corresponding to values of the indices on the x-axis. 44
Figure 3-1. Percent change in the frequency of extreme events (calculated based on the difference in the number of extreme events in 1983–2017 relative to 1948–1982). Maps indicate the geography of changes in daytime maxima for HI_Xf (a), T_X90 (b), SH_X90 (c), and for extreme nighttime values in HI_Nf (d), T_N90 (e), and SH_N90 (f). 69
Figure 3-2. Spatial patterns of grid cell specific 70-year averages of the maximum and minimum of temperature (T °C) and heat index (HI °C) values for the warm season. Specific humidity maxima (a) and minima (b) contours are shown in Kg of vapor per Kg of air..... 70
Figure 3-3. The changes in the frequency of extreme events after the significant change point for HI_Xf (a), T_X90 (b), SH_X90 (c), HI_Nf (d), T_N90 (e), and SH_N90 (f). Colored grid cells show significant changes-points classified based on their decade of change. Red and blue triangles show if the number of extreme events was higher or lower after the change-point, respectively. Change-points mainly happened during the 1980s and 1990s. 71

Figure 3-4. Mann-Kendall trend test results for the entire period (1948–2017). Red and blue triangles indicate upward and downward trends, respectively in HI_Xf (a), T_X90 (b), SH_X90 (c), HI_Nf (d), T_N90 (e), and SH_N90 (f). The highlighted regions had a statistically significant trend. The white regions in plot (d) show the grid cells with zero HI_Nf. 72
Figure 3-5. Analysis of Mann-Kendall trend test in MRB before the significant change-point. Red and blue triangles represent upward and downward trend in the HI_Xf (a), T_X90 (b), SH_X90 (c), HI_Nf (d), T_N90 (e), and SH_N90 (f). The highlighted regions represent a significant trend. The white regions with no triangle had no significant change-point. 73
Figure 3-6. Analysis of Mann-Kendall trend test in the MRB after the significant change-point. Red and blue triangles represent upward and downward trends in the HI_Xf (a), T_X90 (b), SH_X90 (c), HI_Nf (d), T_N90 (e), and SH_N90 (f). The highlighted regions represent a significant trend. The white regions with no triangle had no significant change-point. 73
Figure 3-7. The empirical CDF of HI_Xf (a), T_X90 (b), SH_X90 (c), HI_Nf (d), T_N90 (e), and SH_N90 (f) for 1948–1982 (blue) and 1983–2017 (red). The x-axes represent the frequency of extreme indices in the MRB..... 74
Figure 3-8. 70-year average of HI_Xf (a) and HI_Nf (b) based on NCEP/NCAR (background map) and HadISD (solid red circles). NCEP/NCAR overestimated the HI_Xf and underestimated the HI_Nf. The pattern of distribution is same for both data sets. The higher frequency of HI_Xf and HI_Nf are expected in the south and south-west MRB..... 79
Figure 4-1. Location of stations analyzed in the central United States. The number of available stations increased from 27 to 44 when the study period decreased from 70 to 50 years (a). Annual mean frequency of hourly warm season HDWs in 50-year (b) and 70-year (c) periods. Highest values were determined for Dodge City, Kansas, for both periods. 99
Figure 4-2. The annual multi-station average frequency of hourly HDWs in 50-year (red) and 70-year (blue) periods for all stations in the central United States (top) and for Dodge City (bottom). The highest frequencies occurred in 2011 and 1980. Dodge City, in southwest Kansas, recorded the highest frequency of HDWs among all stations. The difference between 50-year and 70-year average frequency values for the study area is due to the different number of stations analyzed for each period..... 100
Figure 4-3. The annual multi-station average frequency of hourly HDWs in 50-year (red) and 70-year (blue) periods for all stations in the central United States (top) and for Dodge City

(bottom). The highest frequencies occurred in 2011 and 1980. Dodge City, in southwest Kansas, recorded the highest frequency of HDWs among all stations. The difference between 50-year and 70-year average frequency values for the study area is due to the different number of stations analyzed for each period..... 101
Figure 5-1. Location of analyzed stations in the central United States from 1949–2018. Data was retrived from HadISD. 118
Figure 5-2. Random samples of Elliptical and Archimedean copulas. Plots show 1000 random samples from a Gaussian (a), Student-t (b), Frank (c), Clayton (d), Gumbel (e), and Joe (f) copulas. The Elliptical and Archimedean copulas were created using $\boldsymbol{\rho = 0.8}$ and $\boldsymbol{\theta = 5}$, respectively. 121
Figure 5-3. The 3-dimensional distribution of normally transformed temperature, relative humidity, and wind speed (a) and the contour plots of fitted and empirical copula for temperature and relative humidity (b), temperature and wind speed (c), and relative humidity and wind speed (d) for the station located at Brownsville in Texas at 97.4°W and 25.9°N. Frank copula was the best-fitted copula for all three bivariate random variable combinations (b-d) and the trivariate random variables. 122
Figure 5-4. The annual co-occurrence of HDWs in the central United States based on copula (a) and empirical (b) methods. Percentiles used in the copula analysis correspond to the same fixed thresholds that were applied for the empirical method. Stations surrounded by the dashed line are the ones with the highest probability of HDWs (the southern Great Plains hotspot). 126
Figure 5-5. Annual averages of the percentiles corresponding to a temperature of 35°C (a), a relative humidity of 30% (b), and a wind speed of 7m/s (c)..... 128
Figure 5-6. Mann-Kendall correlation values between temperature, wind speed, and relative humidity. The correlation values are negative between temperature and relative humidity, and wind speed and relative humidity. The highest and lowest correlation was discovered between temperature and relative humidity (a) and temperature and wind speed (b), respectively. 130
Figure 5-7. The annual co-occurrence probability of extreme temperature and relative humidity (a), temperature and wind (b), and wind and relative humidity (c) in the central United

States. The threshold was defined based on the temperature higher than 35°C, relative humidity less than 30%, and the wind speed higher than 7m/s. 132
Figure 5-8. Spatial patterns of 70-year temporal trends for extreme HDWs (a), hot events (b), dry events (c), and windy events (d) in the central United States. Circled symbols indicate a significant trend (α=0.05). 135

List of Tables

Table 2-1. Temperature indices analyzed in this study. 28
Table 2-2. The statistics of HWDI (days) for the entire period of record and 10-year periods. ... 43
Table 3-1. Temperature, humidity, and HI extreme indices analyzed in this study. 67
Table 3-2. The percentage of the MRB with a significant change-point, as well as the upward and downward trends before and after change-points. Percentages were calculated in relation to the number of grid cells with significant change-point. The values in parentheses show the percentage of grid cells with a significant trend. 75
Table 3-3. Two-sample K-S test results for extreme indices in the MRB between 1948–1982 and 1983–2017. P-values smaller than 0.05 indicate that the two distributions are significantly different. 75
Table 4-1. Definition and categorization of hot, dry wind events based on different studies. 95
Table 4-2. Two-tailed Mann-Kendall trend test results indicate the temporal changes of HDW events in the central United States. The values indicate the percentage of stations with a significant positive or negative trend with α=0.05 in 50-year (1969–2018) and 70-year (1949–2018) periods. 104
Table 5-1. Two-sample K-S test for changes in extreme HWD events in the central United States between 1949–1983 and 1984–2018. P-values smaller than 0.05 indicate that the two distributions are significantly different. The plus and minus signs in the D Statistics column indicate if the period 1984–2018 had higher or lower frequency of HDWs compared to 1949–1983. The Mann-Kendall trend test indicates the temporal changes of compound (HDW) and single (hot, dry, or windy) extreme events. Values show the slope of the linear fit on data. The bold values indicate a significant trend with α=0.05. The location of stations is indicated by station ID in Figures 1 and 8. 134

Acknowledgements

This work has definitely been a challenge that could not have been accomplished without the assistance of many individuals. My deepest gratitude goes to Dr. Vahid Rahmani for his guidance and support throughout my doctoral program. I sincerely thank Dr. Rahmani for everything that he has done for me. I would like to thank my dissertation chairman, Dr. Charles Rice, and the rest of my committee members Dr. John Harrington, Dr. Stacy Hutchinson, and Dr. Shawn Hutchinson for their time and efforts. I am pleased to thank Dr. Harrington for all his help and feedback on my research. His profound knowledge and expertise in this area of research have always led me throughout my work. Dr. Stacy Hutchinson and Dr. Shawn Hutchinson provided excellent feedback that helped me broaden my research perspectives. I am also thankful for the knowledge I gained while attending my advisor and my committee members' doctoral classes and conducting research with them.

Finally, I would like to thank my family and friends for all of the support that they gave me over the last few years.

Ameneh Tavakol

January 2020

Dedication

To my loving parents, Hossain and Sonat, for their unconditional love and support.

To my special sister Azadeh, who has never left my side, and to my little Ava.

Special thanks to my husband, Amir, who has been a constant source of support and encouragement during the challenges of graduate.

Chapter 1 - **Introduction and Literature Review**

Introduction

Climate is defined by the average temperature and precipitation as well as the frequency, duration, and severity of climate extremes such as heatwave, drought, storms, and flood (EPA, 2017). The World Meteorological Organization (WMO) has defined climate extremes as infrequent climatological and meteorological phenomena that surpass a stated threshold (Das et al., 2003). Extreme events can greatly influence the environment and society resulting in loss of habitat, property, and even life. The National Centers for Environmental Information (NCEI) has reported 241 billion dollar weather disasters (extremes) in the United States since 1980 with a profound economic impact exceeding 1.6 trillion dollars (NOAA NCEI, 2020). A large increase in the number of annual disasters (e.g., heatwave, drought, and flood) from 10 to 35 in less than half of a century (1950–1990) was identified for the United States (Changnon 1998). Additionally, an upward trend in the probability of extreme events that was reported by the Intergovernmental Panel on Climate Change (IPCC: Hartmann et al., 2013). These trends will affect disaster risk due to the increasing level of exposure and vulnerability to these events (Field et al., 2012). In this dissertation, three climate variables, including temperature, humidity (relative and specific), and wind speed, were analyzed to study the changes in the single and concurrent occurrence of extreme events.

Climate change and changes in temperature, humidity and wind speed

The IPCC has documented a warmer planet since 1901 (Figure 1-1), with more pronounced upward trends over 1910–1940 and from 1970 onwards (Hartmann et al., 2013). However, the changes in air temperature differ regionally. In Europe, the downward trend of temperature for 1950–2005 changed to an increase since the 1970s in western Europe

(Makowski et al., 2008). In the United States, the annual average temperature has been rising since the beginning of the 20th century (USGCRP, 2017). Analyzing the changes in temperature in the United States between 1900 and 2000 showed high temperatures in 2000 that were cooler than the mean air temperature in the 1930s and 1990s (Hansen et al., 2001). Easterling et al., (2000) provided an overview of the literature on variations in extreme temperature. A slight downward trend was discovered in the frequency of exceedances of a 32°C threshold (DeGaetano & Allen, 2002; Easterling, D. R. et al., 2000).

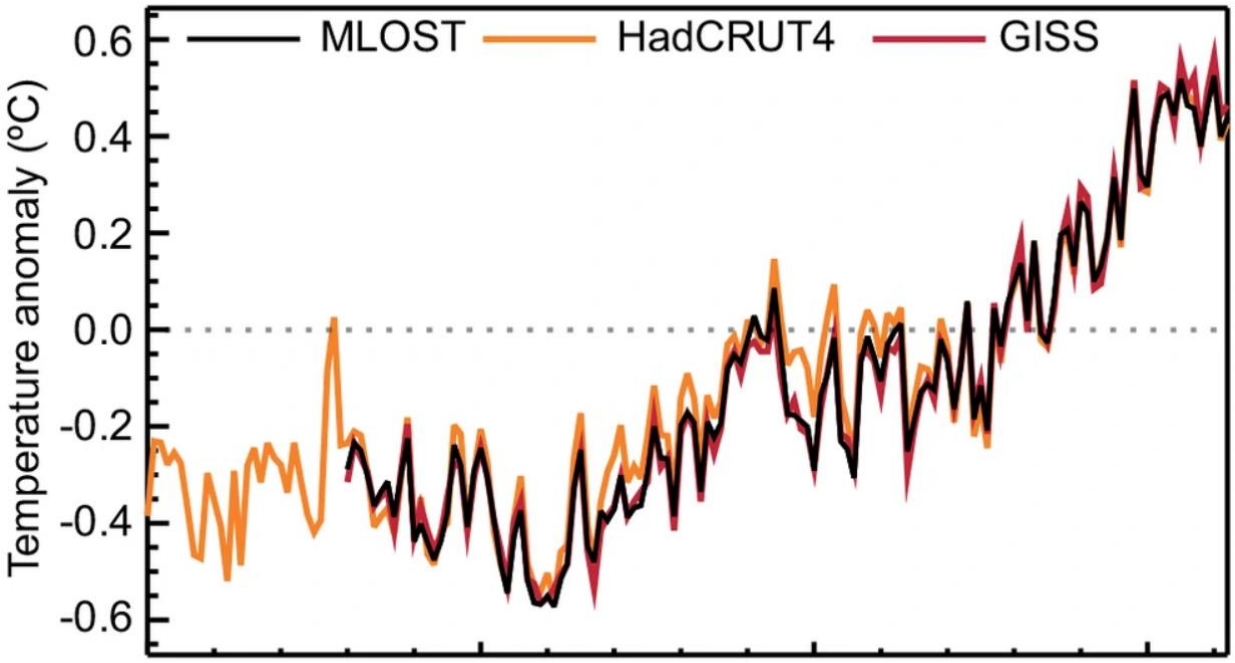

Figure 1-1. The worldwide annual average surface temperature anomalies relative to 1961–1990 retrieved from IPCC based on three combined air temperature and sea surface temperature data sets (Hartmann et al., 2013).

An increase in humidity is expected as a result of a warmer troposphere and an increase in evaporation (Figure 1-2). Surface relative humidity has relatively small inter-annual; however spatial variations are considerable, with a mean value of 30%–60% in deserts and high terrains,

70%–80% over remaining land areas, and 75%–80% over oceans in all seasons (Dai, 2006). Globally, the surface specific humidity has increased significantly between 1973 and 2003 with larger upward trends in the Northern Hemisphere and the tropics during summer (Willett et al., 2008). Considering the increase in both temperature and specific humidity, trends in relative humidity are generally not significant (Hartmann et al., 2013). However, some changes in relative humidity at the seasonal time scale are significant over the landmass of the globe, Northern Hemisphere, and tropics (Willett et al., 2008). A recently discovered decrease in global relative humidity over land areas can be explained by the lower rise in sea surface temperature compared to land temperatures which limits moisture supply from oceans (Simmons et al., 2010). A comparative reduction in water supplied from land evapotranspiration may also be a factor (Vicente-Serrano et al., 2018). A long-term (1961–95) analysis of specific humidity in the United States documented larger upward trend slopes for nighttime humidity than daytime trends (Gaffen & Ross, 1999). The trend of relative humidity is weaker than specific humidity with the maximum increase of specific humidity in summer and relative humidity in winter (Brown & DeGaetano, 2013; Gaffen & Ross, 1999). Spatially, a long-term moistening has been found in the central United States while other portions of the United States are experienced drying (Brown & DeGaetano, 2013).

For winds, a 25 percent increase in peak gusts has caused a sevenfold rise in building damage in the United States (Kezunovic et al., 2008). In Europe, a six percent increase in average winter gust caused a 44 percent insurance losses (Schwierz et al., 2010). Pryor et al., (2009) analyzed the changes in wind speed in the United States using observational, reanalysis, and model-based data over different periods. They found a decline in the annual mean wind speed for events at the 50^{th} and 90^{th} percentiles. Another study confirmed a clear reduction in

mean annual wind speed in North America for different periods of data, based on a literature review of previous studies (Wu et al., 2018). Klink (1999) analyzed the mean monthly wind speed in the United States over the period 1961–1990 and reported a decrease in west and south-west winds related to variable topography and high-pressure systems. However, the monthly mean maximum wind speed, which is higher in the central and northeastern United States than in other parts of the United States, had an increase for the entire United States.

Climate extreme events; single and compound events

Global warming is expected to increase the frequency of extreme climate events. The extreme climate events can influence water quantity and quality, food production, infrastructure, and even human health with profound economic and security effects (Mora et al., 2018). In 2018 alone, 14 billion dollar weather events resulted in the deaths of 247 people (NOAA NCEI, 2020). With multiple simultaneous hazards (compound/concurrent extreme events), a greater influence on event severity is expected in the future (Hartmann et al., 2013; Leonard et al., 2014). With the ongoing emission of greenhouse gases (GHGs), by 2100 the world's population may experience an annual frequency of extremes with the equivalent of at least three contemporary hazards occurring concurrently with a maximum of six concurrent extremes in coastal regions (Mora et al., 2018). The IPCC defines the compound events as "(1) two or more extreme events occurring successively or simultaneously, (2) combinations of extreme events that amplify the impact of the events with underlying conditions, or (3) combinations of events that are not extremes by themselves but lead to an extreme event when combined" (Seneviratne et al., 2012). Leonard et al., (2014) defined compound extremes as "an extreme impact that depends on multiple statistically dependent variables or events".

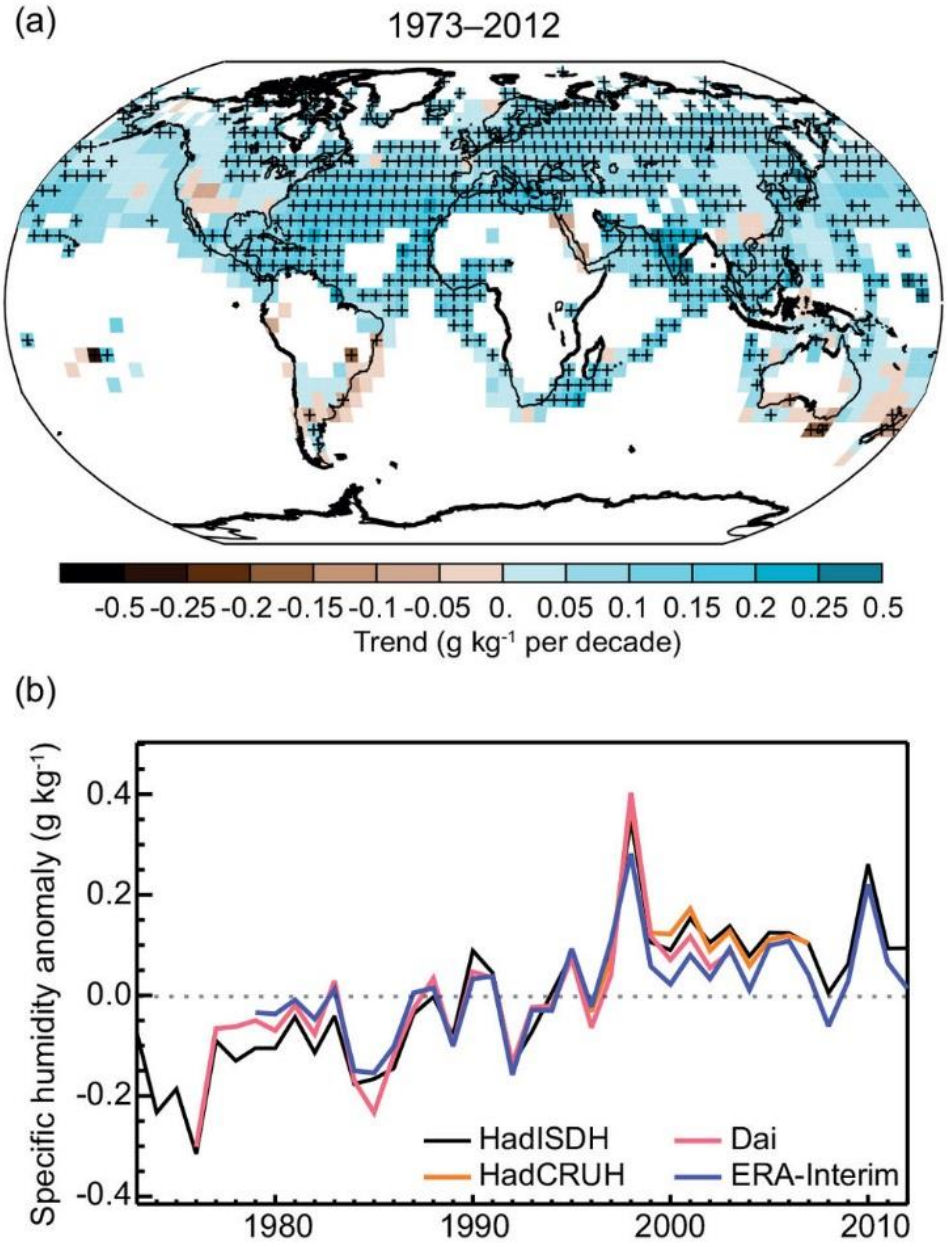

Figure 1-2. (a) Trends in surface specific humidity (g of moisture per kg of air) using different sets of data over 1973–2012. (b) Global annual average anomalies in land surface specific humidity. Anomalies are relative to the 1979–2003 climatology. The figure has been retrieved from IPCC (Hartmann et al., 2013).

Heatwaves are single extreme events defined by one variable, temperature. Heatwaves, with a larger number of record-breaking events in recent decades (Coumou & Rahmstorf, 2012), are among the 10 deadliest natural disasters (Guha-Sapir et al., 2012). Devastating and severe heatwaves of 2003 in Europe and 2010 in Russia exceeded long-term temperature records; the impacts negatively influenced crop production, water resources, and wildfires (Barriopedro et al., 2011; Garcia-Herrera et al., 2010; Miralles et al., 2014). The upward trend of heatwaves worldwide (Donat, M. G. et al., 2013; Hartmann et al., 2013; Meehl & Tebaldi, 2004; Perkins et al., 2012) has been significant since about 1950, consistent with global warming (Donat, Markus G. & Alexander, 2012; Hartmann et al., 2013). In the United States alone, the annual expenditure to address extreme heat and the associated droughts exceeds several billion dollars (NOAA NCEI, 2020). In 2012, most of the central United States experienced prolonged extreme heat leading to $33 billion economic losses, 123 human deaths, a 10 percent drop of corn production, and considerable losses in the beef industry (NOAA NCEI, 2020). While heatwave frequency has been studied in the United States, there is a knowledge gap regrading changes in heatwaves of different durations (Tavakol & Rahmani, 2018). In addition, there is no knowledge about the abrupt change in the frequency and duration of heatwaves (objective I in the research objectives section).

A warmer world would trigger an increase in the frequency and severity of other extreme events (e.g., drought) (Easterling, G. et al., 2000; Hartmann et al., 2013; Perkins et al., 2012) and can substantially increase the probability of concurrent extreme events (e.g., Rahmani & Tavakol, 2019; Tavakol & Rahmani, 2019a; Tavakol & Rahmani, 2019b; Tavakol et al., 2020). Different methods have been developed to study concurrent extreme events (Hao et al., 2018). Empirical approaches involve simply counting the number of either compound or the

consecutive concurrence of multiple events. Indicator approaches study the concurrent extremes of multiple variables as a unique index (e.g., heat index or apparent temperature). Finally, in a multivariate distribution approach (e.g., copula) are developed to assess the joint behavior of the multiple variables in a compound extreme event. Joint probability, in general, is defined as a statistical measure that computes the likelihood of two events occurring together at the same time.

Hot-humid conditions, as a concurrent extreme, result from the high level of moisture in the air that hinders the body's ability to cool off through sweating. The heatwaves of Shanghai (2003) and Chicago (1995) are two examples of hot-humid conditions (Russo et al., 2017) that resulted in 258 and 600 excess deaths (Dematte et al., 1998; Huang et al., 2010). The events mentioned would not be considered severe based only on hot temperatures (single extreme) (Russo et al., 2017). Hot-humid conditions limit the ability of the human body to adapt to heat stress (Sherwood & Huber, 2010), increase the mortality rate with prolonged exposure to heat (Yip *et al.*, 2008), affect livestock by influencing their thermoregulation (Deshazer, 2009), reduce livestock production (Fuquay, 1981; Morrison, 1983), and limit outdoor physical activities (Obradovich & Fowler, 2017). Considering the documented increase of temperature and humidity in the United States (DeGaetano & Allen, 2002; Elliott & Angell, 1997; Gaffen & Ross, 1998; Gaffen & Ross, 1999; Hartmann et al., 2013; Karl et al., 1996), there is an expected increase in hot-humid conditions (Gaffen & Ross, 1998; Knutson & Ploshay, 2016; Pal & Eltahir, 2016; Rieck, 2014).

The heat index (Rothfusz, 1990), a combination of temperature and humidity, calculates a "feels-like" temperature (Knutson & Ploshay, 2016). The heat index incorporates the limiting influence of humidity that would make temperature feel hotter than it actually is and reduce

evaporative cooling. National Weather services (NWS) has developed a technical report "the result of extensive biometeorological studies" to explain how hot-humid conditions affect human health (Rothfusz, 1990). The heat index was developed using regression models to analyze the influence of combined hot and humid conditions on human health, categorizing the exact impact of each heat index values on the human body (Ahrens & Samson, 2010; Havenith & Fiala, 2011). There is limited knowledge on the combined influence of temperature and humidity on the exact number of days when hot-humid condition surpasses the defined NWS thresholds and where or not changes have happened over time (objective II in the research objectives section).

While any single extreme of high temperature, low humidity, or high wind speed can have a negative influence on human and natural systems, a combination of all these weather e;ements, "compound hot, dry, and windy events (HDWs)", can result in a much more profound influence on crop yield (Curtis, 1891; Wang et al., 2016; Yang & Wang, 1978), impact the efficiency of irrigation systems (Haman et al., 2002), and begin or intensify wildfires (Flannigan & Harrington, 1988; Jolly et al., 2015; Srock et al., 2018), influence water resources, and impact human and animal health. HDWs are a type of compound extreme event that is defined by high temperature, low humidity, and moderately high wind speed. HDWs can significantly increase the fire weather season length (Jolly et al., 2015) and lead to more severe wildfires (Flannigan & Harrington, 1988). The factors involved in the definition of HDWs have been used to develop a fire-weather prediction index for weather that makes a wildfire difficult to manage (Srock et al., 2018). Generally, the water demand of plants, required for their growth and cooling, increases on sunny days with HDWs (Derrel et al., 1993). When hot-dry winds reach the soil surface, the soil will dry faster because of higher evaporation rates and the water below the surface moves upward by capillary action. If evaporation continues, the drier soil causes resistance in the rate of

water flow in the soil that limits evaporation. When evaporation is limited, excess energy at the soil surface heats the soil and the air above the soil surface (Derrel et al., 1993). The decrease of soil water will change the partitioning of energy moving from the soil to the atmosphere (with more sensible heat exchanged) and affect the energy budget of the crop.

Very few studies have analyzed the spatial patterns and temporal changes in HDWs. For example, Lydolph and Williams (1982) applied hourly data for a decade (1951–1960) to analyze the spatial occurrence of HDWs in the US to the east of the Rocky Mountains. While almost the entire region was subject to the occurrence of HDWs, or "sukhovey", the results demonstrated a decrease in the frequency of these events eastward from the Great Plains (Lydolph & Williams, 1982). They defined the events using five different categories with temperature higher than 29°C in the first category to temperature higher than 38°Cin the fifth category. With the more intense definition of HDWs (temperature higher than 38°C), the area of occurrence was limited to the Great Plains (Lydolph & Williams, 1982). Leathers and Harrington (2001) analyzed the frequency of HDWs, or "furnace winds" in the regions between the Great Plains and the west coast for 1948–1993. Higher frequency of hot and hot-dry extremes were found in the southwest as a result of aridity and lower cloud coverage in the deserts (Leathers & Harrington, 2001). Higher frequency of HDWs was captured in the Great Plains where high-speed winds are more frequent (Leathers & Harrington, 2001). With documented changes of humidity, temperature, and wind speed, the interest was to study how the compound HDWs are changing over time and space in the central United States (objective III in the research objectives section).

Although the empirical methods can simply asses the occurrence of concurrent extreme events, they may fall short in communicating the risks related to the effects of climate extremes when more than one variable is responsible for the extreme impacts (Raynal-Villasenor & Salas,

1987; Yue et al., 2001). There are many approaches to build a multivariate distribution, such as entropy, parametric distribution, copula, and nonparametric models (Hao & Singh, 2016). Copulas are the preferred joint distribution functions to determine the dependence properties of the distribution regardless of their univariate distribution function (Genest & Favre, 2007).

AghaKouchak et al., (2014) identified the 2014 California drought as a model of an extreme event characterized not only by low precipitation but also with high temperatures. While the precipitation was not the lowest in the record (1896–2014), the extremely high temperature was the highest in the record that intensified the dry condition with severe impacts across the state. This event confirmed that while global warming may not cause drought, it might intensify the severity of the drought (Trenberth et al., 2013).

On the global scale, Zscheischler and Seneviratne (2017) applied copula to show how the dependence structure between temperature and precipitation can influence the concurrency of multivariate extremes. The 90^{th} and 10^{th} percentiles were used respectively on temperature and precipitation data to specify the hot and dry extremes. The dependence structure of data was modeled with copula as well as the bivariate return period of concurrent hot-dry events. Four Archimedean copulas including Gumbel, Frank, Clayton, and Joe were used and demonstrated the importance of the multivariate perspective of climate extremes for risk assessment and design of adaptation strategies.

Sarhadi et al (2018), recently developed a new framework to quantify temporal and spatial concurrency of temperature and precipitation anomalies for the entire globe using data from 1931-2015, a period of non-stationary climate. They found an increase in concurrent warm and dry years from 20% in the mid-20^{th} century to 40% in the early 21^{st} century applying canonical vine (C-vine) copula. The copula approach has been increasingly used in hydrology

and climatology. In this study, the interest was to use it for analyzing compound HDWs (objective IV in the research objectives section).

Research Objectives

Considering the fact that most regions in the world are experiencing warmer than average temperature, it is possible to have an increase in the frequency of single and concurrent extremes. In the United States, all regions are likely to be warmer in the future because of the history of anthropogenic GHG emissions (past emissions), natural variability, and further changes in the human-related emissions (Wuebbles et al., 2014). This increase may increase the probability of concurrent temperature and other climate extremes such as wind and humidity. The overarching goal of this study is to address the mentioned research gaps with the following objectives:

Objective I: Analyzing temporal changes and spatial pattern in a single climate extreme (heatwave)

A long record (1948–present) of temperature was used to analyze the changes in the frequency and duration of the heatwaves in the Mississippi River Basin (MRB; Chapter 2). MRB was selected because of the inclusion of diverse climate and land use. Statistical methods used to test the probable connection between major circulations (e.g., El Niño) and heatwave.

Objective II: Analyzing temporal changes and spatial pattern in a bivariate concurrent climate extreme (hot-humid conditions)

Considering the population of MRB (100 million people), the changes in hot-humid conditions can severely influence morbidity and mortality in the region. The heat index was calculated for MRB to analyze the spatiotemporal risk of extreme heat index (Chapter 3). The high-risk regions were specified along with the temporal changes hot-humid condition, temperature, and humidity.

Objective III: Analyzing changes in a trivariate concurrent climate extreme (HDWs) using the empirical method

Based on previous studies that found the highest occurrence of HDWs in the Great Plains (Leathers & Harrington, 2001; Lydolph & Williams, 1982), the spatial and temporal changes of compound HDWs were analyzed in the central United States using empirical methods (Chapter 4). Applying sub-daily data, the hot spots where the most risk of compound events is expected were specified. Temporal changes of HDWs were analyzed by considering the role of each single variable (wind, relative humidity, and temperature) in the changes of events.

Objective IV: Analyzing changes in a trivariate compound climate extreme (HDWs) using copula

Considering the shortcoming of the empirical method in communicating an accurate risk of concurrent events, a trivariate copula was developed to analyze the probability of HDWs events in the central United States (Chapter 5). The dependent structure among variables was calculated based on the best-fitted copula families. The probable influence of dependence on the probability of concurrent events was analyzed.

A sixth chapter concludes the discussion of extreme events with a summary of important research findings. Limits of the work, along with suggestions for moving forward are also discussed.

References

Aghakouchak, A., Cheng, L., Mazdiyasni, O., & Farahmand, A., 2014. Global warming and changes in risk of concurrent climate extremes: Insights from the 2014 California drought. *Geophysical Research Letters.* 41: 8847-8852. http://doi.org/10.1002/2014GL062308

Ahrens, C. D., & Samson, P. J., 2010. Extreme weather and climate. *Cengage Learning.* Belmont, CA, USA. 531p.

Barriopedro, D., Fischer, E. M., Luterbacher, J., Trigo, R. M., & Garcia-Herrera, R., 2011. The hot summer of 2010: redrawing the temperature record map of Europe. *Science.* 332: 220-224. http://science.sciencemag.org/content/332/6026/220

Brown, P. J.& DeGaetano, A. T., 2013. Trends in US surface humidity, 1930–2010. *Journal of Applied Meteorology and Climatology.* 52: 147-163. https://doi.org/10.1175/JAMC-D-12-035.1

Changnon, S., 1998. "METEOROL APPL." Meteorol. Appl. 5: 125.

Coumou, D., & Rahmstorf, S., 2012. A decade of weather extremes. *Nature climate change.* 2: 491-496. https://doi.org/10.1038/nclimate1452

Curtis, G. E. 1891. The hot winds of the plains. *Seventh Biennial Report, Kansas Department of Agriculture.* 7: 162-183. https://www.kansasmemory.org/item/225333

Dai, A. 2006. Recent climatology, variability, and trends in global surface humidity. *Journal of Climate.* 19: 3589-3606. https://doi.org/10.1175/JCLI3816.1

Das, H. P., Adamenko, T. I., Anaman, K. I., Gommes, R. G., & Johnson, G., 2003. Agrometeorology related to extreme events . *Secretariat of the WMO.* Geneva.

DeGaetano, A. T., & Allen, R. J., 2002. Trends in twentieth-century temperature extremes across the United States. *Journal of Climate.* 15: 3188-3205. https://doi.org/10.1175/1520-0442(2002)0152.0.CO;2

Dematte, J. E., O'mara, K., Buescher, J., Whitney, C. G., Forsythe, S., McNamee, T., ..., and Ndukwu, I. M., 1998. Near-fatal heat stroke during the 1995 heat wave in Chicago. *Annals of Internal Medicine.* 129: 173-181.

Derrel, M. L., Gilley, J. R., & Baumer, O. W., 1993. Irrigation Handbooks and Manuals (Part 623, Chapter 2) Irrigation Water Requirements. *United States Department of Agriculture.* Washington, DC, USA. https://www.nrcs.usda.gov/wps/portal/nrcs/detailfull/national/water/manage/irrigation/?cid=stelprdb1045075.

Deshazer, J. A.2009. Basic principles of the thermal environment and livestock energetics. *In: Livestock energetics and thermal environmental management.* (pp. 1-22). American Society of Agricultural and Biological Engineers. MI, USA.

Donat, M. G., Alexander, L. V., Yang, H., Durre, I., Vose, R., Dunn, R., ..., and Caesar, J., 2013. Updated analyses of temperature and precipitation extreme indices since the beginning of the twentieth century: The HadEX2 dataset. *Journal of Geophysical Research: Atmospheres.* 118: 2098-2118. http://www.doi.org/10.1002/jgrd.50150

Donat, M. G.& Alexander, L. V., 2012. The shifting probability distribution of global daytime and night-time temperatures. *Geophysical Research Letters.* 39: L14707. https://doi.org/10.1029/2012GL052459

Easterling, D. R., Evans, J. L., Groisman, P. Y., Karl, T. R., Kunkel, K. E., & Ambenje, P., 2000. Observed variability and trends in extreme climate events: a brief review. *Bulletin of the American Meteorological Society.* 81: 417-426. https://doi.org/10.1175/1520-0477(2000)0812.3.CO;2

Easterling, G., Meehl, C., Parmesan, S. A., Changnon, T., Karl, L., & Mearns, L., 2000. Climate extremes: Observations, modeling, and impacts. *Science (Washington).* 289: 2068-2074. http://science.sciencemag.org/content/289/5487/2068

Elliott, W. P.& Angell, J. K., 1997. Variations of cloudiness, precipitable water, and relative humidity over the United States: 1973–1993. *Geophysical Research Letters.* 24: 41-44. https://doi.org/10.1029/96GL03616

EPA. (2017). Climate change indicators: Weather and climate. Retrieved from https://www.epa.gov/climate-indicators/weather-climate; January2020.

Field, C. B., Barros, V., Stocker, T. F., & Dahe, Q., 2012. IPCC 2012; Managing the risks of extreme events and disasters to advance climate change adaptation: special report of the intergovernmental panel on climate change. *Cambridge University Press.* Cambridge, Uk and New York, NY, USA. 582p.

Flannigan, M. D.& Harrington, J. B., 1988. A study of the relation of meteorological variables to monthly provincial area burned by wildfire in Canada (1953–80). *Journal of Applied Meteorology.* 27: 441-452. https://doi.org/10.1175/1520-0450(1988)0272.0.CO;2

Fuquay, J. W. 1981. Heat Stress as it Affects Animal Production. *Journal of Animal Science.* 52: 164-174. https://doi.org/10.2527/jas1981.521164x

Gaffen, D. J.& Ross, R. J., 1998. Increased summertime heat stress in the US. *Nature.* 396: 529-530. https://doi.org/10.1038/25030

Gaffen, D. J.& Ross, R. J., 1999. Climatology and trends of US surface humidity and temperature. *Journal of Climate.* 12: 811-828. https://doi.org/10.1175/1520-0442(1999)0122.0.CO;2

Garcia-Herrera, R., Diaz, J., Trigo, R. M., Luterbacher, J., & Fischer, E. M., 2010. A review of the European summer heat wave of 2003. *Critical Reviews in Environmental Science and Technology.* 40: 267-306. https://doi.org/10.1080/10643380802238137

Genest, C.& Favre, A., 2007. Everything you always wanted to know about copula modeling but were afraid to ask. *Journal of Hydrologic Engineering.* 12: 347-368. https://doi.org/10.1061/(ASCE)1084-0699(2007)12:4(347)

Guha-Sapir, D., Vos, F., Below, R., & Ponserre, S., 2012. Annual disaster statistical review 2011: the numbers and trends. *Centre for Research on the Epidemiology of Disasters.* Brussels, Belgium. http://www.cred.be/sites/default/files/ADSR_2011.pdf.

Haman, D. Z., Smajstrla, A. G., & Pitts, D. J., 2002. BUL247 Efficiencies of irrigation systems used in Florida nurseries. *Citeseer.* https://www.researchgate.net/profile/Gary_Clark9/publication/237646861_Efficiencies_of_Florida_Agricultural_Irrigation_Systems_1/links/54bd08440cf27c8f2813746d/Efficiencies-of-Florida-Agricultural-Irrigation-Systems-1.pdf

Hansen, J., Ruedy, R., Sato, M., Imhoff, M., Lawrence, W., Easterling, D., ..., and Karl, T., 2001. A closer look at United States and global surface temperature change. *Journal of Geophysical Research: Atmospheres.* 106: 23947-23963. https://doi.org/10.1029/2001JD000354

Hao, Z.& Singh, V. P., 2016. Review of dependence modeling in hydrology and water resources. *Progress in Physical Geography.* 40: 549-578. https://doi.org/10.1177/0309133316632460

Hao, Z., Singh, V., & Hao, F., 2018. Compound extremes in hydroclimatology: a review. *Water.* 10: 718. https://doi.org/10.3390/w10060718

Hartmann, D. L., Tank, A. M. K., Rusticucci, M., Alexander, L. V., Brnnimann, S., Charabi, Y. A. R., ..., and Kaplan, A., 2013. Observations: Atmosphere and surface. *In: Climate change 2013 the physical science basis: Working group I contribution to the fifth assessment report of the intergovernmental panel on climate change.* (pp. 159-254). Cambridge University Press. Cambridge, United Kingdom and New York, NY, USA.

Havenith, G.& Fiala, D., 2011. Thermal indices and thermophysiological modeling for heat stress. *Comprehensive Physiology.* 6: 255-302. https://doi.org/10.1002/cphy.c140051

Huang, W., Kan, H., & Kovats, S., 2010. The impact of the 2003 heat wave on mortality in Shanghai, China. *Science of the Total Environment.* 408: 2418-2420. https://doi.org/10.1016/j.scitotenv.2010.02.009

Jolly, W. M., Cochrane, M. A., Freeborn, P. H., Holden, Z. A., Brown, T. J., Williamson, G. J., & Bowman, D. M., 2015. Climate-induced variations in global wildfire danger from 1979 to 2013. *Nature Communications.* 6: 7537. https://doi.org/10.1038/ncomms8537

Karl, T. R., Knight, R. W., Easterling, D. R., & Quayle, R. G., 1996. Indices of climate change for the United States. *Bulletin of the American Meteorological Society.* 77: 279-292. https://doi.org/10.1175/1520-0477(1996)0772.0.CO;2

Kezunovic, M., Dobson, I., & Dong, Y., 2008. Impact of extreme weather on power system blackouts and forced outages: New challenges. In: *7th Balkan Power Conf,*

Klink, K. 1999. Trends in mean monthly maximum and minimum surface wind speeds in the coterminous United States, 1961 to 1990. *Climate Research.* 13: 193-205. www.doi.org/10.3354/cr013193

Knutson, T. R.& Ploshay, J. J., 2016. Detection of anthropogenic influence on a summertime heat stress index. *Climatic Change.* 138: 25-39. https://doi.org/10.1007/s10584-016-1708-z

Leathers, N.& Harrington, J., 2001. Furnace winds of the West. *Journal of the West.* 40: 48-57.

Leonard, M., Westra, S., Phatak, A., Lambert, M., van den Hurk, B., McInnes, K., ..., and Stafford-Smith, M., 2014. A compound event framework for understanding extreme impacts. *Wiley Interdisciplinary Reviews: Climate Change.* 5: 113-128. https://doi.org/10.1002/wcc.252

Lydolph, P. E.& Williams, T. B., 1982. The North American Sukhovey. *Annals of the Association of American Geographers.* 72: 224-236. https://doi.org/10.1111/j.1467-8306.1982.tb01821.x

Makowski, K., Wild, M., & Ohmura, A., 2008. Diurnal temperature range over Europe between 1950 and 2005. *Atmospheric Chemistry and Physics.* 8: 6483-6498. https://doi.org/10.5194/acp-8-6483-2008

Meehl, G. A.& Tebaldi, C., 2004. More intense, more frequent, and longer lasting heat waves in the 21st century. *Science.* 305: 994-997. http://science.sciencemag.org/content/305/5686/994

Miralles, D. G., Teuling, A. J., Van Heerwaarden, C. C., & de Arellano, J. V., 2014. Mega-heatwave temperatures due to combined soil desiccation and atmospheric heat accumulation. *Nature Geoscience.* 7: 345-349. https://doi.org/10.1038/ngeo2141

Mora, C., Spirandelli, D., Franklin, E. C., Lynham, J., Kantar, M. B., Miles, W., ..., and Louis, L. V., 2018. Broad threat to humanity from cumulative climate hazards intensified by greenhouse gas emissions. *Nature Climate Change.* 8: 1062. https://doi.org/10.1038/s41558-018-0315-6

Morrison, S. R. 1983. Ruminant heat stress: effect on production and means of alleviation. *Journal of Animal Science.* 57: 1594-1600. https://doi.org/10.2527/jas1983.5761594x

NOAA NCEI. (2020). Billion-dollar weather and climate disasters. Retrieved from https://www.ncdc.noaa.gov/billions; 3/9/2019.

Obradovich, N.& Fowler, J. H., 2017. Climate change may alter human physical activity patterns. *Nature Human Behaviour.* 1: 0097. https://doi.org/10.1038/s41562-017-0097

Pal, J. S.& Eltahir, E. A., 2016. Future temperature in southwest Asia projected to exceed a threshold for human adaptability. *Nature Climate Change.* 6: 197-200. https://doi.org/10.1038/nclimate2833

Perkins, S. E., Alexander, L. V., & Nairn, J. R., 2012. Increasing frequency, intensity and duration of observed global heatwaves and warm spells. *Geophysical Research Letters.* 39: n/a. https://doi.org/10.1029/2012GL053361

Pryor, S. C., Barthelmie, R. J., Young, D. T., Takle, E. S., Arritt, R. W., Flory, D., ..., and Roads, J., 2009. Wind speed trends over the contiguous United States. *Journal of Geophysical Research: Atmospheres.* 114: http://www.doi.org/10.1029/2008JD011416

Rahmani, V., & Tavakol, A., 2019. Spatiotemporal Changes of Correlated Hot, Dry, and Windy Conditions in the Central United States. In: *AGU Fall Meeting 2019,* https://agu.confex.com/agu/fm19/meetingapp.cgi/Paper/594147.

Raynal-Villasenor, J. A.& Salas, J. D., 1987. Multivariate extreme value distributions in hydrological analyses. *IAHS Publication.* 111-119. http://hydrologie.org/redbooks/a164/iahs_164_0111.pdf

Rieck, T. 2014. Heat index climatology for the north-central United States. *Http://Www.Crh.Noaa.Gov/Crh/Ssd/Pdf/tsp_17.Pdf and Accessed on November.* 15: 2014. https://mrcc.illinois.edu/living_wx/heatwaves/HeatIndexClim-tsp17-Rieck.pdf

Rothfusz, L. P.1990. The heat index equation (or, more than you ever wanted to know about heat index). *National Oceanic and Atmospheric Administration, National Weather Service, Office of Meteorology.* Forth Worth, TX.

Russo, S., Sillmann, J., & Sterl, A., 2017. Humid heat waves at different warming levels. *Scientific Reports.* 7: 7477. https://doi.org/10.1038/s41598-017-07536-7

Sarhadi, A., Ausín, M. C., Wiper, M. P., Touma, D., & Diffenbaugh, N. S., 2018. Multidimensional risk in a nonstationary climate: Joint probability of increasingly severe warm and dry conditions. *Science Advances.* 4: eaau3487. http://doi.org/10.1126/sciadv.aau3487

Schwierz, C., Köllner-Heck, P., Mutter, E. Z., Bresch, D. N., Vidale, P., Wild, M., & Schär, C., 2010. Modelling European winter wind storm losses in current and future climate. *Climatic Change.* 101: 485-514. https://doi.org/10.1007/s10584-009-9712-1

Seneviratne, S. I., Nicholls, N., Easterling, D., Goodess, C. M., Kanae, S., Kossin, J., ..., and Zwiers, F. W., 2012. Changes in climate extremes and their impacts on the natural physical environment: An overview of the IPCC SREX report. *Cambridge University Press. Cambridge.* New York, NY, USA. 109-230p.

Sherwood, S. C.& Huber, M., 2010. An adaptability limit to climate change due to heat stress. *Proceedings of the National Academy of Sciences.* 107: 9552-9555. https://doi.org/10.1073/pnas.0913352107

Simmons, A. J., Willett, K. M., Jones, P. D., Thorne, P. W., & Dee, D. P., 2010. Low-frequency variations in surface atmospheric humidity, temperature, and precipitation: Inferences

from reanalyses and monthly gridded observational data sets. *Journal of Geophysical Research: Atmospheres.* 115: https://doi.org/10.1029/2009JD012442

Srock, A., Charney, J., Potter, B., & Goodrick, S., 2018. The Hot-Dry-Windy Index: A New Fire Weather Index. *Atmosphere.* 9: 279. https://doi.org/10.3390/atmos9070279

Tavakol, A., & Rahmani, V., 2018. Changes of heat wave duration in the Mississippi River Basin. In: *2018 ASABE Annual International Meeting*, Michigan, USA. https://doi.org/10.13031/aim.201801071.

Tavakol, A., & Rahmani, V., 2019a. Analysis of compound hot, dry winds using Copula. In: *AGU Fall Meeting 2019*, https://agu.confex.com/agu/fm19/meetingapp.cgi/Paper/552421.

Tavakol, A., & Rahmani, V., 2019b. Changes in the frequency of hot, humid conditions in the Mississippi River Basin. In: *2019 ASABE Annual International Meeting*, http://www.doi.org/10.13031/aim.201901502.

Tavakol, A., Rahmani, V., & Harrington, J., 2020. Changes in the frequency of hot, humid days and nights in the Mississippi River Basin. *Int J Climatol.* 1-16. https://doi.org/10. 1002/joc.6484

Trenberth, K. E., Dai, A., Gerard Van, D. S., Jones, P. D., Barichivich, J., Briffa, K. R., & Sheffield, J., 2013. Global warming and changes in drought. *Nature Climate Change.* 4: 17-22. https://doi.org/10.1038/nclimate2067

USGCRP.2017. Climate Science Special Report: Fourth National Climate Assessment, Volume I. *U.S. Global Change Research Program.* Washington, DC, USA. https://science2017.globalchange.gov/chapter/front-matter-about/.

Vicente-Serrano, S. M., Nieto, R., Gimeno, L., Azorin-Molina, C., Drumond, A., El Kenawy, A., ..., and Peña-Gallardo, M., 2018. Recent changes of relative humidity: Regional connections with land and ocean processes. https://doi.org/10.5194/esd-9-915-2018

Wang, S., Zheng, H., Liu, S., Miao, Y., & Li, J., 2016. Numerical study on the stomatal responses to dry-hot wind episodes and its effects on land-atmosphere interactions. *PloS One.* 11: e0162852. https://doi.org/10.1371/journal.pone.0162852

Willett, K. M., Jones, P. D., Gillett, N. P., & Thorne, P. W., 2008. Recent changes in surface humidity: Development of the HadCRUH dataset. *Journal of Climate.* 21: 5364-5383. https://doi.org/10.1175/2008JCLI2274.1

Wu, J., Zha, J., Zhao, D., & Yang, Q., 2018. Changes in terrestrial near-surface wind speed and their possible causes: an overview. *Climate Dynamics.* 51: 2039-2078. https://doi.org/10.1007/s00382-017-3997-y

Wuebbles, D. J., Kunkel, K., Wehner, M., & Zobel, Z., 2014. Severe weather in United States under a changing climate. *Eos, Transactions American Geophysical Union.* 95: 149-150. https://doi.org/10.1002/2014EO180001

Yang, Z.& Wang, S., 1978. The climatal analysis and forecast on Dry-hot wind at Guangzhong, Shaanxi. *Meterology Shaanxi.* 3: 6-13.

Yip, F. Y., Flanders, W. D., Wolkin, A., Engelthaler, D., Humble, W., Neri, A., ..., and Rubin, C., 2008. The impact of excess heat events in Maricopa County, Arizona: 2000–2005. *International Journal of Biometeorology.* 52: 765-772. https://doi.org/10.1007/s00484-008-0169-0

Yue, S., Ouarda, T., & Bobee, B., 2001. A review of bivariate gamma distributions for hydrological application. *Journal of Hydrology.* 246: 1-18. https://doi.org/10.1016/S0022-1694(01)00374-2

Zscheischler, J.& Seneviratne, S. I., 2017. Dependence of drivers affects risks associated with compound events. *Science Advances.* 3: e1700263. http://doi.org/10.1126/sciadv.1700263

Chapter 2 - **Evaluation of hot temperature extremes and heatwaves in the Mississippi River Basin**

Chapter 3 - **in the Mississippi River Basin**

This chapter is a peer-reviewed publication in the *International Journal of Climatology* with the following citation: Tavakol, A.; Rahmani, V.; Harrington, J.Jr. (2020). Evaluation of hot temperature extremes and heat waves in the Mississippi River Basin." Atmospheric Research (2020): 104907. https://doi.org/10.1016/j.atmosres.2020.104907. This publication was granted permission to be included in this dissertation.

Introduction

A large number of record-breaking hot temperature extremes and heatwaves (HW) have been reported in recent years all around the world (Coumou & Rahmstorf, 2012) suggesting that this increased frequency is symptomatic of ongoing global climate change. HWs are among the 10 deadliest global natural disasters (Guha-Sapir et al., 2012). Lack of cooling at night and multi-day atmospheric heat accumulation (Miralles et al., 2014) have been linked to human and livestock mortality (Anderson & Bell, 2011; CDC, 1996; Fouillet et al., 2008; Nienaber & Hahn, 2007). The connections between HWs and water scarcity (Seneviratne et al., 2006), human mortality (Basu & Samet, 2002; Patz et al., 2005), livestock health (Hahn, 1999; Thornton et al., 2009), and crop loss (Deryng et al., 2014; Lobell et al., 2012; Lobell et al., 2013) have raised serious concerns about the future impacts of climate change (Kovats & Hajat, 2008). The Intergovernmental Panel on Climate Change (IPCC) Fourth Assessment Report indicated an increase in warm extreme indices for a majority of global land areas (Hartmann et al., 2013).

Since 1950, this increase is significant and consistent with global climate change (Donat & Alexander, 2012; Hartmann et al., 2013).

In 2003, 2010, and 2015, European areas experienced devastating HWs that broke long-standing temperature records and caused extensive crop loss, water scarcity, wildfires and loss of life (Barriopedro et al., 2011; Garcia-Herrera et al., 2010; Krzyżewska et al., 2019; Miralles et al., 2014). Atmospheric blocking with the presence of persistent high-pressure areas (Meehl & Tebaldi, 2004) has been identified as a key synoptic weather pattern causing temperature escalation to recorded extremes. Maximum summer temperatures that were observed during 2010 in western Russia were exceptional based on the observational record that dates back to 1871 (Barriopedro et al., 2011). This HW lasted from June into August and the heat and dry conditions set the stage for extensive wildfires (Trenberth & Fasullo, 2012). Barriopedro et al. (2011) suggest that the probability of summer with a mega-HW in Europe will increase by a factor of 5-10 in the next 40 years. In China, a warming trend was found for extremely hot days and nights (Shi et al., 2018). HWs were found to be generally concurrent with warm season drought in most regions in China (Chen et al., 2019). In Pakistan, a positive trend was found for HWs with a maximum temperature greater than 40°C (Zahid & Rasul, 2012). Stronger winds and lower relative humidity are distinctive characteristics of HWs in Pakistan (Khan et al., 2019a).

In the United States, the 1995 Chicago HW was described as the “urban inferno” (Klinenberg, 2015). Although this HW was relatively short (3 days), extreme temperatures accompanied by high humidity made for severe heat index conditions (Kaiser et al., 2007; Russo et al., 2017). Tavakol and Rahmani (2019) have documented an upward trend in severe heat index conditions for the central MRB. Results from HW studies in the United States show an

increasing frequency of HW, especially over the Great Plains and eastern United States (Alexander, L. V. et al., 2006; Smith et al., 2013). While the changes in the frequency of HW events have been studied, there is still limited knowledge on changes in HW length which is expected to increase in the 21st century (Meehl & Tebaldi, 2004).

Considering the impacts of HW on water availability and human and animal mortality, and the projected probabilities of more frequent, more intense, and longer hot summers in North America (Meehl & Tebaldi, 2004), it is important to understand and analyze changes in high temperatures and HWs in the United States. The objective of this study is to assess spatial patterns and temporal changes for HWs in the MRB and specify regions and times with more risk of experiencing a HW. Previous studies used different sets of data, study periods, HW definitions, and diverse temperature variables to analyze HWs in the United States (Alexander, L. V. et al., 2006; DeGaetano & Allen, 2002; Lyon & Barnston, 2017; Oswald, 2018; Smith et al., 2013). Station-based temperature observations are limited by missing information and cannot perfectly represent the spatial pattern of HWs. To cope with this issue, researchers have used either interpolated (*i.e.*, gridded) (Oswald, 2018) or model-based (*i.e.*, reanalysis) data (Smith et al., 2013) to spatially and temporally provide a complete dataset. In this study, the National Centers for Environmental Prediction/National Center for Atmospheric Research (NCEP-NCAR) reanalysis data covering 1948 – 2017 were used. In addition, a change-point detection analysis was completed to determine any sudden change in HW frequency. Analysis of trends before and after the change-point will provide a better understanding of temporal change in HWs.

Materials and Methods

Data

Daily maximum temperature (TX) values (at 2 meters above ground surface) were retrieved from the NCEP-NCAR reanalysis data. These data offer the advantage of assimilating information from many different sources and are available at multiple space and time resolutions. The NCEP-NCAR reanalysis project began in 1991 motivated by climate change and the need for improvement in climate forecasts (Kalnay et al., 1996). The success of any statistical analysis is highly dependent on the existence of a sufficient sample size. NCEP-NCAR reanalysis data provide a longer record (1948–present) of climate variables compared to other available gridded products (Kalnay et al., 1996) with the inclusion of more observational data as well as a better quality control scheme (Bromwich & Fogt, 2004). The NCEP-NCAR data are the most commonly re-analysis products in recent decades (Liléo et al., 2013).

Daily TX values were used for a 70-year period from 1948 through 2017. Data were obtained from the surface flux level of the NCEP-NCAR reanalysis dataset (www.esrl.noaa.gov/psd/data), which is available with a global Gaussian T62 grid (192x94 grid points) with a 1.9° latitude × 1.875° longitude spatial resolution. All 137 grid cells that were either completely or partly inside the MRB were included in the study. Daily TX values, obtained from NCEP-NCAR products, were validated against HadISD observation data (https://www.metoffice.gov.uk/hadobs/hadisd/). HadISD (Dunn et al., 2012; Dunn et al., 2016) is a quality-controlled, station-based, sub-daily, global dataset developed based on the Integrated Surface Database (ISD) at the National Oceanic and Atmospheric Administration's National Centre for Environmental Information (NOAA/NCEI). HadISD data are available from 1931 to the present. 83 Stations with less than 10% missing data, randomly distributed in MRB, were

used in this study. The linear correlation showed acceptable agreement between the gridded and station-based datasets ranging from R=0.66 (R^2=43%) in the south to R=0.92 (R^2=85%) in the north and north-west of the MRB.

Study area

The MRB, with a population of approximately 100 million, is located in the central United States and covers parts or all of 31 states in the United States plus parts of two Canadian provinces (Figure 2-1). Boreal summer in the MRB extends from May through September (Perkins et al., 2012). Covering approximately 41% of the contiguous United States, the basin has an area of 3.3 million km^2. Waters from the MRB account for the 90 percent inflow of fresh water to the Gulf of Mexico (Rabalais et al., 1996). The MRB includes six 2-digit HUC watersheds and is the largest watershed in North America and the third largest river basin in the world. Extending from the Rocky Mountains in the west to the Allegheny Mountains in the northeast, southern Canada in the north to the Gulf of Mexico in the south, the basin is comprised of diverse natural and agricultural ecosystems.

Figure 3-1. Location of the Mississippi River Basin (MRB) in North America.

With a population of about 100 million in MRB, HW eventscan critically influence societal affairs. For instance, Coppola (2006) attributed about 10,000 excess deaths in the United State to excessive heat between 1979 and 2001. A majority of the MRB regions experienced a catastrophic HW in the spring and summer 2012. The prolonged heat event contributed to 123 human deaths, along with economic impacts (NOAA NCEI, 2020a).

The MRB is one the most agriculturally productive regions in the world containing 58% cropland, 21% range and barren land, 18% woodland, 2.4% water and wetland, and 0.6% urban land (Goolsby, 2000). While diverse crops show different responses to heat stress (Hatfield et al., 2014), crop yields decrease when temperatures exceed the crop's optimum growth temperature (Deryng et al., 2014; Pryor et al., 2014). Considering that the land use of the MRB is dominated by cropland, HWs like the one that occurred in 2012 (NOAA NCEI, 2019b) have pronounced negative impacts on water resources, agriculture and the economy of the region.

Methods

Temperature Indices

Establishing a threshold is necessary for identifying a hot temperature extreme. A TX higher than the 90th percentile was identified as a hot extreme based on the IPCC definition (Stocker, 2014). The 90th percentile threshold was calculated for every warm season calendar day for 1961–1990 (the reference period) for each grid cell.

The 1961-1990 period has been suggested by the World Meteorological Organization (WMO) as a standard reference period for long-term climate change assessments (Klein Tank et al., 2009) and has been used in many recent studies (Habeeb et al., 2015; Hirschi et al., 2011; Sun et al., 2017). Gridded TX values were then compared to the daily thresholds. The analysis was done on a daily basis for five warm season months (May through September). The identified threshold values change on a daily basis with highest values in mid-summer. Spatial variation in the identified threshold values tends to have a south-to-north spatial pattern.

Typically, a HW is defined as a period of consecutive days exceeding an extreme temperature threshold (Meehl & Tebaldi, 2004; Perkins & Alexander, 2013). However, there is no universal definition for a HW (Khan et al., 2019c; Perkins 2015; Smith et al., 2013). Previous studies have considered the length of the hot day sequence from at least two (Anderson & Bell, 2011; Robinson, 2001; Smith et al., 2013) or three (Ceccherini et al., 2017; Hirschi et al., 2011; Meehl & Tebaldi, 2004; Nissan et al., 2017; Perkins & Alexander, 2013) to a longer sequence of consecutive hot days (Clark et al., 2006; Mazdiyasni & Aghakouchak, 2015). Selecting a longer length for HW event will decrease the number of captured extreme events (Robinson, 2001) while omitting short-lasting HWs that have a huge social impact like the 3-day HW of Chicago in 1995 (Klinenberg, 2015). In this study, a 2-day duration was selected to define a HW. The

shortest length of HW (two consecutive days) has been selected to capture a greater number of HWs in each grid cell and to provide a better understanding of HW trends over time. Changes in HW length were also analyzed separately. In addition to assessing the spatial pattern and temporal change in TX, five indices were calculated (Table 2-1) to study changes in the frequency of hot days (TX90), the frequency of heatwaves (HW_f), the frequency of hot years (TX_X90P; HW_X90P), and heatwave duration (HWDI). The selected indices are modifications of metrics used in previous studies (Fischer et al., 2007; Fischer & Schär, 2010; Frich et al., 2002; Hirschi et al., 2011; Tavakol & Rahmani, 2018).

Examination of the impact of possible teleconnections from the tropical Pacific and Atlantic was assessed using the Oceanic Niño Index (ONI) and North Atlantic Oscillation (NAO), respectively. Monthly values of the ONI and NAO were obtained from the Climate Prediction Center (CPC; http://www.cpc.ncep.noaa.gov).

Table 3-1. Temperature indices analyzed in this study.

Index	Units	Definition
TX90	Count of Days	Annual frequency of hot days; Days with TX greater than 90th percentile.
TX**X**90P	%	Percentage of years when the frequency of TX90 is higher than the 90th percentile. The 90th percentile was calculated based on the average for the reference period 1961–1990.
HW**f**	Count of HWs	Annual frequency of HWs*.
HW**X**90P	%	Percentage of years when the frequency of HWs is higher than the 90th percentile. The 90th percentile was calculated based on the average for the reference period 1961–1990.
HWDI	Days	Annual maximum length of a HW.

*A HW was defined as at least two consecutive days of TX90.

Trend Analysis

The non-parametric Mann-Kendall test was used for trend analysis. Mann-Kendall is a rank-based, distribution-free test to specify whether or not there is a monotonic trend in a time series (Kendall, 1975; Mann, 1945). This method was selected because it does not require a normal distribution for the residuals. Mann-Kendall and modified Mann-Kendall (Hamed, 2008) have been widely used in previous studies to analyze temperature (Khan et al., 2019b), streamflow (Fathian et al., 2016), and precipitation (Rahmani et al., 2016). Mann-Kendall is not sensitive to the effect of outliers in the time series and has been widely used for different climate variables (Ahiablame et al., 2017; Rahmani & Harrington Jr, 2018). In using this method, the null hypothesis (H_0) states that there is no trend in the data. However, there are three alternative hypotheses (H_a) that determine an upward, downward or either an upward or a downward monotonic trend in data. An advantage of this method is its non-sensitivity to missing data and outliers.

The first step, to specify a trend in a time series $x_1, x_2, \ldots, x_n$ of length n, was to compute the indicator function $sgn(x_i - x_j)$ and determine if the difference between the data at time i and j is positive, negative or zero.

$$sgn(x_i - x_j) = \begin{cases} 1, & x_i - x_j > 0 \\ 0, & x_i - x_j = 0 \\ -1, & x_i - x_j < 0 \end{cases} \quad (1)$$

The test statistic S and standard deviation (σ_s) of S were calculated using equations (2) and (3), respectively. In these equations, p is the number of tied groups and q_k is the number of data points in the k^{th} group.

$$S = \sum_{i=1}^{n-1} \sum_{j=i+1}^{n} sgn(x_i - x_j) \quad (2)$$

$$\sigma_s = \sqrt{\frac{1}{18}[(n)(n-1)(2n+5) - \sum_{k=1}^{p}(q_k)(q_k-1)(2q_k+5)]} \quad (3)$$

Using S and σ_s, the Mann-Kendall test statistic (Z_{MK}) was calculated by applying the transformation in equation (4). This function ensures a normal distribution of Z_{MK} for data with a large sample size. At a significance level α (here $\alpha = 0.1$), H_0 was rejected if $|Z_{MK}| > Z_{1-\alpha/2}$.

$$Z_{MK} = \begin{cases} \frac{S-1}{\sigma_s}, & S > 0 \\ 0, & S = 0 \\ \frac{S+1}{\sigma_s}, & S < 0 \end{cases} \quad (4)$$

Change-point Analysis

The Pettitt test was used for detecting potential abrupt changes in the time series for each of the indices considered (Anandhi et al., 2016; Rahmani et al., 2015). This test is a rank-based,

distribution-free, non-parametric test which is resistant to outliers (Pettitt, 1979). The variable U_k was calculated based on the rank of the i^{th} observation (R_{y_i}) after sorting the data in ascending order:

$$U_k = 2\sum_{i=1}^{k} R_{y_i} - k(n+1) \quad (5)$$

where n is the total number of observations and k ranges from 1 to n. The change-point statistic (K) was defined as the maximum value of U_k.

$$K = \max_{1 \le k \le n} |U_k| \quad (6)$$

where α is the significance level of the test (here $\alpha = 0.05$), the change-point is statistically significant if K is greater than the critical value (K_α) given by:

$$K_\alpha = [-ln\alpha(n^3 + n^2)/6]^{0.5} \quad (7)$$

Mann-Kendall and Pettitt tests were applied to capture changing and/or nonstationary conditions (trend and non-homogeneity) of indices for the MRB. The tests were run for the average or sum of all values in all of the grid cells in the MRB and for every grid point separately. Trends were studied for the whole period and then before and after the years in which a change-point was identified. Temporal and spatial changes in index values were analyzed, including dividing the 70-year record into two halves so that the two halves could be compared. Temporal findings are also presented for the different 10-year periods (decades) covered by the available data. In some cases, the decades begin with the first year of available data (*i.e.,* 1948-1957, 1958-1967, …), and in other cases, the data are reported using decades that align with the base-10 number system (*i.e.,* 1951-1960, 1961-1970, …).

Results

Daily maximum temperature (TX)

Spatial distributions of the 70-year average of TX for the entire warm season as well as the monthly averages of TX are shown in Figure 2-2. The average values decreased from the south-west (north Texas) toward the north, north-east, and north-west of the MRB. The lowest average TX value (11.2°C) was recorded in May on the border between Montana and Wyoming. Highest values were recorded in July from 24.8 to 36.8°C (Figure 2-2d) and in August from 25.6 to 37.0°C (Figure 2-2e).

Changes in TX90 summarized for the MRB for 1948–2017 are shown in Figure 2-3. Annual values were computed by summing the TX90 (count of days) for all grid cells across the entire MRB. For the basin as a whole, TX90 ranged from a low of 1080 days in 1993 to highs of 5351 days in 1952 and 5155 days in 2012. Patterns of TX90 in the MRB are different for each year (See the supplemental material; Figure S2). When annual totals are averaged for a decade, the period from 1948-1957 had the greatest average of TX90 (3417) following by 1998–2007 (3096), and 2008–2017 (3041). The intervening four decades from 1958 to 1997 clearly had lower TX90 sums (Figure 2-3). In the analysis of yearly values, a non-homogeneity was detected by the Pettitt test in TX90 counts. A statistically significant downward trend is evident before the change-point and a non-significant upward trend occurs after 1997 (Figure 2-3). Average annual counts of TX90 were 2300 days before the change-point and increased to 2995 days following 1997.

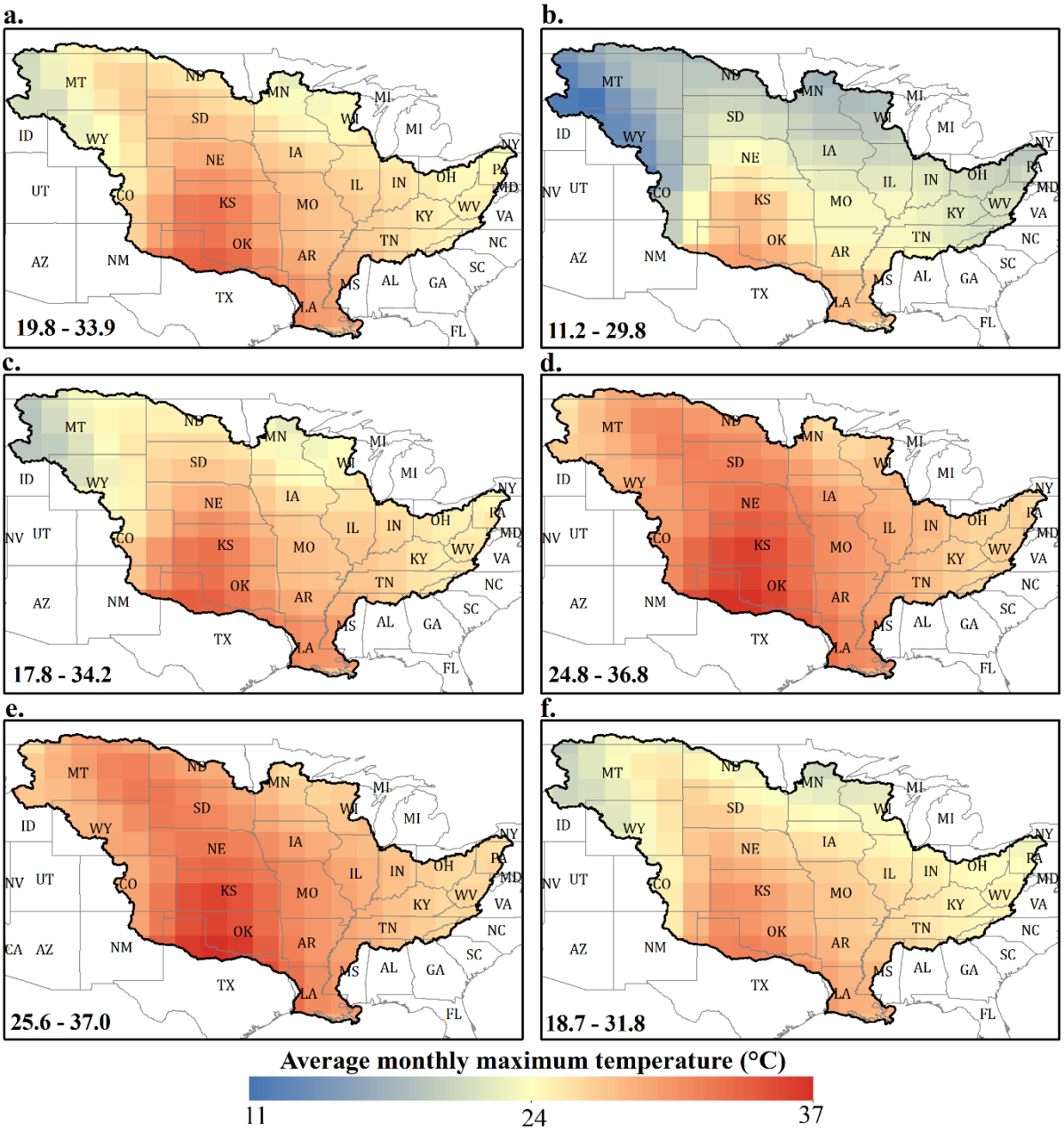

Figure 3-2. The 70-year (1948–2017) five month average of TX for the warm season (a), May (b), June (c), July (d), August (e) and September (f). Values on the bottom left of the plots show the range of monthly values.

Spatial analysis of the data for individual grid cells indicates that the average annual TX90 increased from the south and east to the west and north-west of MRB for 1948–2017 (Figure 2-4a). Lowest TX90 values (13 days) are near the confluence of the Ohio and Mississippi Rivers and a grid cell in central Wyoming had the highest average annual count (28 days). TX90

values have large interannual variability for each grid cell and do not follow the same temporal pattern as total TX90 averaged for the MRB. To examine the temporal distribution of TX90 over the entire record, the TX_X90P index was calculated (Figure 2-4b). Western and north-western grid cells have higher TX_X90P values. Greatest TX_X90P (51%) was observed in Wyoming. Generally, in central parts of the watershed, especially in Missouri, Iowa, South Dakota, Nebraska, and Kansas, less than 20% of the 70-yr data period had TX90 values that exceeded the 1961–1990 90th percentile threshold. Different parts of the MRB were influenced by extreme temperature in each year. During the year with highest TX90 (5351 days in 1952), much of the southern and western MRB experienced severe hot weather (See the supplemental material; Figure S2).

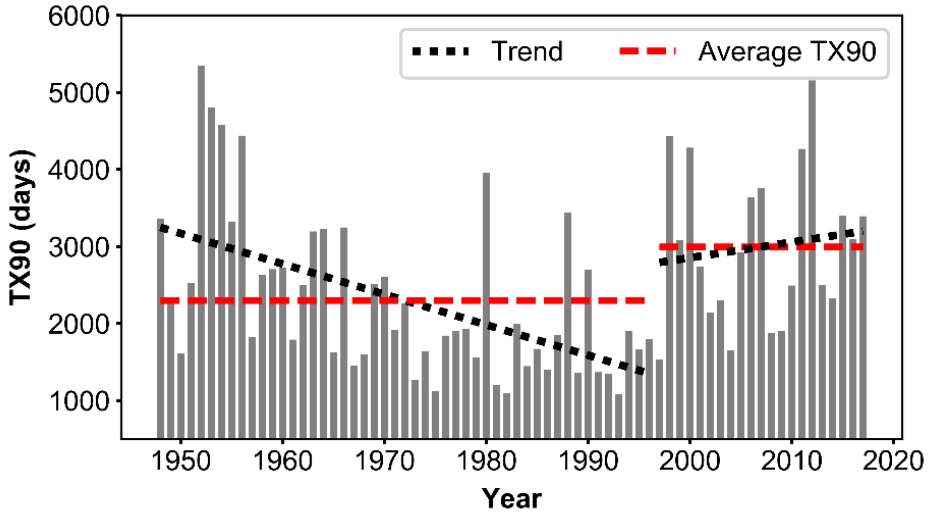

Figure 3-3. Annual frequency of hot days (TX90) in MRB for 1948 to 2017 (bars). Dotted black lines indicate the trend lines before and after the change-point (1997); and dashed red lines show the average of TX90 before and after change-point.

After dividing the whole time period into two 35-year subsets, average TX90 values exhibited different spatial patterns (Figures 2-4c and 2-4d). In the first 35-year period, the range of TX90 values was smaller (from 15 days in northcentral areas to 25 days in the west). However, for the second 35-year period, TX90 values ranged from 10 days near the middle of

Mississippi River to 34 days in southern Louisiana; values also increased westward toward Wyoming. Comparing TX90 values from the first 35-yr period to the second, the eastern, central, and center-western areas of the MRB experienced a decrease, while an increase occurred in southern Louisiana along with northern, north-western, and western areas. The increase was prominent in southern Louisiana (72%) and central Montana (36%). Analyzing the changes in TX90 before and after the change-point showed that identification of a change-point will influence the average (see the supplemental material; Figure S3).

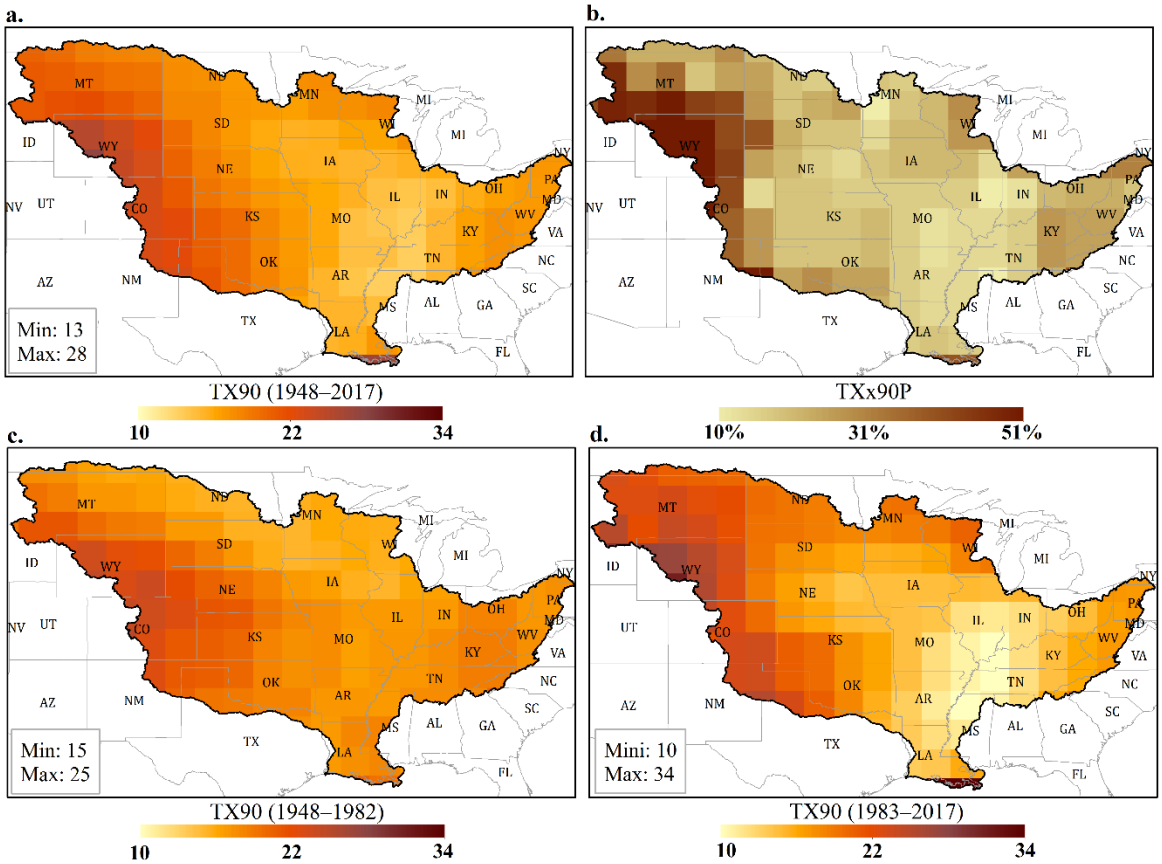

Figure 3-4. The spatial distribution of average annual TX90 for 1948–2017 (whole period) (a). The spatial pattern of TX$_X$90 for every grid cell (b) and the spatial distribution of annual average TX90 in the first 35-year period (1948–1982) (c) and the second 35-year period (1983–2017) (d).

Pettitt test analysis on TX90 values indicated a significant change-point in the time series for 61% of the grid cells across the MRB (Figure 2-5a). A majority (60%) of these grid cells had

a higher average of TX90 after the change-point. Most of the grid cells with a decrease in the average value of TX90 after a significant change-point were in the eastern and west-central portions of the MRB. Figure 2-5a shows a significant change-point during the decade of the 1990s for 34% of the grid cells. For grid cells where the 1960s and 1970s showed an abrupt change, the patterns of change in the average TX90 after these change-points differed but mainly decreased. Most of the grid cells with a non-significant change-point were in the central MRB.

Trend analysis of the entire period (1948–2017) indicates a decreasing trend for a majority of the grid cells (54%). However, only a few cells in the east (12%) showed a significant downward trend (Figure 2-5b). For grid cells that had a significant change-point, a majority of cells (90%; 55% significant) had downward trends before the change-point (Figure 2-5c). No significant upward trend was observed. Significant downward trends occurred mainly in western and north-western areas of the MRB. After the change-points, a majority of the grid cells (89%; 27% significant) had upward trends (Figure 2-5d). Most of the girds with a significant upward trend were in the western MRB. For all grid cells with a statistically significant change-point, the trends before and after the change-point were downward and upward, respectively.

Annual frequency of HW (HWf)

Temporal changes of HW_f for 1948–2017 are shown in Figure 2-6. Summary annual values were computed by summing the HW_f values from all grid cells across the entire MRB. The values ranged from a minimum of 199 events in 1982 and a maximum of 1275 events in 2012. The years, 1952 and 1954, had the second and third highest values of HW_f. Decadal analysis of HW_f values for the entire MRB found similar results as with TX90 values.

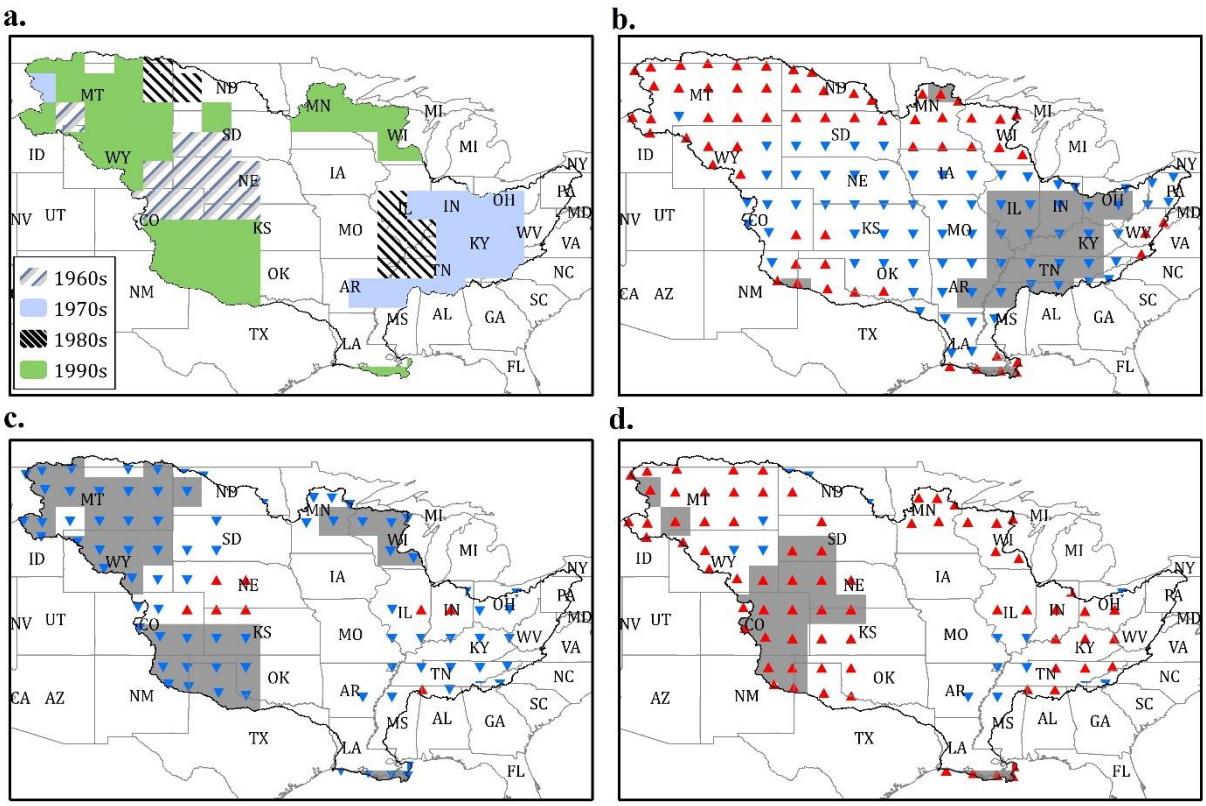

Figure 3-5. Change-point and trend analysis of TX90 for the MRB. Spatial and temporal distribution of significant change-points by decade (a), trends of TX90 for the entire period (1948–2017) (b), and for before (c) and after (d) the change-point for the grid cells that had a significant change-point. The upward (red) and downward (blue) triangles show positive and negative trends, respectively. Shaded areas indicate significant trends. The regions with no triangle in (c) and (d) had no significant change-point.

The first decade (1948–1957) had the highest average HW_f (803 events) following by 1998–2007 (755), and 2008–2017 (728). The other four decades from 1958 to 1997 had fewer HWs (Figure 2-6). Pettitt test analysis detected 1997 as a significant change-point for HW_f with an increase from an average HW_f of 547 events for 1948–1996 compared with an average of 724 for 1997–2017. A significant downward trend before the change-point and a non-significant upward trend after 1997 were found for HW_f (Figure 2-6).

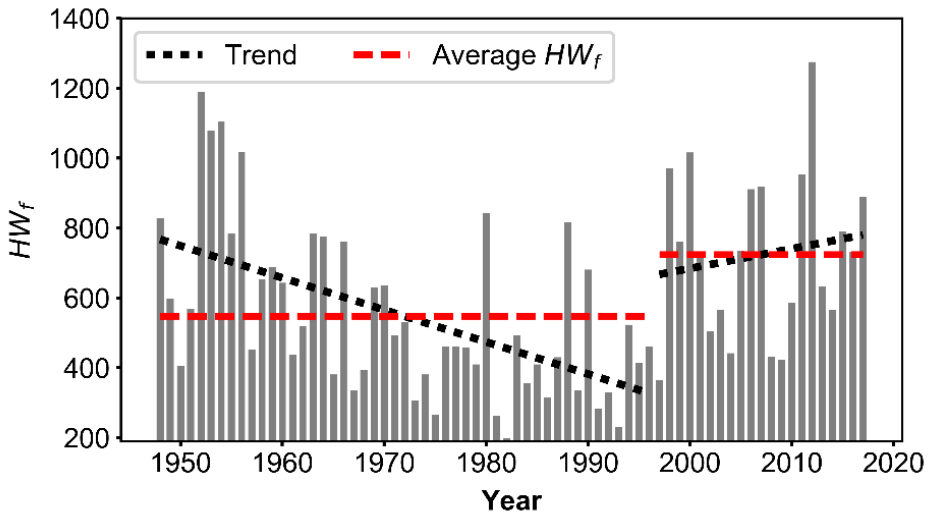

Figure 3-6. Temporal changes in HW_f for the MRB from 1948 to 2017. Bars indicate annual values of HW_f. Dotted black lines are trend lines and the dashed red lines show the average of HW_f before and after change-point in 1997.

The spatial pattern of HW_f (the average of annual values) shows a gradual increase away from the areas with the lowest values in the south-central region (Figure 2-7a). Grid cells in Arkansas and Wyoming had the lowest (3) and highest (7) average HW_f values, respectively (Figure 2-7a). To examine the spatial distribution of HW_f, the percentage of years with high HW_f (HWx90P) was computed (Figure 2-7b). The grid cells with the greatest (49%) and the least (4%) frequency of HWx90P were in the western and eastern parts of the MRB, respectively.

Temporal analysis of HW_f documented the highest decadal frequencies at the beginning (1948–1957) and at the end (1998–2017) of the study period. After dividing the whole period into two 35-year periods, the spatial patterns for HW_f (Figure 2-7c and 2-7d) are different. In the first 35-year period (Figure 2-7c), HW_f ranges from three in the south-center (Arkansas) to a maximum of six in the north-western MRB (western South Dakota and eastern Wyoming). However, in the second 35-year period (Figure 2-7d), values ranged from seven for grid cells in the northwest to two for grid cells near the Mississippi River from Illinois to the Gulf of Mexico. Comparing the difference between the time periods, HW_f generally decreased in the southern,

eastern, and north-central areas. Grid cells in western, northern, and north-western areas had slightly larger HW_f values in the second 35-year period. The greatest increases were in Montana (38% increase) and along the Gulf Coast in southern Louisiana (37% increase). It is worth mentioning that the reference period has lower HW_f compared to the whole period, which helps explain the sizeable percentage of HWx90P (Figure 2-7b) in some parts of MRB (See the supplemental material; Figure S4).

Pettitt test analysis on the HW_f data indicates a significant change-point in 68% of the grid cells (Figure 2-8a). A majority of these grid cells (78%) had an increase in average HW_f after the change-point. Grid cells with a decrease in average HW_f after the change-point (22%) were generally located in eastern and west-central areas of the MRB. Among all grid points in the MRB, a significant change-point was detected for 46% of the grid cells during the 1990s. For all grid cells with a significant change-point in the 1990s and 2000s, the average of HW_f increases after the change-point. On the other hand, trends in HW_f decreased after the change-point if a transition was detected for the 1960s and 1970s. For grid cells where the 1980s showed an abrupt change, the patterns of change in the average HW_f after these change-points were mixed but mainly decreased.

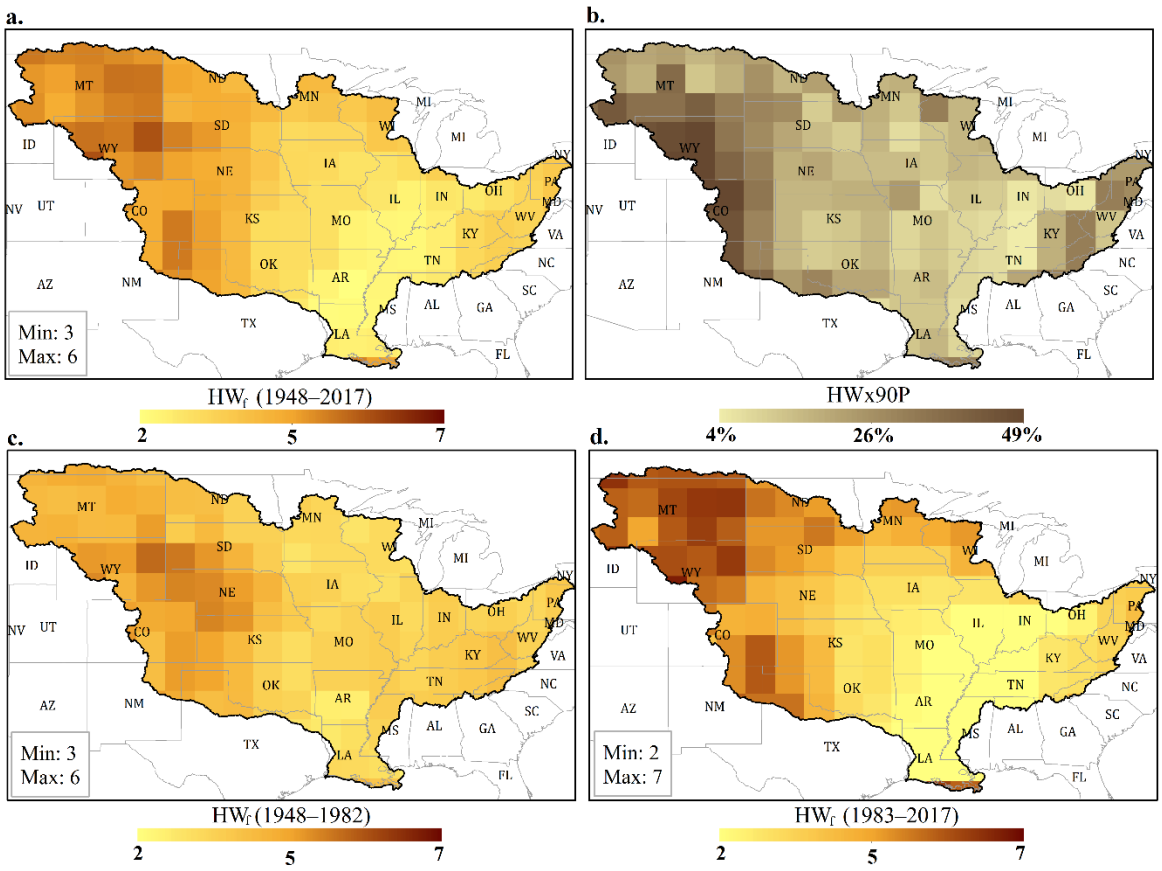

Figure 3-7. Spatial distribution of HW_f for 1948–2017 (a), the spatial distribution of HW_X90 for 1948-2017 (b), the spatial distribution of HW_f in the first 35-year period (1948–1982) (c) and the second 35-year period (1983–2017) (d).

Trend analysis of the entire period (1948–2017) documents an increasing trend for a majority of the grid cells (52%). However, only a few grid cells (5%) had significant upward trends (Figure 2-8b). Before the change-points at individual cells, a majority of the grid cells (87%; 57% significant) had downward trends (Figure 2-8c) and for the few grid cells with an upward trend, none of the trends were significant. After the change-points, a majority of the grid cells (80%; 11% significant) had an upward trend. However, some grid cells (20%; 5% significant) in central and western parts of the MRB had a downward trend (Figure 2-8d).

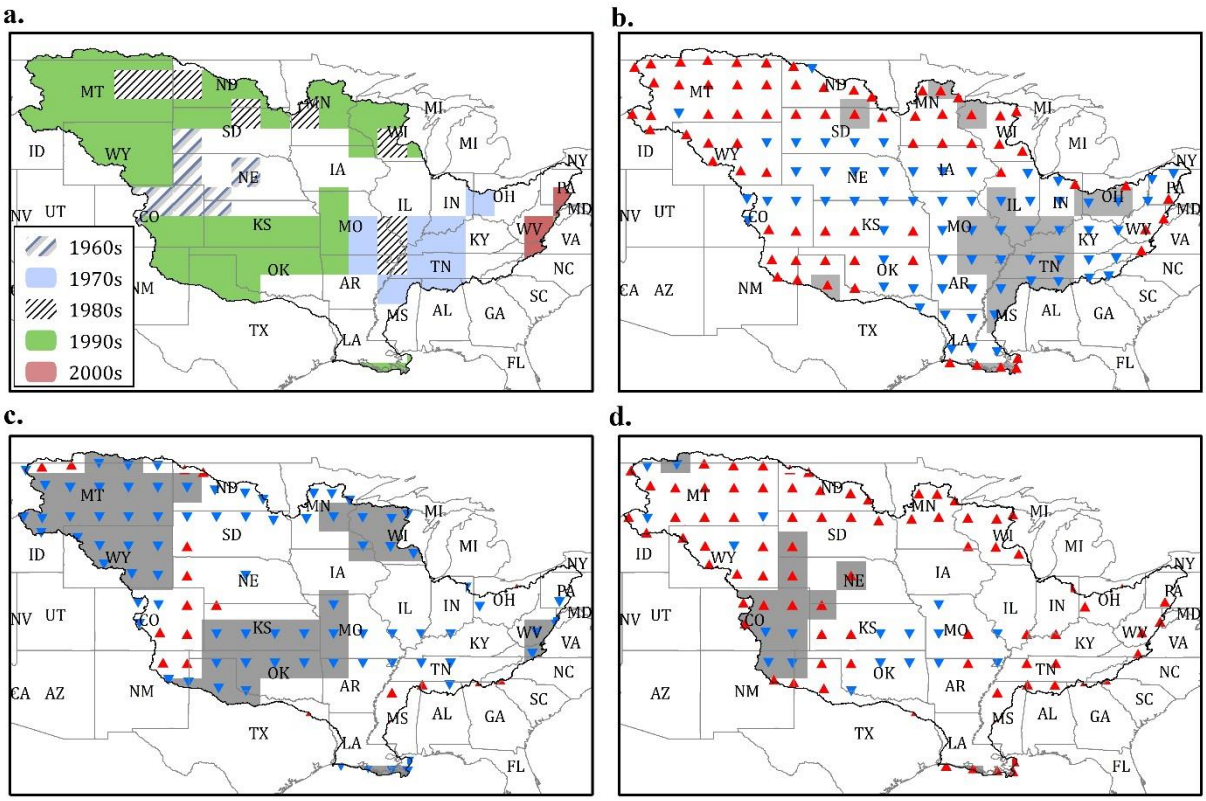

Figure 3-8. Change-point and trend analysis of HW_f in the MRB. Decade of occurrence for significant change-points (a), trend of HW_f for the entire period (1948–2017) (b), and for before (c) and after (d) the change-point for the grid cells that had a significant change-point. The upward (red) and downward (blue) triangles show positive and negative trends, respectively. The shaded areas indicate cells with significant trends. The regions with no triangle in plots (c) and (d) did not have a significant change-point.

Annual maximum length of HW (HWDI)

Previous studies clearly report the impact of HW duration on mortality rates (Díaz et al., 2002; Nakai et al., 1999). The length of a HW can be analyzed by applying different indices (Tavakol & Rahmani, 2018). HWDI, the length of the longest HW each year, was computed for each grid cell and analyzed to assess if this metric of duration has changed during the 70-year study period. The greatest value of HWDI (30 days) was found in southern Louisiana in both 2005 and 2011. However, in 1982 and 1993, almost 30% of MRB had no HW. A significant change-point was identified for nearly half of the grid cells (47%) in the MRB (Figure 2-9a).

When the change-point was significant, the decade of the 1990s was recognized as the critical period for 69% of grid cells. Most of the grid cells with a non-significant change-point are located in central and eastern parts of the MRB (Figure 2-9a). A majority (91%) of the grid cells with a significant change-point had a greater average length of HWDI after the change-point. Grid cells with a decrease in the average of HWDI after a significant change-point (9%) are located mainly in western parts of the MRB.

Trend analysis for the entire period (1948–2017) indicates a decrease in HWDI for a majority of the grid cells (64%). However, only a few cells had significant trends (21%) and for those that were significant, the trend was mainly downward (16%) (Figure 2-9b). Before the grid-based change-point (Figure 2-9c), a majority (95%) of grid cells had downward trends (83% significant). After the grid-based change-points (Figure 2-9d), 89% of grid cells with significant change-point showed upward trends (32% significant). Most of the gird cells with a significant upward trend were located within the western half of the MRB.

For each year, HWDI values were calculated for each grid cell and summarized for the seven decades (Table 2-2). Substantial areas of the MRB experienced a HWDI value greater than 10 consecutive days in 1980 (32%), 1953 (20%), and 2000 (18%). Except for HWDI values of 4-5 days, other lengths of HWDI had a statistically significant change-point. HWDI of 2-3 days and 6-7 days, had a decrease after the change-point of 1966. The percentage of MRB with HWDI of 8-10 days and greater than 10 days increased after 1997 and 1994 (change-points), respectively. These shifts in trends may impact the probability of having longer HWs in the future.

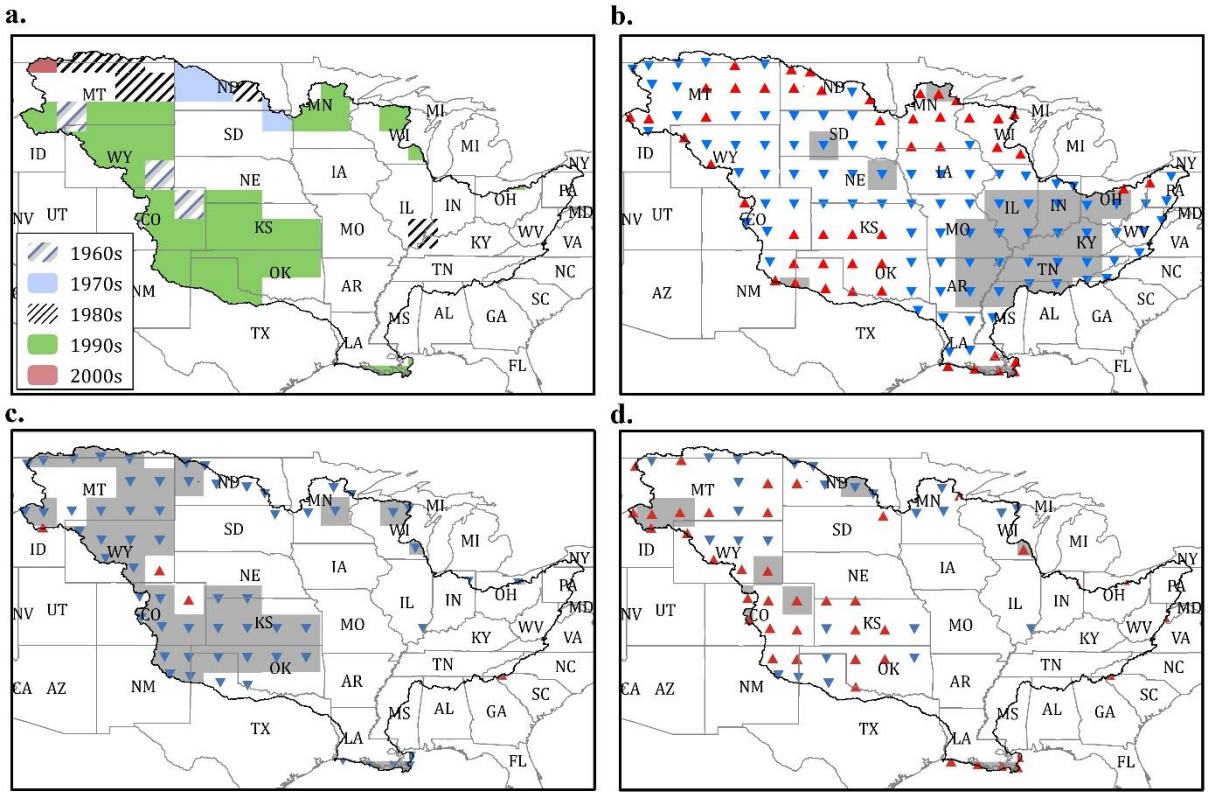

Figure 3-9. Spatial and temporal distribution of significant change-points (a), trends of HWDI for the entire period (1948–2017) (b) and for before (c) and after (d) the change-point for the grid cells that had a significant change-point. The upward (red) and downward (blue) triangles show positive and negative trends, respectively. The shaded areas show significant trends. The regions with no triangle in plots (c) and (d) did not have a significant change-point.

Other parameters, like increasing minimum temperature and the associated reduction in the diurnal temperature range, could result in a reduction in cooling/stress relief during the night and impact how warm the next day high temperature becomes (Miralles et al., 2014). The decadal analysis showed a higher percentage of the MRB experiencing a longer HWDI in the two decades at the beginning (1948–1967) and the two decades at the end of the study period (1998–2017; Table 2-2). 1998–2007 had the highest percentage for the MRB with HWDI values greater than 10 consecutive days. Maximum values of HWDI for the entire MRB have happened in two last decades in southern Louisiana.

Table 3-2. The statistics of HWDI (days) for the entire period of record and 10-year periods.

Period	Average of HWDIs (days)	Maximum of HWDIs (days)	Percentage of MRB with HWDI of				
			2-3 days	4-5 days	6-7 days	8-10 days	>10 days
1948–2017	4.4	30	34.8	33.5	14.5	7.5	3.0
1948–1957	5.3	19	20.7	34.7	22.6	12.3	5.3
1958–1967	4.7	19	28.4	38.8	16.1	10.5	2.4
1968–1977	3.6	12	45.7	35.3	8.9	3.0	0.1
1978–1987	3.6	24	48.1	24.5	9.1	2.7	3.6
1988–1997	3.6	19	47.5	27.9	9.2	5.5	0.7
1998–2007	5.0	30	26.6	34.1	17.4	10.8	5.5
2008–2017	4.9	30	26.6	39.3	18.5	7.6	3.6

Impact of teleconnections on HWs

Teleconnections may impact the changes of hot extremes in the MRB. In many parts of the world, the El Niño Southern Oscillation (ENSO) impacts both mean and extreme temperatures (Alexander, Lisa V. et al., 2009; Min et al., 2013). Analyzing a change-point for the data representing the entire MRB, the major change in TX90 (Figure 2-3) and HW_f (Figure 2-6) occurred in 1997, coincident with the major El Niño Event of 1997-1998 (Held, 2013). To study this possible teleconnection for the MRB, an index of tropical sea surface temperatures (the ONI), was analyzed. The ONI is a monthly index based on a 3-month moving average of SST values. To specify the El Niño years, the years when the average of ONI in three consecutive windows (including November–January, December–February, and January–March) was higher than 0.5 were identified (Murari et al., 2016; Yu et al., 2011). For an analysis involving annual data, ONI values were calculated using the first window (November–January) from the past year to the last window (January–March) of each year. As the ONI data starts in 1950, the analysis was run for 1951-2017. Comparing the distribution of the annual TX90 for El Niño years with

the remaining years for the entire MRB (Figure 2-10a) indicates that more grid cells experienced a larger count of of TX90 in El Niño years. A similar analysis of frequency histograms for HW_f (Figure 2-10b), and HWDI (Figure 2-10c) also show greater extremes for El Niño years.

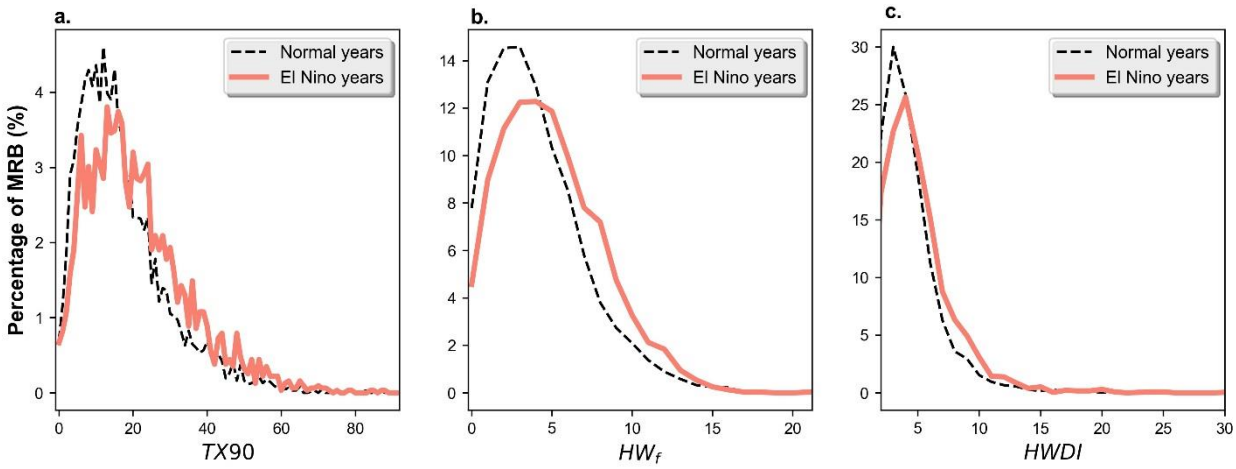

Figure 3-10. The percentage of the MRB covered by TX90 (a), HW_f (b), and HWDI (c) during normal and EL Niño years. The percentage of the MRB represents the fraction of the grid cells corresponding to values of the indices on the x-axis.

The present study suggests the probability of a link between El Niño conditions and hotter conditions in the following summer in the western parts of the MRB that increase the probability of a HW through feedback between dryness and temperature (Alexander, Lisa, 2011; Hirschi et al., 2011). However, the Kolmogorov–Smirnov test results indicated that the differences are not statistically significant.

Another prominent Earth system oscillation pattern is the NAO (Barnston & Livezey, 1987). Extreme negative NAO events tend to be associated with below-normal temperatures in the eastern United States (Barry & Hall-McKim, 2014). A similar analysis, as was done with El Niño, was done for the NAO. No specific impact from either phase of the NAO was detected for the study area.

Discussion

Hot temperatures and HWs are important climate extremes with extensive impacts on the economy, society, human and animal health, the environment, and agriculture (e.g. Schlenker & Roberts, 2009; White et al., 2006). In this study, historical changes in the hot days and HWs were analyzed in the MRB for 1948–2017 using available reanalysis data. Results show that the average TX was larger in 62% of the MRB mainly in western and north-western areas for the entire analysis period (1948–2017) compared to the reference period (1961–1990) (Figure 2-4). Grid-based analysis indicated the western and north-western areas of the MRB as hot spots where TX, TX90, and HW_f showed greater values in the second half of the period of study (Figures 2-4 and 2-7).

In addition, coastal locations in the southern MRB in Louisiana were one of the main hot spots with an increase in TX90 and HW_f after 1990 (Figures 2-4 and 2-7) and the largest recorded HWDI in MRB during 1948–2017 (Figure 2-9b). The subtropical characteristics of southern Louisiana and the influence of the Gulf of Mexico results in hot and humid summers in this area. Tropical maritime air from the Gulf of Mexico advected by southerly currents associated with the western Atlantic Subtropical High usually causes warm to hot summers (Henderson, 1994). The prominent impact of the regional subtropical circulation on warm days in the south-central United States (Henderson & Muller, 1997) may help explain the high frequency of hot extremes in southern Louisiana. The role of an increase in cloudiness and a lack of cooling at night associated with the advection of Gulf of Mexico moisture may influence the local weather extremes.

For the entire period, the years 2012, 1952, and 1954 had the hottest warm seasons with the greater HW_f and TX90. Based on a National Oceanic and Atmospheric Administration report

(NOAA, 2018), 2012 was the hottest year for the contiguous United States. During 2012, precipitation was below the United States precipitation average, producing a hot, dry year (NOAA, 2018). Previous studies addressing the mean daily temperature in the contiguous United States for the period 1895 to 2008 add to the findings of this study by reporting 1952, 1953, 1954, 1998 and 2000 as hot summers (e.g. Guttorp & Kim, 2013; Shen et al., 2012). However, it is important to recognize that the analysis of hot extremes is different than an analysis of average temperatures.

Results identify one decade at the beginning (1948–1957) and two decades at the end (1998–2017) of the analysis period as the hotter decades for the MRB (Figures 2-3 and 2-6). Previous analysis also had a peak in TX values in the 1950s, a major multi-year drought episode in the United States (DeGaetano & Allen, 2002; Diaz, 1983). The other four decades of this study had lower TX90 and HW_f. These findings agree with an earlier study where the 1960s had the fewest number of HWs (Peterson et al., 2013). During the period 1960–1996, data from a number of stations document an upward trend in the number of hot extremes for the eastern and central United States (DeGaetano & Allen, 2002).

Eastern areas of the MRB had the lowest occurrence of hot extremes and a significant downward trend in TX90 and HW_f. Oswald (2018) analyzed the gridded TX observations and found a similar pattern of HW change with the area of lowest HWs extending from the Great Plains toward the east to the Tennessee and Ohio valleys. This region with a very low occurrence of HW events corresponds with the existence of the “warming hole” in the United States (Meehl et al., 2012; Pan et al., 2004).

Western sections of the MRB have been recognized for a large variability in mean temperature (Mo, 2003) along with variations in summer soil moisture and evapotranspiration

(Huang et al., 1996; Koster & Suarez, 2003) which help explain a strong influence of land surface conditions on the air temperature. In addition, correlation analysis of Palmer Drought Severity Index (PDSI) and TX values indicates a strong impact of dry conditions on high temperature in Wyoming and Idaho (Alfaro et al., 2006), just to the west of the location where results from this study report the highest value of TX90s (Figure 2-4a).

Results from this study might serve as a warning for the probability of experiencing longer HWs over the larger area of MRB. Two decades in the beginning and two decades at the end of the study period reported the greatest number of HWs with a duration longer than 10 consecutive days. In the eastern MRB, at the same location where TX90 and HW_f showed a decrease, there was a significant downward trend in the HWDI. Lau et al (2012) applied reanalysis data as well as simulations by two general circulation models and showed considerable increases in the average duration of HW during the 21st century. They also reported the highest average HW duration in Central Gulf Coast extending into Texas and Oklahoma which is similar to the results of this study for the maximum length of HWs.

This study also examined the influence of El Niño teleconnections on the frequency and duration of HWs. Temporal analysis of ONI during 1950–2017 suggests some differences in the western MRB but revealed no statistically significant connection between HWs and El Niño years. Halpert and Ropelewski (1992) examined temperature teleconnections for North America for positive and negative phases of the Southern Oscillation. They found little evidence of an impact of tropical deviations during the warm season and much stronger relationships in the cold season, but for areas other than the MRB. Wolter et al. (1999) showed the same results during summer for the United States. A similar temporal disconnect was found between HWs and NAO in MRB.

Summary and Conclusion

While the nature of a HW may differ in southern compared to the northern, western, and north-western sections of the MRB, southern areas are among the most vulnerable regions to climate change, a result of having more HWs and upward trends in the frequency (Figure 2-7d and 2-8d). Hot days with TX higher than the 90^{th} percentile for the reference period (TX90) and hot events or heatwaves that last at least two consecutive TX90 (HW_f) were analyzed. Temporal analysis for entire MRB documents a downward trend for both TX90 and HW_f from 1948 to the change-point year (1997) and then a positive trend from 1997 to 2017. It is perhaps relevant that 1997 was a major El Niño event. A majority of grid cells had an increase in the average of TX90 (57%) and HW_f (75%) after the change-point. Hot extremes in the 1950s and in 2012 have an impact on the long-term temporal trends.

Considering the MRB with its high human population and density of farmlands and livestock, it is critical to know which areas may face a higher risk of hot extremes. Hotspots with an increasing risk of experiencing hot conditions were found in the southern Louisiana, western, and north-western areas of the MRB. Eastern sections of the MRB had a lower frequency of hot extremes and a decreasing trend from 1948 through 2017, which was significant for most of the grid cells. Results of this paper add to existing warnings about an increase in the frequency of HWs in the MRB and a need for adaptation to future changes in these hot climate extremes associated with ongoing global climate change (Hartmann et al., 2013; Trenberth et al., 2013).

References

Ahiablame, L., Sheshukov, A. Y., Rahmani, V., & Moriasi, D., 2017. Annual baseflow variations as influenced by climate variability and agricultural land use change in the Missouri River Basin. *Journal of Hydrology.* 551: 188-202. https://doi.org/10.1016/j.jhydrol.2017.05.055

Alexander, L. V., Zhang, X., Peterson, T. C., Caesar, J., Gleason, B., Tank, A. K., ..., and Rahimzadeh, F., 2006. Global observed changes in daily climate extremes of temperature and precipitation. *Journal of Geophysical Research: Atmospheres.* 111: https://doi.org/10.1029/2005JD006290

Alexander, L. 2011. Climate science. *Nature Geoscience.* 4: 12-13. https://doi.org/10.1038/ngeo1045

Alexander, L. V., Uotila, P., & Nicholls, N., 2009. Influence of sea surface temperature variability on global temperature and precipitation extremes. *Journal of Geophysical Research: Atmospheres.* 114: D18116. https://doi.org/10.1029/2009JD012301

Alfaro, E. J., Gershunov, A., & Cayan, D., 2006. Prediction of summer maximum and minimum temperature over the central and western United States: The roles of soil moisture and sea surface temperature. *Journal of Climate.* 19: 1407-1421. https://doi.org/10.1175/JCLI3665.1

Anandhi, A., Hutchinson, S., Harrington, J., Rahmani, V., Kirkham, M. B., & Rice, C. W., 2016. Changes in spatial and temporal trends in wet, dry, warm and cold spell length or duration indices in Kansas, USA. *International Journal of Climatology.* 36: 4085-4101.

Anderson, G. B.& Bell, M. L., 2011. Heat waves in the United States: mortality risk during heat waves and effect modification by heat wave characteristics in 43 US communities. *Environmental Health Perspectives.* 119: 210-218. http://doi.org/10.1289/ehp.1002313

Barnston, A. G., & Livezey, R. E., 1987. Classification, seasonality and persistence of low-frequency atmospheric circulation patterns. *Monthly Weather Review.* 115: 1083-1126. https://doi.org/10.1175/1520-0493(1987)1152.0.CO;2

Barriopedro, D., Fischer, E. M., Luterbacher, J., Trigo, R. M., & Garcia-Herrera, R., 2011. The hot summer of 2010: redrawing the temperature record map of Europe. *Science.* 332: 220-224. http://science.sciencemag.org/content/332/6026/220

Barry, R. G., & Hall-McKim, E. A., 2014. Essentials of the Earth's climate system. *Cambridge University Press.* Cambridge, UK. 214p.

Basu, R.& Samet, J. M., 2002. Relation between elevated ambient temperature and mortality: a review of the epidemiologic evidence. *Epidemiologic Reviews.* 24: 190-202. https://doi.org/10.1093/epirev/mxf007

Bromwich, D. H., & Fogt, R. L., 2004. Strong trends in the skill of the ERA-40 and NCEP–NCAR reanalysis in the high and mid-latitudes of the Southern Hemisphere, 1958–2001. *Journal of Climate.* 17: 4603-4619. https://doi.org/10.1175/3241.1

CDC. 1996. Heat wave related mortality-Milwaukee, Wisconsin, July 1995. *MMWR: Morbidity and Mortality Weekly Report.* 45: 505-507. https://www.cdc.gov/mmwr/preview/mmwrhtml/00042616.htm

Ceccherini, G., Russo, S., Ameztoy, I., Marchese, A. F., & Carmona-Moreno, C., 2017. Heat waves in Africa 1981-2015, observations and reanalysis. *Natural Hazards and Earth System Sciences.* 17: 115-125. http://dx.doi.org/10.5194/nhess-17-115-2017

Chen, L., Chen, X., Cheng, L., Zhou, P., & Liu, Z., 2019. Compound hot droughts over China: Identification, risk patterns and variations. *Atmospheric Research.* 227: 210-219. https://doi.org/10.1016/j.atmosres.2019.05.009

Clark, R. T., Brown, S. J., & Murphy, J. M., 2006. Modeling northern hemisphere summer heat extreme changes and their uncertainties using a physics ensemble of climate sensitivity experiments. *Journal of Climate.* 19: 4418-4435. https://doi.org/10.1175/JCLI3877.1

Coppola, D. P. 2006. Introduction to international disaster management. *Elsevier.* Boston, US. 696p.

Coumou, D., & Rahmstorf, S., 2012. A decade of weather extremes. *Nature climate change.* 2: 491-496. https://doi.org/10.1038/nclimate1452

DeGaetano, A. T., & Allen, R. J., 2002. Trends in twentieth-century temperature extremes across the United States. *Journal of Climate.* 15: 3188-3205. https://doi.org/10.1175/1520-0442(2002)0152.0.CO;2

Deryng, D., Conway, D., Ramankutty, N., Price, J., & Warren, R., 2014. Global crop yield response to extreme heat stress under multiple climate change futures. *Environmental Research Letters.* 9: 034011. https://doi.org/10.1088/1748-9326/9/3/034011

Diaz, H. F.1983. Drought in the United States. *Journal of Applied Meteorology and Climatology.* 22: 3-16. https://doi.org/10.1175/1520-0450(1983)0222.0.CO;2

Díaz, J., Jordan, A., García, R., López, C., Alberdi, J., Hernández, E., & Otero, A., 2002. Heat waves in Madrid 1986–1997: effects on the health of the elderly. *International Archives of Occupational and Environmental Health.* 75: 163-170. https://doi.org/10.1007/s00420-001-0290-4

Donat, M. G.& Alexander, L. V., 2012. The shifting probability distribution of global daytime and night-time temperatures. *Geophysical Research Letters.* 39: L14707. https://doi.org/10.1029/2012GL052459

Dunn, R. J., Willett, K. M., Parker, D. E., & Mitchell, L., 2016. Expanding HadISD: quality-controlled, sub-daily station data from 1931. *Geoscientific Instrumentation, Methods and Data Systems.* 5: 473-491. http://www.doi.org/10.5194/gi-5-473-2016

Dunn, R. J., Willett, K. M., Thorne, P. W., Woolley, E. V., Durre, I., Dai, A., ..., and Vose, R. E., 2012. HadISD: a quality-controlled global synoptic report database for selected variables at long-term stations from 1973--2011. *arXiv Preprint arXiv:1210.7191.* htpp://www.doi.org/10.5194/cp-8-1649-2012

Fathian, F., Dehghan, Z., Bazrkar, M. H., & Eslamian, S., 2016. Trends in hydrological and climatic variables affected by four variations of the Mann-Kendall approach in Urmia Lake basin, Iran. *Hydrological Sciences Journal.* 61: 892-904. https://doi.org/10.1080/02626667.2014.932911

Fischer, E. M.& Schär, C., 2010. Consistent geographical patterns of changes in high-impact European heatwaves. *Nature Geoscience.* 3: 398–403. https://doi.org/10.1038/ngeo866

Fischer, E. M., Seneviratne, S. I., Lüthi, D., & Schär, C., 2007. Contribution of land-atmosphere coupling to recent European summer heat waves. *Geophysical Research Letters.* 34: L06707. https://doi.org/10.1029/2006GL029068

Fouillet, A., Rey, G., Wagner, V., Laaidi, K., Empereur-Bissonnet, P., Le Tertre, A., ..., and De Crouy-Chanel, P., 2008. Has the impact of heat waves on mortality changed in France since the European heat wave of summer 2003? A study of the 2006 heat wave. *International Journal of Epidemiology.* 37: 309-317. https://doi.org/10.1093/ije/dym253

Frich, P., Alexander, L. V., Della-Marta, P., Gleason, B., Haylock, M., Tank, A., & Peterson, T., 2002. Observed coherent changes in climatic extremes during the second half of the twentieth century. *Climate research.* 19: 193-212. https://doi.org/10.3354/cr019193

Garcia-Herrera, R., Diaz, J., Trigo, R. M., Luterbacher, J., & Fischer, E. M., 2010. A review of the European summer heat wave of 2003. *Critical Reviews in Environmental Science and Technology.* 40: 267-306. https://doi.org/10.1080/10643380802238137

Goolsby, D. A. 2000. Mississippi basin nitrogen flux believed to cause Gulf hypoxia. *Eos, Transactions American Geophysical Union.* 81: 321-327. https://doi.org/10.1029/00EO00244

Guha-Sapir, D., Vos, F., Below, R., & Ponserre, S., 2012. Annual disaster statistical review 2011: the numbers and trends. *Centre for Research on the Epidemiology of Disasters.* Brussels, Belgium. http://www.cred.be/sites/default/files/ADSR_2011.pdf.

Guttorp, P., & Kim, T. Y., 2013. Uncertainty in ranking the hottest years of US surface temperatures. *Journal of Climate.* 26: 6323-6328. https://doi.org/10.1175/JCLI-D-12-00760.1

Habeeb, D., Vargo, J., & Stone, B., 2015. Rising heat wave trends in large US cities. *Natural Hazards.* 76: 1651-1665. https://link.springer.com/article/10.1007%2Fs11069-014-1563-z

Hahn, G. L. 1999. Dynamic responses of cattle to thermal heat loads. *Journal of Animal Science.* 77: 10-20. https://doi.org/10.2527/1997.77suppl_210x

Halpert, M. S.& Ropelewski, C. F., 1992. Surface temperature patterns associated with the Southern Oscillation. *Journal of Climate.* 5: 577-593. https://doi.org/10.1175/1520-0442(1992)0052.0.CO;2

Hamed, K. H. 2008. Trend detection in hydrologic data: the Mann–Kendall trend test under the scaling hypothesis. *Journal of Hydrology.* 349: 350-363. https://doi.org/10.1016/j.jhydrol.2007.11.009

Hartmann, D. L., Tank, A. M. K., Rusticucci, M., Alexander, L. V., Brnnimann, S., Charabi, Y. A. R., ..., and Kaplan, A., 2013. Observations: Atmosphere and surface. *In: Climate change 2013 the physical science basis: Working group I contribution to the fifth assessment report of the intergovernmental panel on climate change.* (pp. 159-254). Cambridge University Press. Cambridge, United Kingdom and New York, NY, USA.

Hatfield, J., G., Takle, R., Grotjahn, P., Holden, R. C., Izaurralde, T., Mader, E. M., & Liverman, D., 2014. Agriculture. *In: Climate change impacts in the united states: The third national climate assessment.* (pp. 150-174). U.S. Global Change Research Program. Washington, DC, USA.

Held, I. M. 2013. Climate science: The cause of the pause. *Nature.* 501: 318-319. https://doi.org/10.1038/501318a

Henderson, K. G. 1994. Variations in dew-point temperatures in the southern United States. *Physical Geography.* 15: 23-37. https://www.tandfonline.com/doi/abs/10.1080/02723646.1994.10642502

Henderson, K. G.& Muller, R. A., 1997. Extreme temperature days in the south-central United States. *Climate Research.* 8: 151-162. http://www.jstor.org/stable/24864637

Hirschi, M., Seneviratne, S. I., Alexandrov, V., Boberg, F., Boroneant, C., Christensen, O. B., ..., and Stepanek, P., 2011. Observational evidence for soil-moisture impact on hot extremes in southeastern Europe. *Nature Geoscience.* 4: 17-21. https://doi.org/10.1038/ngeo1032

Huang, J., Van Den Dool, Huug M, & Georgarakos, K. P., 1996. Analysis of model-calculated soil moisture over the United States (1931–1993) and applications to long-range temperature forecasts. *Journal of Climate.* 9: 1350-1362. https://doi.org/10.1175/1520-0442(1996)0092.0.CO;2

Kaiser, R., Le Tertre, A., Schwartz, J., Gotway, C. A., Daley, W. R., & Rubin, C. H., 2007. The effect of the 1995 heat wave in Chicago on all-cause and cause-specific mortality.

American Journal of Public Health. 97: 158-162. https://doi.org/10.2105/AJPH.2006.100081

Kalnay, E., Kanamitsu, M., Kistler, R., Collins, W., Deaven, D., Gandin, L., ..., and Woollen, J., 1996. The NCEP/NCAR 40-year reanalysis project. *Bulletin of the American Meteorological Society.* 77: 437-471. https://doi.org/10.1175/1520-0477(1996)0772.0.CO;2

Kendall, M. G. 1975. Rank Correlation Measures. *Charles Griffin.* London, UK. 202p.

Khan, N., Shahid, S., Juneng, L., Ahmed, K., Ismail, T., & Nawaz, N., 2019a. Prediction of heat waves in Pakistan using quantile regression forests. *Atmospheric Research.* 221: 1-11. https://doi.org/10.1016/j.atmosres.2019.01.024

Khan, N., Shahid, S., bin Ismail, T., & Wang, X., 2019b. Spatial distribution of unidirectional trends in temperature and temperature extremes in Pakistan. *Theoretical and Applied Climatology.* 136: 899-913. https://doi.org/10.1007/s00704-018-2520-7

Khan, N., Shahid, S., Ismail, T., Ahmed, K., & Nawaz, N., 2019c. Trends in heat wave related indices in Pakistan. *Stochastic Environmental Research and Risk Assessment.* 33: 287-302. https://doi.org/10.1007/s00477-018-1605-2

Klein Tank, A M G., Zwiers, F. W., & Zhang, X., 2009. Guidelines on analysis of extremes in a changing climate in support of informed decisions for adaptation. *Climate data and monitoring WCDMP-No. 72.* WMO-TD/No. 1500. https://www.ecad.eu/documents/WCDMP_72_TD_1500_en_1.pdf.

Klinenberg, E. 2015. Heat wave: A social autopsy of disaster in Chicago. *The University of Chicago Press.* London, UK and Chicago USA. 328p.

Koster, R. D., & Suarez, M. J., 2003. Impact of land surface initialization on seasonal precipitation and temperature prediction. *Journal of Hydrometeorology.* 4: 408-423. https://doi.org/10.1175/1525-7541(2003)42.0.CO;2

Kovats, R. S.& Hajat, S., 2008. Heat stress and public health: a critical review. *Annu.Rev.Public Health.* 29: 41-55. https://doi.org/10.1146/annurev.publhealth.29.020907.090843

Krzyżewska, A., Wereski, S., & Demczuk, P., 2019. Biometeorological conditions during an extreme heatwave event in Poland in August 2015. *Weather.* 99: 1-7. https://doi.org/10.1002/wea.3497

Liléo, S., Berge, E., Undheim, O., Klinkert, R., & Bredesen, R. E., 2013. Long-term correction of wind measurements. State-of-the-art, guidelines and future work. *Elforsk Report.* 13: 18.

Lobell, D. B., Hammer, G. L., McLean, G., Messina, C., Roberts, M. J., & Schlenker, W., 2013. The critical role of extreme heat for maize production in the United States. *Nature Climate Change.* 3: 497. https://doi.org/10.1038/nclimate1832

Lobell, D. B., Sibley, A., & Ortiz-Monasterio, J. I., 2012. Extreme heat effects on wheat senescence in India. *Nature Climate Change.* 2: 186. https://doi.org/10.1038/nclimate1356

Lyon, B.& Barnston, A. G., 2017. Diverse Characteristics of US Summer Heat Waves. *Journal of Climate.* 30: 7827-7845. https://doi.org/10.1175/JCLI-D-17-0098.1

Mann, H. B. 1945. Nonparametric tests against trend. *Econometrica: Journal of the Econometric Society.* 13: 245-259. http://www.jstor.org/stable/1907187

Mazdiyasni, O., & Aghakouchak, A., 2015. Substantial increase in concurrent droughts and heatwaves in the United States. *Proceedings of the National Academy of Sciences.* 112: 11484-11489. https://doi.org/10.1073/pnas.1422945112

Meehl, G. A., Arblaster, J. M., & Branstator, G., 2012. Mechanisms contributing to the warming hole and the consequent US east–west differential of heat extremes. *Journal of Climate.* 25: 6394-6408.

Meehl, G. A.& Tebaldi, C., 2004. More intense, more frequent, and longer lasting heat waves in the 21st century. *Science.* 305: 994-997. http://science.sciencemag.org/content/305/5686/994

Min, S., Cai, W., & Whetton, P., 2013. Influence of climate variability on seasonal extremes over Australia. *Journal of Geophysical Research: Atmospheres.* 118: 643-654. https://doi.org/10.1002/jgrd.50164

Miralles, D. G., Teuling, A. J., Van Heerwaarden, C. C., & de Arellano, J. V., 2014. Mega-heatwave temperatures due to combined soil desiccation and atmospheric heat accumulation. *Nature Geoscience.* 7: 345-349. https://doi.org/10.1038/ngeo2141

Mo, K. C.2003. Ensemble canonical correlation prediction of surface temperature over the United States. *Journal of Climate.* 16: 1665-1683. https://doi.org/10.1175/1520-0442(2003)0162.0.CO;2

Murari, K. K., Sahana, A. S., Daly, E., & Ghosh, S., 2016. The influence of the El Niño Southern Oscillation on heat waves in India. *Meteorological Applications.* 23: 705-713. https://doi.org/10.1002/met.1594

Nakai, S., Itoh, T., & Morimoto, T., 1999. Deaths from heat-stroke in Japan: 1968–1994. *International Journal of Biometeorology.* 43: 124-127. https://doi.org/10.1007/s004840050127

National Research Council. 2008. Mississippi River water quality and the Clean Water Act: progress, challenges, and opportunities. *National Academies Press.* Washington, DC. USA. 253p.

Nienaber, J. A.& Hahn, G. L., 2007. Livestock production system management responses to thermal challenges. *International Journal of Biometeorology.* 52: 149-157. https://doi.org/10.1007/s00484-007-0103-x

Nissan, H., Burkart, K., Coughlan de Perez, E., Van Aalst, M., & Mason, S., 2017. Defining and Predicting Heat Waves in Bangladesh. *Journal of Applied Meteorology and Climatology.* 56: 2653-2670. https://doi.org/10.1175/JAMC-D-17-0035.1

NOAA. (2018). State of the climate: National climate report for annual 2012. Retrieved from https://www.ncdc.noaa.gov/sotc/national/201213; 6/15/2018.

NOAA NCEI. (2019a). Billion-dollar weather and climate disasters. Retrieved from https://www.ncdc.noaa.gov/billions; 3/9/2019.

NOAA NCEI. (2019b). Billion-dollar weather and climate disasters: Table of events. Retrieved from https://www.ncdc.noaa.gov/billions/events; 7/1/2019.

Oswald, E. M. 2018. An Analysis of the Prevalence of Heat Waves in the United States between 1948 and 2015. *Journal of Applied Meteorology and Climatology.* 57: 1535-1549. https://doi.org/10.1175/JAMC-D-17-0274.1

Pan, Z., Arritt, R. W., Takle, E. S., Gutowski, W. J., Anderson, C. J., & Segal, M., 2004. Altered hydrologic feedback in a warming climate introduces a "warming hole". *Geophysical Research Letters.* 31: L17109. https://doi.org/10.1029/2004GL020528

Patz, J. A., Campbell-Lendrum, D., Holloway, T., & Foley, J. A., 2005. Impact of regional climate change on human health. *Nature.* 438: 310-317. https://doi.org/10.1038/nature04188

Perkins, S. E., & Alexander, L. V., 2013. On the measurement of heat waves. *Journal of Climate.* 26: 4500-4517. https://doi.org/10.1175/JCLI-D-12-00383.1

Perkins, S. E., Alexander, L. V., & Nairn, J. R., 2012. Increasing frequency, intensity and duration of observed global heatwaves and warm spells. *Geophysical Research Letters.* 39: n/a. https://doi.org/10.1029/2012GL053361

Perkins, S. E. 2015. A review on the scientific understanding of heatwaves—Their measurement, driving mechanisms, and changes at the global scale. *Atmospheric Research.* 164-165: 242-267. https://doi.org/10.1016/j.atmosres.2015.05.014

Peterson, T. C., Heim Jr, R. R., Hirsch, R., Kaiser, D. P., Brooks, H., Diffenbaugh, N. S., ..., and Karl, T. R., 2013. Monitoring and understanding changes in heat waves, cold waves, floods, and droughts in the United States: state of knowledge. *Bulletin of the American Meteorological Society.* 94: 821-834. https://doi.org/10.1175/BAMS-D-12-00066.1

Pryor, S. C., Scavia, D., Downer, C., Gaden, M., Iverson, L., Nordstrom, R., ..., and Robertson, G. P., 2014. Midwest. *In: Climate change impacts in the united states: The third national*

climate assessment. (pp. 418-440). U.S. Global Change Research Program. Washington, DC, USA.

Rabalais, N. N., Turner, R. E., Justić, D., Dortch, Q., Wiseman, W. J., & Gupta, B. K. S., 1996. Nutrient changes in the Mississippi River and system responses on the adjacent continental shelf. *Estuaries.* 19: 386-407. https://doi.org/10.2307/1352458

Rahmani, V.& Harrington Jr, J., 2018. Assessment of climate change for extreme precipitation indices: A case study from the central United States. *International Journal of Climatology.* https://doi.org/10.1002/joc.5858

Rahmani, V., Hutchinson, S. L., Harrington, J. A., & Hutchinson, J. M., 2016. Analysis of frequency and magnitude of extreme rainfall events with potential impacts on flooding: a case study from the central United States. *International Journal of Climatology.* 36: 3578-3587. https://doi.org/10.1002/joc.4577

Rahmani, V., Hutchinson, S. L., Harrington Jr, J. A., Hutchinson, J. M. S., & Anandhi, A., 2015. Analysis of temporal and spatial distribution and change- points for annual precipitation in Kansas, USA. *International Journal of Climatology.* 35: 3879-3887. https://doi.org/10.1002/joc.4252

Robinson, P. J. 2001. On the definition of a heat wave. *Journal of Applied Meteorology.* 40: 762-775. https://doi.org/10.1175/1520-0450(2001)0402.0.CO;2

Russo, S., Sillmann, J., & Sterl, A., 2017. Humid heat waves at different warming levels. *Scientific Reports.* 7: 7477. https://doi.org/10.1038/s41598-017-07536-7

Schlenker, W.& Roberts, M. J., 2009. Nonlinear temperature effects indicate severe damages to US crop yields under climate change. *Proceedings of the National Academy of Sciences.* 106: 15594-15598. https://doi.org/10.1073/pnas.0906865106

Seneviratne, S. I., Lthi, D., Litschi, M., & Schr, C., 2006. Land-atmosphere coupling and climate change in Europe. *Nature.* 443: 205-209. https://doi.org/10.1038/nature05095

Shen, S. S., Lee, C. K., & Lawrimore, J., 2012. Uncertainties, trends, and hottest and coldest years of US surface air temperature since 1895: An update based on the USHCN V2 TOB data. *Journal of Climate.* 25: 4185-4203. https://doi.org/10.1175/JCLI-D-11-00102.1

Shi, J., Cui, L., Ma, Y., Du, H., & Wen, K., 2018. Trends in temperature extremes and their association with circulation patterns in China during 1961–2015. *Atmospheric Research.* 212: 259-272. https://doi.org/10.1016/j.atmosres.2018.05.024

Smith, T. T., Zaitchik, B. F., & Gohlke, J. M., 2013. Heat waves in the United States: definitions, patterns and trends. *Climatic Change.* 118: 811-825. https://doi.org/10.1007/s10584-012-0659-2

Stocker, T. F. 2014. Climate change 2013: the physical science basis: Working Group I contribution to the Fifth assessment report of the Intergovernmental Panel on Climate Change. *Cambridge University Press.* Cambridge, United Kingdom and New York, NY, USA. 1308p.

Sun, Q., Miao, C., AghaKouchak, A., & Duan, Q., 2017. Unraveling anthropogenic influence on the changing risk of heat waves in China. *Geophysical Research Letters.* 44: 5078-85. https://doi.org/10.1002/2017GL073531

Tavakol, A., & Rahmani, V., 2018. Changes of heat wave duration in the Mississippi River Basin. In: *2018 ASABE Annual International Meeting*, Michigan, USA. https://doi.org/10.13031/aim.201801071.

Thornton, P. K., van de Steeg, J., Notenbaert, A., & Herrero, M., 2009. The impacts of climate change on livestock and livestock systems in developing countries: A review of what we know and what we need to know. *Agricultural Systems.* 101: 113-127. https://doi.org/10.1016/j.agsy.2009.05.002

Trenberth, K. E., Dai, A., Gerard Van, D. S., Jones, P. D., Barichivich, J., Briffa, K. R., & Sheffield, J., 2013. Global warming and changes in drought. *Nature Climate Change.* 4: 17-22. https://doi.org/10.1038/nclimate2067

Trenberth, K. E., & Fasullo, J. T., 2012. Climate extremes and climate change: The Russian heat wave and other climate extremes of 2010. *Journal of Geophysical Research: Atmospheres.* 117: D17103. https://doi.org/10.1029/2012JD018020

Turner, R. E.& Rabalais, N. N., 2003. Linking landscape and water quality in the Mississippi River basin for 200 years. *Bioscience.* 53: 563-572. https://doi.org/10.1641/0006-3568(2003)053[0563:LLAWQI]2.0.CO;2

White, M. A., Diffenbaugh, N. S., Jones, G. V., Pal, J. S., & Giorgi, F., 2006. Extreme heat reduces and shifts United States premium wine production in the 21st century. *Proceedings of the National Academy of Sciences.* 103: 11217-11222. https://doi.org/10.1073/pnas.0603230103

Wolter, K., Dole, R. M., & Smith, C. A., 1999. Short-term climate extremes over the continental United States and ENSO. Part I: Seasonal temperatures. *Journal of Climate.* 12: 3255-3272. https://doi.org/10.1175/1520-0442(1999)0122.0.CO;2

Yu, J., Kao, H., Lee, T., & Kim, S. T., 2011. Subsurface ocean temperature indices for Central-Pacific and Eastern-Pacific types of El Nino and La Nina events. *Theoretical and Applied Climatology.* 103: 337-344. https://doi.org/10.1007/s00704-010-0307-6

Zahid, M.& Rasul, G., 2012. Changing trends of thermal extremes in Pakistan. *Climatic Change.* 113: 883-896. https://doi.org/10.1007/s10584-011-0390-4

Chapter 4 - **Changes in the frequency of hot, humid days and nights in the Mississippi River Basin**

This chapter is a peer-reviewed publication in the *International Journal of Climatology* with the following citation: Tavakol, A.; Rahmani, V.; Harrington, J.Jr. (2020). Changes in the frequency of hot, humid days and nights in the Mississippi River Basin. *Int J Climatol*. 2020;1–16. https://doi.org/10.1002/joc.6484. This publication was granted permission to be included in this dissertation.

Introduction

Heatwaves (HWs) are among the top 10 deadliest natural disasters around the world (Guha-Sapir et al., 2012; Scheuren et al., 2007). Extreme impacts of HW on human health may be due to single extreme, consecutive extreme or non-extreme events (Field *et al.*, 2012) such as high temperatures (Oswald, 2018), high temperature and high humidity (Russo et al., 2017), high temperature and dry winds (Rahmani & Tavakol, 2019; Tavakol & Rahmani, 2019a), or high temperature and soil moisture deficit (Alexander, 2011; Hirschi *et al.*, 2011; Miralles *et al.*, 2014). For example, the HWs of 2003 in Europe and 2010 in Russia were intensified by soil moisture deficits (Miralles *et al.*, 2014) and resulted in approximately 40,000 and 55,000 fatalities, respectively (Barry & Hall-McKim, 2014). The HWs of Shanghai in 2003 and Chicago in 1995 are two examples of how the contribution of both relative humidity (RH) and maximum temperature (Russo et al., 2017) resulted in 258 and 600 excess deaths (Dematte et al., 1998; Huang et al., 2010). These HWs would not be considered severe based only on temperature (Russo et al., 2017). Exposing people to a combination of high humidity and temperatures above 35 $°C$ over an extended period can cause hyperthermia and possibly death (Bynum et al., 1978;

Pandolf & Goldman, 1977). A combination of extremely hot days and nights (Murage et al., 2017), extended HW duration (Tavakol & Rahmani, 2018), and high humidity (Russo et al., 2017; Tavakol & Rahmani, 2019b), may increase heat-related mortality (Changnon et al., 1996; Conti et al., 2005; Grize et al., 2005; Steadman, 1979; Trigo et al., 2009).

High humidity limits the ability of the human body to adapt to heat stress (Sherwood & Huber, 2010). Humidity is a well-established meteorological factor that impacts human, livestock, and plant health directly (Arundel et al., 1986; Barreca, 2012; Conti et al., 2005; Pierece, 1922; Wolkoff, 2018) and intensifies mortality and morbidity during a HW (Dematte et al., 1998; Palecki et al., 2001; Russo et al., 2017). Human bodies cool through evaporation of water (sweating) and exchange of heat (ventilation). High humidity limits the evaporative cooling process and increases heat stress (Noji, 1996). Normally, the human body tries to keep the core temperature constant by evaporation. Hot extremes present a condition that can exceed the human body's ability to cool through perspiration and evaporation. High humidity makes it more challenging as the surrounding air has a reduced capacity to accept more moisture.

Hot, humid conditions affect livestock by influencing their thermoregulation (Deshazer, 2009) and reduces livestock production (Fuquay, 1981; Morrison, 1983). In general, animals that gain weight faster or produce more milk are more susceptible because of their higher levels of metabolic heat production (Collier & Collier, 2011). In this way, heat extremes influence the United States' agricultural economy (St-Pierre et al., 2003). Genetic diversity among animals influences their sensitivity to the sultry conditions and, as a result, different temperature-humidity indices were introduced to characterize the influence of hot, humid stress on livestock breeds (Bohmanova et al., 2007).

Atmospheric near-surface moisture content can change with temperature, where the air can theoretically accommodate 7% more moisture per 1 °C of warming. The Clausius-Clapeyron relationship regulates the increase in atmospheric moisture that has occurred in the tropics and extra-tropics during summer over both land and ocean areas (Church *et al.*, 2013). A statistically significant increase in atmospheric moisture is linked to humans through increasing greenhouse gases, a global energy imbalance, and warmer ocean waters (Santer *et al.*, 2007). The fingerprint of global climate system change was found in the rise in wet bulb temperature since the late 20th century, increasing heat stress in most land regions (Knutson & Ploshay, 2016). In association with higher temperatures over land and ocean, specific humidity has increased since 1976 (Hartmann *et al.*, 2013). Willett *et al.* (2008) document a significant increase in specific humidity over the globe, the Northern Hemisphere, and the tropics between 1973 and 2003. Greater increases in specific humidity have occurred during the night rather than in the daytime across the United States (Gaffen & Ross, 1999). Global warming along with the increase of atmospheric moisture may intensify the compound hot, humid condition. Different indices can be used to analyze the simultaneous influence of temperature and humidity including wet bulb temperature, dew point temperature, apparent temperature, and a heat index. Analyzing changes in dew point during 1961–1990 (Robinson, 2000) and 1951–1990 (Gaffen & Ross, 1999) found a slight upward trend over most of the United States in winter, spring, and summer. While wet bulb temperature and dew point temperature are indices that specify the amount of moisture in the air, the Heat Index (HI) is, in contrast, a "feels-like" index (Knutson & Ploshay, 2016). A higher HI incorporates the effects of humidity in limiting evaporative cooling and making the temperature feel hotter than it actually is. HI conveys the non-linear nature of heat stress (Rothfusz, 1990).

Based on the IPCC reports, the increases in surface air temperature and surface humidity are projected to result in rises in HI values with a major impact on human comfort (Houghton *et al.*, 2002). A model scenario showed an increase of about 5 °C in July mean HI over the south-east United States by 2050 (Delworth et al., 1999). Analysis of summer (June, July, August) HI in the north-central United States (1979–2003) showed a pattern with dangerous HI values from the Central Plains toward mid-Mississippi River Valley (Rieck, 2014). Analysis of the changes in the United States in extreme HI or apparent temperature (using 85th percentile) for the period of 1949–1955 showed a greater increase in the frequency of extreme events at night especially in areas west of the continental divide and east of the Mississippi River (Gaffen & Ross, 1998). Kalkstein and Valimont (1986) developed a human weather stress index based on temperature and dew point and showed the highest frequency of extremes during July in the central and south-central United States.

Recent studies show that heat stress will increase in the 21st century, particularly when the effects of temperature and humidity are considered concurrently (Delworth et al., 1999; Knutson & Ploshay, 2016; Pal & Eltahir, 2016; Willett & Sherwood, 2012). Combined hot and humid conditions could limit outdoor physical activities (Obradovich & Fowler, 2017), and also increase the mortality rate with prolonged exposure to heat (Yip *et al.*, 2008). Globally, a larger increase in HI compared to air temperature is expected in the future especially in low latitudes under the high-emission scenario (Li *et al.*, 2018). In the United States, the highest frequency of the daily maximum HI is found in the southeast. For the period 1979–2011, HI increased in the northeast, southeast, and Midwest (Smith et al., 2013). These trends may be correlated with the boundary layer humidity, land surface moisture availability, greater vegetation coverage, and increased plant transpiration in these areas (Ford & Schoof, 2017; Hass et al., 2016; Ma et al.,

2018). Analysis of data from 10 stations near Knoxville, Tennessee, USA, showed higher HI values in regions with greater tree coverage (Hass *et al.*, 2016). Robinson (2001) defined a HW as at least 48 hours with a maximum and minimum HI higher than 103°F and 81°F, respectively and showed the greatest occurrence of events in central and south-central United States for 1951–1990. Using a combination of observed and reanalysis data, Lyon and Barnston (2017) analyzed the changes of extreme HI values using the 85^{th}, 90^{th}, and 95^{th} percentile thresholds and found an influence of HI definition on the spatial distribution of events.

Unlike previous studies that used the percentile threshold (Lyon & Barnston, 2017), shorter periods (Lyon & Barnston, 2017; Robinson, 2001; Smith et al., 2013), or analyzed only daytime HI (Smith et al., 2013), here, a longer period of data was used to analyze the variability of both daytime and nighttime extreme HI values using National Weather Services (NWS) fixed thresholds. Considering the documented increase of temperature and humidity in the United States (DeGaetano & Allen, 2002; Elliott & Angell, 1997; Gaffen & Ross, 1998; Gaffen & Ross, 1999; Hartmann et al., 2013; Karl et al., 1996), the interest was to investigate the hot spots, where the frequency of extremely hot, humid days and nights have increased over time. The selected study area has a population of approximately 100 million and is one of the most productive agricultural regions in the world. The goal of this paper is to evaluate the trends in maximum (daytime) and minimum (nighttime) extreme HI values in the Mississippi River Basin (MRB), USA, for the period 1948 to 2017 using NCEP/NCAR reanalysis data. In addition, the spatiotemporal changes of extreme temperature and extreme specific humidity (applying the 90^{th} percentile) are analyzed along with extreme HI events (applying the fixed thresholds).

Materials and Methods

Data

The National Centers for Atmospheric Prediction (NCEP) and the National Center for Atmospheric Research (NCAR) reanalysis products were used in this study. The NCEP/NCAR re-analysis provides the longest (1948–present) reanalysis data set of atmospheric parameters (Kalnay *et al.*, 1996) and is the most commonly used reanalysis data (Liléo *et al.*, 2013). NCEP/NCAR covers a longer period compared to the second generation of NCEP (NCEP/DOE Reanalysis 2; 1979–present) which makes it a better choice for long-term trend analysis.

Archived observations from weather stations, satellites, balloons, ships, and other sources are interpolated to help produce the reanalysis data. Scarce and unevenly observed humidity data encouraged the use of reanalysis humidity data to analyze trends in HI for the study area. Other studies of HI in the United States have also used the humidity data from a reanalysis (Lyon & Barnston, 2017; Smith et al., 2013). In this study, both temperature and specific humidity were obtained from NCEP/NCAR to get the same spatial resolution. Daily maximum and minimum temperature and 6-hourly specific humidity data at 2-meter height were obtained for 1948–2017 (70 years) from the surface flux level (www.esrl.noaa.gov/psd/data) provided at the global Gaussian T62 grid (192×94 grid points) with 1.9° latitude × 1.875° longitude resolution. RH data were obtained for 4-times daily with 2.5° latitude × 2.5° longitude global grid resolution. RH data were re-gridded to the same grid size as that of temperature and specific humidity using bilinear interpolation. RH data were obtained from the surface level (sigma 0.995) of NCEP/NCAR corresponding to an altitude of approximately 42.2 m above the ground (Liléo *et al.*, 2013). Similar to Smith *et al*. (2012), RH was considered constant vertically for combining with temperature to calculate the HI.

Study area

The MRB is one of the world's major river systems and is characterized by a diversity of land cover types and biological productivity. With an approximately 3.3 million Km^2 area, this basin covers about 41% of the contiguous United States (Turner & Rabalais, 2003) and parts of two Canadian provinces. With around 100 million people and a very high livestock population, the MRB is an ideal area for studying the impacts of hot, humid conditions.

The MRB has diverse climate conditions including subtropical lowlands in the south (near the Gulf of Mexico), temperate humid regions in the north-east (near the Great lakes), humid continental prairies in the north (North Dakota, South Dakota, and Minnesota), and semi-arid prairies in the north-west (Wyoming and Montana), and Rocky Mountains (Vining et al., 2013). Diverse climate of regions in the MRB means that annual precipitation can differ for each sub-region. The northern part of MRB may experience drought at the same time that southern regions are receiving precipitation from tropical systems (Vining et al., 2013). In addition to climate, land use varies widely across the MRB. A primary land use in the MRB is agriculture (58% cropland) and the area produces the majority of corn, wheat, soybean, hogs, chicken, and cattle in the United States (Goolsby, 2000). Land use of the MRB is dominated by intensive corn and soybean productions (David et al., 2010).

Methods

Indices

Six indicators of temperature, humidity, and HI were selected in order to study the changes in the frequency of extremely hot and/or humid events in the MRB (Table 3-1). The World Meteorological Organization (WMO) suggests 1961–1990 as a 30-year reference period to assess aspects of climate change (Klein Tank et al., 2009).

To specify extreme temperature and extreme specific humidity, the 90th percentile of the reference period (1961–1990) was considered as the threshold. The selection of the 90th percentile was based on the Intergovernmental Panel on Climate Change (IPCC) glossary (https://www.ipcc.ch/report/sr15/glossary/) and the WMO definition of extremes (WMO, 2016). The 90th percentile has been used to define extreme temperatures in previous studies (Ceccherini et al., 2017; Fischer et al., 2007; Fischer & Schär, 2010; Hirschi et al., 2011; Lyon, 2009; Perkins et al., 2012; Russo et al., 2017). Daily maximum and minimum temperature and specific humidity values were then compared to the identified daily thresholds that were calculated for each grid cell.

Although there are many heat stress indices that evaluate the combined effects of temperature and humidity (Havenith & Fiala, 2011), the HI has been developed by NWS and has categorized the human health symptoms related to any combination of temperature and humidity on human health (Ahrens & Samson, 2010; Havenith & Fiala, 2011). Calculation of HI values (Rothfusz, 1990; Steadman, 1979) was done using the National Oceanic and Atmospheric Administration (NOAA; http://www.wpc.ncep.noaa.gov/html/heatindex_equation.shtml) equation. Based on a multiple regression analysis, the equation (1) computes the heat index.

$$HI = C_1 + C_2T + C_3T^2 + RH(C_4 + C_5T + C_6T^2) + RH^2(C_7 + C_8T + C_9T^2) \quad (1)$$

Where HI is heat index ($°F$), T is temperature ($°F$), RH is humidity (%) and the coefficients are defined as C_1=-42.379, C_2=2.04901523, C_3=-0 .00683783, C_4=10.14333127, C_5=- 0.22475541, C_6=0.00122874, C_7=- 0.05481717, C_8=0.00085282, and C_9=-0.00000199.

If the RH is less than 13% and T is between 80 and 112 °F, adjusted HI (HI^*) would be calculated as followed:

$$HI^* = HI - \left(\frac{13 - RH}{4}\sqrt{\frac{17 - Abs(T - 95)}{17}}\right) \quad (2)$$

Where Abs is the absolute value. In addition, if RH is greater than 85% while the temperature is between 80 and 87 °F, adjusted HI (HI^*) would be calculated as followed:

$$HI^* = HI + \left(\frac{RH - 85}{10} * \frac{87 - T}{5}\right) \quad (3)$$

Furthermore, if the HI from the previous equations would result in a HI less than 80 °F, then equation (4) would be applied to calculate HI^*.

$$HI^* = 0.5\,(T + 61 + 1.2(T - 68) + 0.094RH) \quad (4)$$

The calculated HI values from equation 4 are consistent with Steadman's results.

Two HI values were calculated for each day. Maximum and minimum RH were available on a 6-hourly basis. From those four time steps each day, the maximum RH and minimum temperature were used to calculate the nighttime HI (minimum HI; HI_N) and the minimum RH and maximum temperature were used to calculate the daytime HI (maximum HI; HI_X) (St-Pierre et al., 2003).

The NWS excessive heat watch and warning system uses 40.6 ℃ (105 °F) and 26.7 ℃ (80 °F) as excessive HI daily and nightly threshold values, respectively (Robinson, 2001). These thresholds were used to identify the annual frequency of hot, humid days (HI_Xf) and hot, humid nights (HI_Nf).

Statistical tests

Three statistical tests were applied to detect a potential change in the six extreme indices. The distribution-free, non-parametric, and rank-based Pettitt test (Pettitt, 1979; Rahmani *et al.*, 2015) was used to detect any abrupt change (a change-point) in a time series. Second, the distribution-free Mann-Kendall test (Ahiablame et al., 2017; Kendall, 1975; Mann, 1945;

Rahmani & Harrington Jr, 2018) was used to recognize monotonic trends in the selected extreme indicators. This test was run for three-time windows: the entire period, before the change-point, and after the change-point. Third, a two-sample Kolmogorov-Smirnov (K-S) test (Massey Jr, 1951) was applied to assess the differences between the cumulative distribution functions (CDFs) of HI values for various time periods. K-S test is mainly sensitive to general distributional changes and not scale and location shifts (Sharkey & Killick, 2014). The same tests were run on both temperature and specific humidity data. A two-sided significant level of 0.05 was used for all parameters.

Table 4-1. Temperature, humidity, and HI extreme indices analyzed in this study.

Index	Definition	Units
$HI_{X}f$	Annual frequency of hot, humid days; Days with a HI greater than 40.6°*C*	Count of Days
$HI_{N}f$	Annual frequency of hot, humid nights; Nights with a HI greater than 26.7°*C*	Count of Nights
$T_{X}90$	Annual frequency of hot days; Days with a maximum temperature greater than the 90^{th} percentile.	Count of Days
$T_{N}90$	Annual frequency of hot nights; Nights with a minimum temperature greater than the 90^{th} percentile.	Count of Nights
$SH_{X}90$	Annual frequency of humid days; Days with a minimum specific humidity greater than the 90^{th} percentile.	Count of Days
$SH_{N}90$	Annual frequency of humid nights; Nights with a maximum specific humidity greater than the 90^{th} percentile.	Count of Nights

Results

Temporal changes in the extreme daily and nightly specific humidity (SH_X90, SH_N90), temperature (T_X90, T_N90) and concurrent humidity and temperature (HI_Xf, HI_Nf) were analyzed for the second half of the study period 1983–2017 relative to the first 35 years (1948–1982; Figure 3-1). Changes were calculated by dividing the index frequency in the more recent 35-yr period by

the frequency for the earlier 35-yr period. More pronounced changes were observed in specific humidity, with increases in both SH_X90 and SH_N90. Greater increases were observed in western MRB where average humidity is less than in other regions of the basin. Warmer regions in the MRB had larger increases in the humidity while northern areas with lower temperature had smaller increases (Figure 3-1c and 3-1f).

Comparing the two time periods, a greater increase was found in T_N90 for the majority of grid cells (99%) compared to the T_X90 (46%). Consistent with previous studies (Easterling et al., 1997; Hartmann et al., 2013; Vose et al., 2005)that showed greater rates of increase in the minimum temperature than maximum temperature at the global scale, our results demonstrated a greater increase in extremely hot nights (T_N90) rather than hot days (T_X90) in the MRB. Although the increase in the frequency of extreme temperature was prominent, a "warming hole" (Pan *et al.*, 2004) was observed in the central United States. The nocturnal southerly low-level jet advects more humid air northward over the central United States that is favorable for cloud development as well as mesoscale convective systems. These phenomena tend to decrease sensible heat and increase precipitation and soil moisture, which both contribute to the "warming hole" development (Pan *et al.*, 2004).

No HI_Nf (Figure 3-1d) were observed in the east, west, north, and north-west of the basin (over 48% of the MRB). Percentages determined for HI_Nf have been calculated using only grid cells with existent HI_Nf (Figure 3-1d). The largest counts of HI_Xf and HI_Nf were recorded in central and southern MRB, with a greater than a 100% increase in HI_Xf in the north and north-west of the MRB (Figure 3-1a). For HI_Nf, the greatest increase corresponds to the area of the low-level jet that brings maritime tropical air northward from the western Gulf of Mexico. West of the 98th meridian, there is usually not enough humidity for high HI values. Calculating the

correlation between the percentage of changes with non-parametric (Mann-Kendall and Spearman) methods (Helsel & Hirsch, 2002), increases of HI_Xf were positively correlated with the changes of T_X90 and the greatest increase occurred in the north-west and northern parts of the MRB.

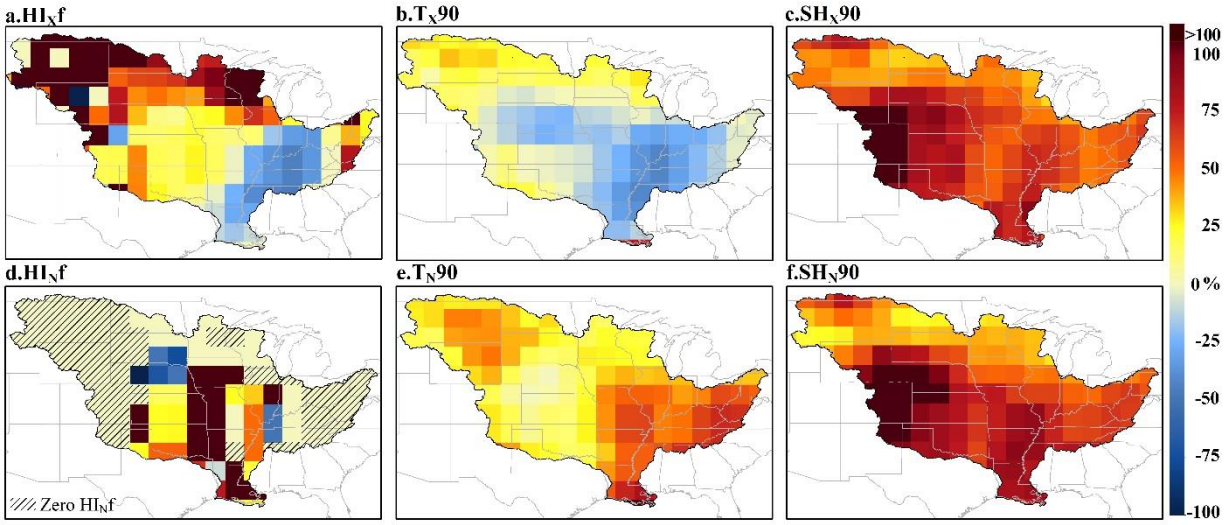

Figure 4-1. Percent change in the frequency of extreme events (calculated based on the difference in the number of extreme events in 1983–2017 relative to 1948–1982). Maps indicate the geography of changes in daytime maxima for HI_Xf (a), T_X90 (b), SH_X90 (c), and for extreme nighttime values in HI_Nf (d), T_N90 (e), and SH_N90 (f).

Analysis of 70-year average values of maximum and minimum HI, specific humidity and temperature (Figure 3-2) showed that spatial patterns of HI mirror the changes of temperature generally, and that an increase in humidity may intensify the HI, as evident in southern MRB (Figure 3-2c). The Gulf of Mexico is the main source of atmospheric moisture for the central United States and a sharp decline in specific humidity across Kansas and Nebraska corresponds to the 98th meridian (the westward extent of the Gulf of Mexico).

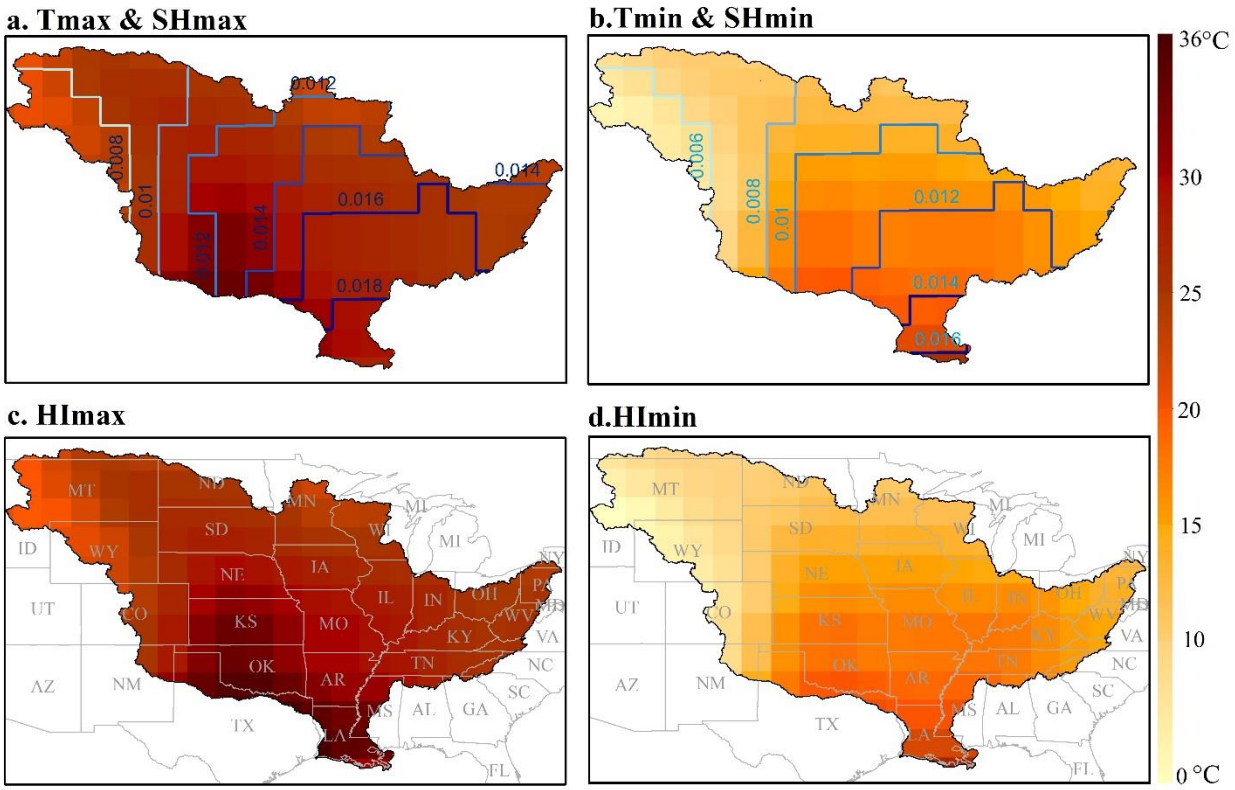

Figure 4-2. Spatial patterns of grid cell specific 70-year averages of the maximum and minimum of temperature (T °C) and heat index (HI °C) values for the warm season. Specific humidity maxima (a) and minima (b) contours are shown in Kg of vapor per Kg of air.

The Pettitt change-point detection test was used to investigate abrupt changes in extreme indices. These changes happened mainly in a 10-year period during the 1980s for the majority of grid cells for SH_X90 (84%), SH_N90 (86%), T_N90 (66%), HI_Xf (56%), and HI_Nf (67%). Decadal percentages were computed based on the number of grid cells with a shift during the ten-year interval. For T_X90, the majority of changes (55%) occurred in the 1990s. Abrupt changes in all indices may be related to the major El Niño events of 1982–83 and 1997–98 (Trenberth & Stepaniak, 2001) and the substantial warming of the oceans during the mid-1990s (Levitus *et al.*, 2000). Averages of the extreme indices showed an increase after the significant change-point for a majority of grids (Figure 3-3) for SH_X90 (100%), SH_N90 (100%), T_N90 (100%), T_X90 (60%), HI_Xf (93%), and HI_Nf (83%).

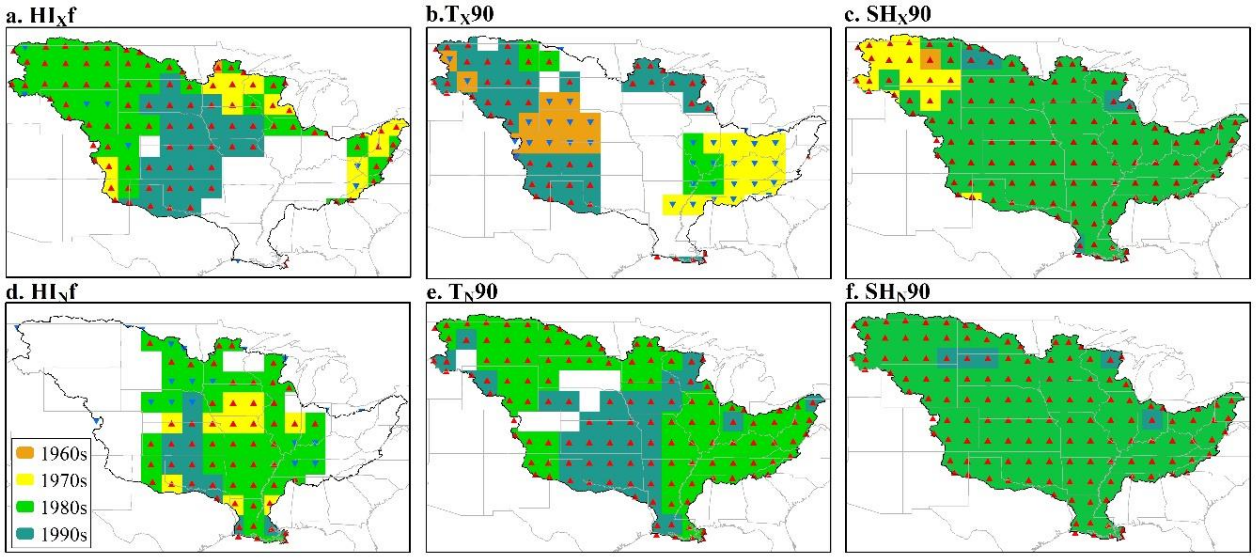

Figure 4-3. The changes in the frequency of extreme events after the significant change point for HIXf (a), TX90 (b), SHX90 (c), HINf (d), TN90 (e), and SHN90 (f). Colored grid cells show significant changes-points classified based on their decade of change. Red and blue triangles show if the number of extreme events was higher or lower after the change-point, respectively. Change-points mainly happened during the 1980s and 1990s.

The Mann-Kendall trend test was completed on the extreme indices in all grid cells for the entire period (1948–2017; Figure 3-4). An upward trend was observed in the majority of grid cells for SH_X90 (100%; 97% significant), SH_N90 (100%; 93% significant), T_N90 (97%; 72% significant), HI_Xf (63%; 16% significant), and HI_Nf (76%; 17% significant). For T_X90, a majority of grid cells mainly located in the eastern MRB had a downward trend (54%; 12% significant). Warm-season HI values increased faster than temperature as humidity has increased in all regions.

Analyzing the trends before and after change-points in grid cells with a significant abrupt change provided interesting results (Table 3-2, Figure 3-5 and 3-6). Before a change-point, the trend was downward for a majority of grids for SH_X90 (93%; 68% significant), SH_N90 (96%; 70% significant), T_X90 (90%; 54% significant), T_N90 (100%; 73% significant), and HI_Xf (81%; 27% significant). For HI_Nf, however, a majority of grid cells (82%; 24% significant) had an upward trend.

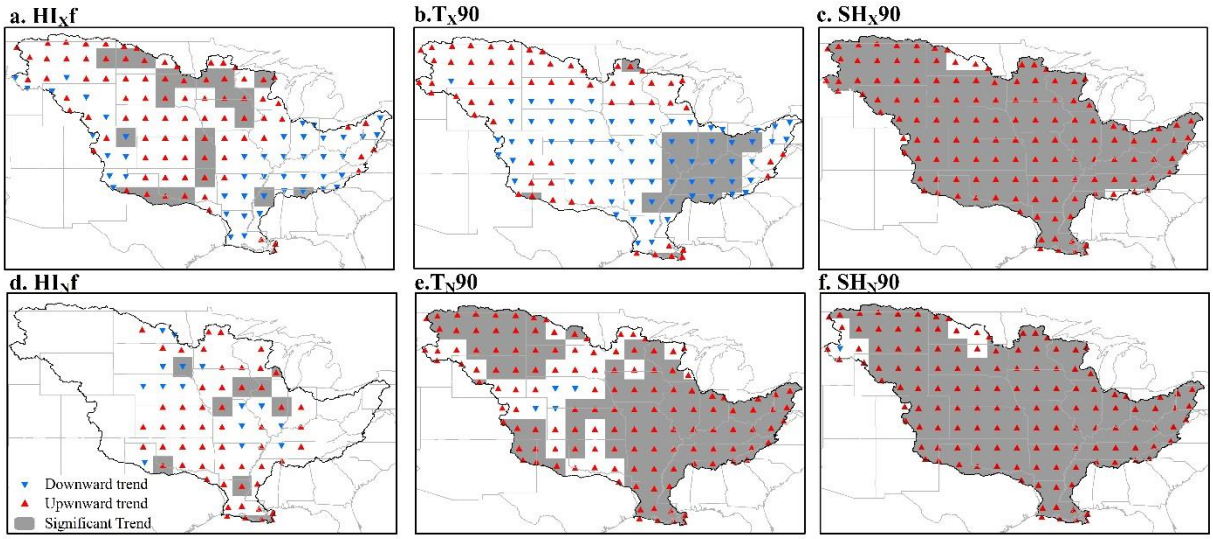

Figure 4-4. Mann-Kendall trend test results for the entire period (1948–2017). Red and blue triangles indicate upward and downward trends, respectively in HI_Xf (a), T_X90 (b), SH_X90 (c), HI_Nf (d), T_N90 (e), and SH_N90 (f). The highlighted regions had a statistically significant trend. The white regions in plot (d) show the grid cells with zero HI_Nf.

After the change-point, however, a majority of grid cells had an upward trend for SH_X90 (77%; 12% significant), SH_N90 (85%; 22% significant), T_X90 (89%; 20% significant), T_N90 (90%; 26% significant), and HI_Xf (54%; 5% significant). HI_Nf had a downward trend in a majority (52%; 18% significant) of grid cells. Previous studies found an increase in HI only in certain areas of the western and eastern United States during 1949–1995 (Gaffen & Ross, 1998). The results of this study indicate a significant upward trend for HI mostly for the grid cells in the central United States considering the whole period (Table 3-2). Eastern regions were different with a decrease in T_X90 and HI_Xf, suggesting a reduced risk of both maximum and minimum HI extremes.

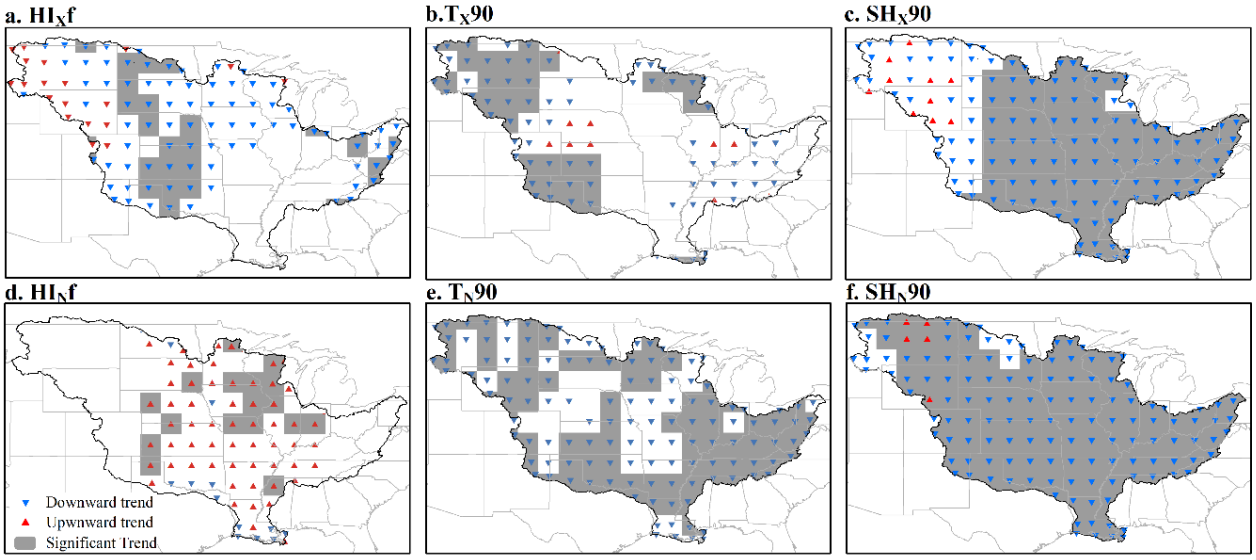

Figure 4-5. Analysis of Mann-Kendall trend test in MRB before the significant change-point. Red and blue triangles represent upward and downward trend in the HIXf (a), TX90 (b), SHX90 (c), HINf (d), TN90 (e), and SHN90 (f). The highlighted regions represent a significant trend. The white regions with no triangle had no significant change-point.

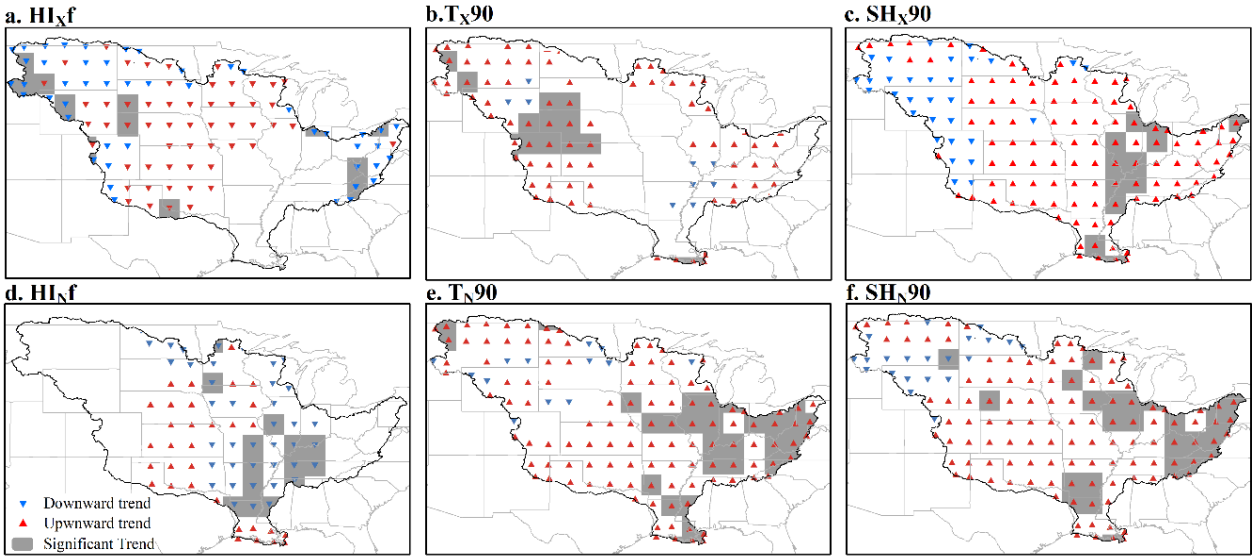

Figure 4-6. Analysis of Mann-Kendall trend test in the MRB after the significant change-point. Red and blue triangles represent upward and downward trends in the HIXf (a), TX90 (b), SHX90 (c), HINf (d), TN90 (e), and SHN90 (f). The highlighted regions represent a significant trend. The white regions with no triangle had no significant change-point.

Investigating the empirical cumulative distribution function (CDF) of the extreme indices for the two halves of the study period revealed a major change in humidity as well as minimum temperature and HI indicators for 1983–2017 (Figure 3-7). During the second 35-year period, the upper tail of the CDF (red line) has shifted to the right for SH_X90, HI_Nf , T_N90, and SH_N90 compared to 1948–1982 (blue line).

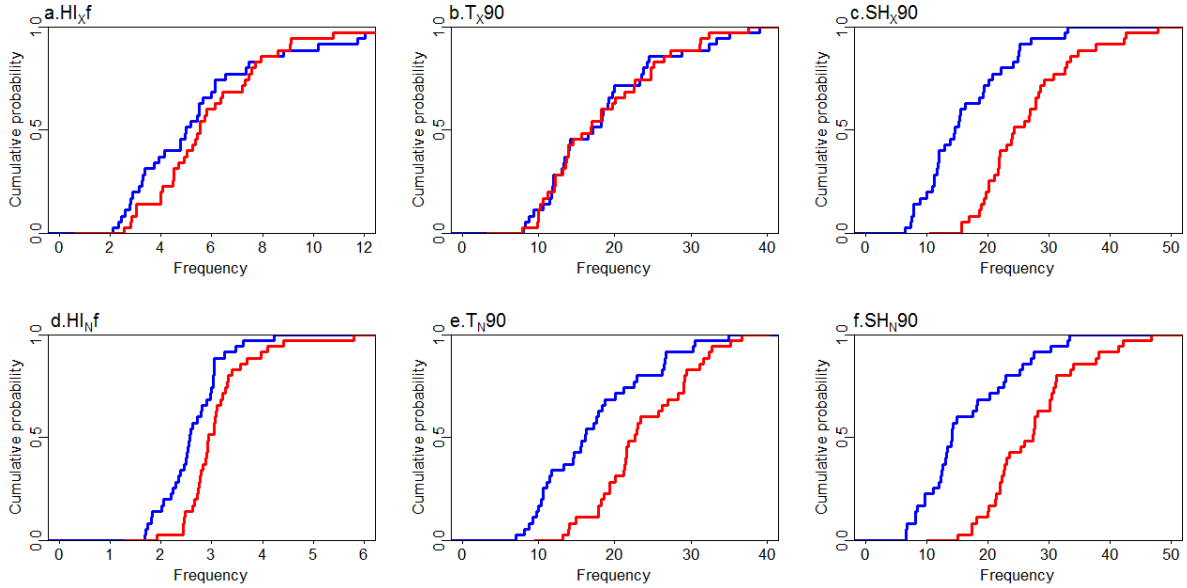

Figure 4-7. The empirical CDF of HI_Xf (a), T_X90 (b), SH_X90 (c), HI_Nf (d), T_N90 (e), and SH_N90 (f) for 1948–1982 (blue) and 1983–2017 (red). The x-axes represent the frequency of extreme indices in the MRB.

The two-sample K-S test confirmed these changes are significant with the 0.05 significance level (Table 3-3). Dividing the study period (1948-2017) into two 35-year periods showed the significant change during the second 35-year period, compared to 1948–1982, for 4%, 2%, 9%, 60%, 19%, and 17% of grid cells for HI_Xf, HI_Nf ,T_X90, T_N90, SH_X90, and SH_N90. The grid cells with a significant change are randomly distributed within the MRB. All grid cells with significant change (K-S test) in two 35-year periods showed a positive (increasing) change in the frequency of events. Except, 6% and 3% of grid cells that showed negative (decreasing) change for TX90 and SHX90, respectively.

Table 4-2. The percentage of the MRB with a significant change-point, as well as the upward and downward trends before and after change-points. Percentages were calculated in relation to the number of grid cells with significant change-point. The values in parentheses show the percentage of grid cells with a significant trend.

Indices	Trend 1948–2017 (%)		Significant Change-point (%)	Trend before the change-points (%)		Trend after the change-points (%)	
	Upward	Downward		Upward	Downward	Upward	Downward
HI_Xf	63 (16)	37 (2)	74	19 (1)	81 (27)	54 (5)	46 (12)
HI_Nf	76 (17)	24 (1)	50	82 (24)	18 (0)	48 (0)	52 (18)
T_X90	46 (4)	54 (12)	50	10 (0)	90 (54)	89 (20)	11 (0)
T_N90	97 (72)	3 (0)	77	0 (0)	100 (73)	90 (26)	10 (0)
SH_X90	100 (97)	0 (0)	61	7 (0)	93 (68)	77 (12)	23 (17)
SH_N90	100 (93)	0 (0)	94	4 (0)	96 (70)	85 (22)	15 (11)

Results of the K-S test reinforce the idea of warmer and more humid nights which are an indicator of ongoing climate change (Table 3-3, Figure 3-7e-f). Although Held (2013) suggested a pause in global atmospheric warming since 1999 by analyzing the global mean surface temperature, the results of this study show an increase in the frequency of extreme temperature events by analyzing maximum temperature in the MRB. Seneviratne *et al.* (2014) also found an increasing trend for extreme temperature events since 1997.

Table 4-3. Two-sample K-S test results for extreme indices in the MRB between 1948–1982 and 1983–2017. P-values smaller than 0.05 indicate that the two distributions are significantly different.

Indices	D-Statistic	*P*-value
HI_Xf	0.23	0.32
HI_Nf	0.43	0.00
T_X90	0.11	0.98
T_N90	0.49	0.00
SH_X90	0.60	0.00
SH_N90	0.60	0.00

Discussion

Global near-surface specific humidity has increased since the 1970s (Hartmann *et al.*, 2013) consistent with the trend of temperature (Peterson et al., 2011; Willett et al., 2008). Considering the fact that the warmer air has the energy to maintain more moisture in the gaseous state, specific humidity is expected to increase with warming (Dai, 2006; Willett *et al.*, 2008), but RH is expected to stay constant (Hartmann *et al.*, 2013). In the MRB, warmer regions had larger increases in specific humidity (Figure 3-1c and 3-1f). The increase in temperature and humidity will eventually modify the occurrence of extreme HI events in the MRB.

The highest HI_Xf and HI_Nf were found in southern and south-western areas of the MRB consistent with the results of previous studies (Lyon & Barnston, 2017; Robinson, 2001; Smith et al., 2013). Lyon and Barnston (2017) used daily temperature and humidity data and defined HW based on different durations (3-day and 5-day periods) when the HI is higher than either the 80^{th}, 90^{th}, or 95^{th} percentiles. The highest frequency of summer HWs was found in the west and the south-eastern United States. Although they considered percentile-based thresholds to define HWs with different durations, the southern MRB had the highest frequency of events with a decreasing pattern toward the northern MRB. The slight difference between the spatial patterns of results may be explained by the nature of the data and also the different periods of study. Smith *et al.* (2013) used fixed thresholds and calculated the number of days when the daytime HI exceeded 80 °F, 90 °F, 105 °F, or 130 °F. For lower thresholds (80 °F and 90 °F), extreme daytime HI extended from the central United States toward east. With an increase in threshold values, the area with a high frequency of extreme HI shrunk toward the southern MRB, and regions next to the Gulf of Mexico (Smith, Zaitchik, Gohlke, 2013). Applying the same fixed threshold (105 °F) as in this study, the highest annual frequency of extreme events from 1979–

2011 was found in southern MRB. Schoof *et al.* (2017) used one observed and four reanalysis products and analyzed HW changes using air temperature and equivalent temperature (temperature and specific humidity) over the period 1981–2015. While we found a downward trend in both T_X90 and HI_Xf in the eastern MRB (1948–2017), the regional analysis of hot, humid events (1981–2015) showed a negative trend in northern Plains (Schoof et al., 2017). The reason for the lack of agreement may be due to using different datasets, data periods, and applied indices to define oppressive (i.e., high temperature and high humidity) HWs.

Trend analysis documented the upward trend of HI_Xf in northern, central, and southwestern areas of the MRB. Overall, regions associated with the low-level jet extending from the Gulf of Mexico toward the central and northern MRB are more at the risk of hot and humid conditions and this finding is consistent with previous studies (Lyon & Barnston, 2017; Smith et al., 2013). Slight differences in the exact locations of upward trends in different studies may be explained with the different nature of the data sets used and the periods of study. Dividing the 70-year period (1948–2017) into two 35-year periods (1948–1982 and 1983–2017), reinforced the idea of warmer and more humid nights since 1983 (Figure 3-1 and 3-7).

To better understand the variations of HI_Xf and HI_Nf, the changes in extreme (higher than the 90^{th} percentile) temperature and specific humidity were analyzed in the MRB (Figure 3-4 and Table 3-2). Geographically, the regions located adjacent to the Gulf of Mexico have the highest level of specific humidity during summer (Figure 3-2) with a high and significant correlation between temperature and specific humidity (Gaffen & Ross, 1999) that explains the highest frequency of extreme HI. However, the long-term decrease of maximum temperature (significant) and HI (non-significant) identified in this research suggests that the eastern regions of the MRB are less at the risk of an extreme HI (Figure 3-4). Generally, the historical average

distribution of HI_Xf and HI_Nf had a pattern similar to the average maximum and minimum temperature and did not show a relationship with the geographical pattern of specific humidity (Figure 3-2). The highest frequencies of SH_X90 and SH_N90 were in southern MRB with a decreasing pattern toward the north-west. Both SH_X90 and SH_N90 had a significant upward trend (Figure 3-4) in a majority of the MRB consistent with IPCC and other previous studies (Brown & DeGaetano, 2013; Gaffen & Ross, 1999; Hartmann et al., 2013).

For temperature, the highest annual average frequency of T_X90 was captured in the western and north-western areas of the MRB. However, the highest average frequency of T_N90 was found in the southern and eastern sections of the MRB. There was a significant decrease in the frequency of T_X90 (Figure 3-3 and 3-4) consistent with previous studies that found the "warming hole" in the eastern MRB (Meehl et al., 2012; Pan et al., 2004) where more precipitation may reduce the maximum temperature (Donat *et al.*, 2013). Donat *et al*. (2013) analyzed the global changes of extreme temperature and precipitation indices and showed a downward trend in T_X90 over the period 1951–2010 in the central and eastern United States (eastern MRB). Similar to the findings from previous studies (Donat *et al.*, 2013; Hartmann *et al.*, 2013), results from this research showed that the minimum temperature extremes warmed significantly faster than the maximum temperature extremes. The trend was mostly positive for T_N90 grid cells with a few regions in central MRB showing a non-significant trend (Figure 3-4) that was consistent with previous studies (Hartmann *et al.*, 2013; Oswald, 2018). Oswald (2018) defined HWs based on minimum temperature and showed a significant positive trend over the United States except for regions in the central Great Plains. Donat *et al.* (2013) analyzed the trend of T_N90 over the period 1951–2010 and showed a significant positive trend over a majority of the United States except in eastern MRB. The slight difference in the geographical location of

the downward trend may be explained by using different data sets and study periods. Defining the extreme heat events based on both absolute and relative thresholds over the period of 1980–2016 produced an upward trend in the frequency of heat events in southern MRB (Sheridan & Lee, 2018).

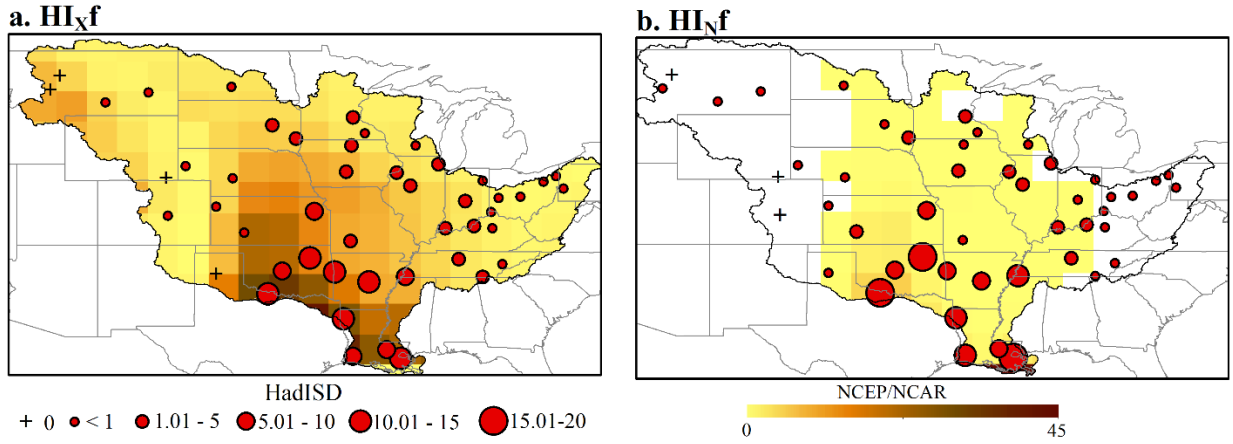

Figure 4-8. 70-year average of HI_Xf (a) and HI_Nf (b) based on NCEP/NCAR (background map) and HadISD (solid red circles). NCEP/NCAR overestimated the HI_Xf and underestimated the HI_Nf. The pattern of distribution is same for both data sets. The higher frequency of HI_Xf and HI_Nf are expected in the south and south-west MRB.

To discover the sensitivity of the results to the selected dataset, RH and temperature data were obtained from station-based, quality-controlled, sub-daily HadISD database (Dunn et al., (2016); https://www.metoffice.gov.uk/hadobs/hadisd/). HI was calculated for 48 stations in the MRB with less than 10% missing data. Calculated daily maximum and minimum HI values from HadISD observation data showed a good agreement with the HI values from NCEP/NCAR. The linear correlation showed acceptable association for maximum HI values between datasets ranging from R=0.62 (R^2=38%) in the south to R=0.78 (R^2=61%) in the northern MRB. For minimum HI, however, the correlation was stronger ranging from R=0.77 (R^2=59%) in the north-west and south to R=0.94 (R^2=88%) in the east MRB. Excluding the HI values lower than the fixed thresholds (40.6 °C for HI_X and 26.7 °C for HI_N) and eliminating the stations with zero

values higher than the thresholds, 58% and 48% of stations showed significant correlation for HI_X (R^2=0.50% to R^2=88%) and HI_N (R^2=1.70% to R^2=85%) between datasets, respectively.

Distributions of annual average HI_Xf and HI_Nf calculated from HadISD showed the same spatial pattern with the highest average number of events in the south and south-west of the MRB (Figure 3-8). However, results based on NCEP/NCAR overestimated the frequency of maximum HI and underestimated the number of average minimum HI events in the MRB. This finding might be due to the fact that NCEP/NCAR data provide only four data points per day (6-hourly) for RH which may not exactly represent the real minimum and maximum of RH in each day. Although reanalysis products have no missing data and cover complete periods of time, it is worth mentioning that changes in observational systems as well as model biases are their relative weak points (Berg et al., 2003; Bosilovich et al., 2011) that sometimes make the use of these data products unable to detect a realistic long-term trend (Trenberth, 2011).

Satellite observations are included in NCEP/NCAR reanalysis beginning in 1979. To check if the change-points identified in this study were biased with this observational system change, the Pettit test was used to analyze observation-based HI_Xf and HI_Nf values. The 1980s was the decade of abrupt change for a majority of the MRB based on both NCEP/NCAR (67%) and HadISD (42%). For HI_Xf, however, the abrupt change in a majority of the MRB was reported in the 1980s based on NCEP/NCAR (56%) and in the 1970s based on HadISD (63%). Other studies showed a robust agreement between the trends calculated based on observed and reanalysis temperature and humidity data (Schoof et al., 2017; Simmons et al., 2010).

Conclusion

Changes in extreme specific humidity (SH_X90, SH_N90), temperature (T_X90, T_N90) and concurrent humidity and temperature (HI_Xf, HI_Nf) were analyzed over the MRB during 1948–

2017. The 90th percentile of the reference period (1961–1990), calculated separately for each grid cell, were used as criteria to specify extreme humidity and temperature events. Results indicate a significant increase in SH_X90 and SH_N90 over the MRB with an upward trend either for the whole period or after the significant change-point. Analysis of extreme temperature indices revealed the probability of having more hot nights rather than hot days. Mesoscale atmospheric feedbacks may explain the decrease of both T_X90 and T_N90 in the central MRB.

For the combination of humidity and temperature, HI was calculated and the days and nights with a HI higher than 40.6° C and 26.7° C were considered as extreme events. For areas in the central and southern MRB, 52% of the grid cells had at least one HI_Nf during the 70-year study period. Many areas of the MRB showed no extreme nocturnal HI values. For HI_Xf, the highest frequency was observed in southern and central MRB, but greater changes in 1983–2017 compared to the baseline period (1948–1982) occurred in the north-west and northern sections of the MRB.

Change-point detection revealed an abrupt change in all indices during either the 1980s or1990s. Analyzing the distribution of extreme indices in two 35-year periods and applying the K-S test reinforced the idea of having hotter and more humid nights since the 1980s. Changes in the frequency and intensity of HI values, which are projected to increase as the result of continued summertime temperature and humidity rise, may adversely affect human health, agriculture, dairy cattle, and livestock production.

References

Ahiablame L, Sheshukov AY, Rahmani V, Moriasi D (2017) Annual baseflow variations as influenced by climate variability and agricultural land use change in the Missouri River Basin. *Journal of hydrology*, 551: 188-202. https://doi.org/10.1016/j.jhydrol.2017.05.055.

Ahrens CD, Samson PJ (2010) *Extreme weather and climate.* Cengage Learning. Belmont, CA, USA.

Alexander L (2011) Climate science: Extreme heat rooted in dry soils. *Nature Geoscience*, 4: 12-3. https://doi.org/10.1038/ngeo1045.

Arundel AV, Sterling EM, Biggin JH, Sterling TD (1986) Indirect health effects of relative humidity in indoor environments. *Environmental health perspectives*, 65: 351-61. www.doi.org/10.1289/ehp.8665351.

Barreca AI (2012) Climate change, humidity, and mortality in the United States. *Journal of Environmental Economics and Management*, 63: 19-34. https://doi.org/10.1016/j.jeem.2011.07.004.

Barry RG, Hall-McKim EA (2014) *Essentials of the Earth's climate system.* Cambridge University Press. Cambridge, UK.

Berg AA, Famiglietti JS, Walker JP, Houser PR (2003) Impact of bias correction to reanalysis products on simulations of North American soil moisture and hydrological fluxes. *Journal of Geophysical Research: Atmospheres*, 108: https://doi.org/10.1029/2002JD003334.

Bohmanova J, Misztal I, Cole JB (2007) Temperature-humidity indices as indicators of milk production losses due to heat stress. *Journal of dairy science*, 90: 1947-56. https://doi.org/10.3168/jds.2006-513.

Bosilovich MG, Robertson FR, Chen J (2011) Global energy and water budgets in MERRA. *Journal of Climate*, 24: 5721-39. https://doi.org/10.1175/2011JCLI4175.1.

Brown PJ, DeGaetano AT (2013) Trends in US surface humidity, 1930–2010. *Journal of Applied Meteorology and Climatology*, 52: 147-63. https://doi.org/10.1175/JAMC-D-12-035.1.

Bynum GD, Pandolf KB, Schuette WH, Goldman RF, Lees DE, Whang-Peng J, Atkinson ER, Bull JM (1978) Induced hyperthermia in sedated humans and the concept of critical thermal maximum. *American Journal of Physiology-Regulatory, Integrative and Comparative Physiology*, 235: R228-36. https://doi.org/10.1152/ajpregu.1978.235.5.R228.

Ceccherini G, Russo S, Ameztoy I, Marchese AF, Carmona-Moreno C (2017) Heat waves in Africa 1981-2015, observations and reanalysis. *Natural Hazards and Earth System Sciences*, 17: 115-25. http://dx.doi.org/10.5194/nhess-17-115-2017.

Changnon SA, Kunkel KE, Reinke BC (1996) Impacts and responses to the 1995 heat wave: A call to action. *Bulletin of the American Meteorological Society*, 77: 1497-506. https://doi.org/10.1175/1520-0477(1996)0772.0.CO;2.

Church JA, Clark PU, Cazenave A, Gregory JM, Jevrejeva S, Levermann A, Merrifield MA, Milne GA, Nerem RS, Nunn PD (2013) Sea Level Change. In: Anonymous *Climate Change 2013 the Physical Science Basis: Working Group I Contribution to the Fifth Assessment Report of the Intergovernmental Panel on Climate Change*. Cambridge, United Kingdom and New York, NY, USA: Cambridge University Press, 1137-1216.

Collier RJ, Collier JL (2011) *Environmental physiology of livestock.* John Wiley & Sons, Inc. New Jersey, USA.

Conti S, Meli P, Minelli G, Solimini R, Toccaceli V, Vichi M, Beltrano C, Perini L (2005) *Epidemiologic study of mortality during the Summer 2003 heat wave in Italy.* Cambridge Univ Press. Cambridge, UK.

Dai A (2006) Recent climatology, variability, and trends in global surface humidity. *Journal of Climate*, 19: 3589-606. https://doi.org/10.1175/JCLI3816.1.

David MB, Drinkwater LE, McIsaac GF (2010) Sources of nitrate yields in the Mississippi River Basin. *Journal of environmental quality*, 39: 1657-67. http://www.doi.org/10.2134/jeq2010.0115.

DeGaetano AT, Allen RJ (2002) Trends in twentieth-century temperature extremes across the United States. *Journal of Climate*, 15: 3188-205. https://doi.org/10.1175/1520-0442(2002)0152.0.CO;2.

Delworth TL, Mahlman JD, Knutson TR (1999) Changes in heat index associated with CO2-induced global warming. *Climatic Change*, 43: 369-86. https://doi.org/10.1023/A:1005463917086.

Dematte JE, O'mara K, Buescher J, Whitney CG, Forsythe S, McNamee T, Adiga RB, Ndukwu IM (1998) Near-fatal heat stroke during the 1995 heat wave in Chicago. *Annals of Internal Medicine*, 129: 173-81. .

Deshazer JA (2009) Basic principles of the thermal environment and livestock energetics. In: Anonymous *Livestock energetics and thermal environmental management*. MI, USA: American Society of Agricultural and Biological Engineers, 1-22.

Donat MG, Alexander LV, Yang H, Durre I, Vose R, Dunn R, Willett KM, Aguilar E, Brunet M, Caesar J (2013) Updated analyses of temperature and precipitation extreme indices since the beginning of the twentieth century: The HadEX2 dataset. *Journal of Geophysical Research: Atmospheres*, 118: 2098-118. http://www.doi.org/10.1002/jgrd.50150.

Dunn RJ, Willett KM, Parker DE, Mitchell L (2016) Expanding HadISD: quality-controlled, sub-daily station data from 1931. *Geoscientific Instrumentation, Methods and Data Systems*, 5: 473-91. http://www.doi.org/10.5194/gi-5-473-2016.

Easterling DR, Horton B, Jones PD, Peterson TC, Karl TR, Parker DE, Salinger MJ, Razuvayev V, Plummer N, Jamason P (1997) Maximum and minimum temperature trends for the globe. *Science*, 277: 364-7. https://doi.org/0.1126/science.277.5324.364.

Elliott WP, Angell JK (1997) Variations of cloudiness, precipitable water, and relative humidity over the United States: 1973–1993. *Geophysical Research Letters*, 24: 41-4. https://doi.org/10.1029/96GL03616.

Field CB, Barros V, Stocker TF, Dahe Q (2012) *IPCC 2012; Managing the risks of extreme events and disasters to advance climate change adaptation: special report of the intergovernmental panel on climate change.* Cambridge University Press. Cambridge, Uk and New York, NY, USA.

Fischer EM, Schär C (2010) Consistent geographical patterns of changes in high-impact European heatwaves. *Nature Geoscience*, 3: 398–403. https://doi.org/10.1038/ngeo866.

Fischer EM, Seneviratne SI, Lüthi D, Schär C (2007) Contribution of land-atmosphere coupling to recent European summer heat waves. *Geophysical Research Letters*, 34: L06707. https://doi.org/10.1029/2006GL029068.

Ford TW, Schoof JT (2017) Characterizing extreme and oppressive heat waves in Illinois. *Journal of Geophysical Research: Atmospheres*, 122: 682-98. https://doi.org/10.1002/2016JD025721.

Fuquay JW (1981) Heat Stress as it Affects Animal Production. *Journal of animal science*, 52: 164-74. https://doi.org/10.2527/jas1981.521164x.

Gaffen DJ, Ross RJ (1999) Climatology and trends of US surface humidity and temperature. *Journal of Climate*, 12: 811-28. https://doi.org/10.1175/1520-0442(1999)0122.0.CO;2.

Gaffen DJ, Ross RJ (1998) Increased summertime heat stress in the US. *Nature*, 396: 529-30. https://doi.org/10.1038/25030.

Goolsby DA (2000) Mississippi basin nitrogen flux believed to cause Gulf hypoxia. *Eos, Transactions American Geophysical Union*, 81: 321-7. https://doi.org/10.1029/00EO00244.

Grize L, Huss A, Thommen O, Schindler C, Braun-Fahrlander C (2005) Heat wave 2003 and mortality in Switzerland. *Swiss Medical Weekly*, 135: 200-5. https://doi.org/2005/13/smw-11009.

Guha-Sapir D, Vos F, Below R, Ponserre S (2012) Annual disaster statistical review 2011: the numbers and trends. *Centre for Research on the Epidemiology of Disasters (CRED)*http://www.cred.be/sites/default/files/ADSR_2011.pdf.

Hartmann DL, Tank AMK, Rusticucci M, Alexander LV, Brnnimann S, Charabi YAR, Dentener FJ, Dlugokencky EJ, Easterling DR, Kaplan A (2013) Observations: atmosphere and surface. In: Anonymous *Climate Change 2013 the Physical Science Basis: Working Group I Contribution to the Fifth Assessment Report of the Intergovernmental Panel on Climate Change*. Cambridge, United Kingdom and New York, NY, USA: Cambridge University Press, 159-254.

Hass A, Ellis K, Reyes Mason L, Hathaway J, Howe D (2016) Heat and humidity in the city: neighborhood heat index variability in a mid-sized city in the southeastern United States. *International journal of environmental research and public health*, 13: 117. https://doi.org/10.3390/ijerph13010117.

Havenith G, Fiala D (2011) Thermal indices and thermophysiological modeling for heat stress. *Comprehensive Physiology*, 6: 255-302. https://doi.org/10.1002/cphy.c140051.

Held IM (2013) Climate science: The cause of the pause. *Nature*, 501: 318-9. https://doi.org/10.1038/501318a.

Helsel DR, Hirsch RM (2002) *Statistical methods in water resources.* Techniques of Water Resources Investigations of the United States Geological Survey (2002). .

Hirschi M, Seneviratne SI, Alexandrov V, Boberg F, Boroneant C, Christensen OB, Formayer H, Orlowsky B, Stepanek P (2011) Observational evidence for soil-moisture impact on hot extremes in southeastern Europe. *Nature Geoscience*, 4: 17-21. https://doi.org/10.1038/ngeo1032.

Houghton JT, Ding DJ, Griggs M, Noguer PJ, van der Linden X, Dai KM, Johnson CA (2002) *Climate change 2001: the scientific basis. Contribution of Working Group 1 to the Third Assessment Report of the Intergovernmental Panel on Climate Change.* Cambridge University Press. Cambridge, United Kingdom and New York, NY, USA.

Huang W, Kan H, Kovats S (2010) The impact of the 2003 heat wave on mortality in Shanghai, China. *Science of the total environment*, 408: 2418-20. https://doi.org/10.1016/j.scitotenv.2010.02.009.

Kalkstein LS, Valimont KM (1986) An evaluation of summer discomfort in the United States using a relative climatological index. *Bulletin of the American Meteorological Society*, 67: 842-8. https://doi.org/10.1175/1520-0477(1986)0672.0.CO;2.

Kalnay E, Kanamitsu M, Kistler R, Collins W, Deaven D, Gandin L, Iredell M, Saha S, White G, Woollen J (1996) The NCEP/NCAR 40-year reanalysis project. *Bulletin of the American Meteorological Society*, 77: 437-71. https://doi.org/10.1175/1520-0477(1996)0772.0.CO;2.

Karl TR, Knight RW, Easterling DR, Quayle RG (1996) Indices of climate change for the United States. *Bulletin of the American Meteorological Society*, 77: 279-92. https://doi.org/10.1175/1520-0477(1996)0772.0.CO;2.

Kendall MG (1975) *Rank Correlation Measures.* Charles Griffin. London, UK.

Klein Tank, A M G, Zwiers FW, Zhang X (2009) Guidelines on analysis of extremes in a changing climate in support of informed decisions for adaptation56. https://www.ecad.eu/documents/WCDMP_72_TD_1500_en_1.pdf.

Knutson TR, Ploshay JJ (2016) Detection of anthropogenic influence on a summertime heat stress index. *Climatic Change*, 138: 25-39. https://doi.org/10.1007/s10584-016-1708-z.

Levitus S, Antonov JI, Boyer TP, Stephens C (2000) Warming of the world ocean. *Science*, 287: 2225-9. https://doi.org/10.1126/science.287.5461.2225.

Li J, Chen YD, Gan TY, Lau N (2018) Elevated increases in human-perceived temperature under climate warming. *Nature Climate Change*, 8: 43. https://doi.org/10.1038/s41558-017-0036-2.

Liléo S, Berge E, Undheim O, Klinkert R, Bredesen RE (2013) Long-term correction of wind measurements. State-of-the-art, guidelines and future work. *Elforsk report*, 13: 18. .

Lyon B (2009) Southern Africa summer drought and heat waves: Observations and coupled model behavior. *Journal of Climate*, 22: 6033-46. .

Lyon B, Barnston AG (2017) Diverse Characteristics of US Summer Heat Waves. *Journal of Climate*, 30: 7827-45. https://doi.org/10.1175/JCLI-D-17-0098.1.

Ma S, Pitman A, Yang J, Carouge C, Evans JP, Hart M, Green D (2018) Evaluating the effectiveness of mitigation options on heat stress for Sydney, Australia. *Journal of applied meteorology and climatology*, 57: 209-20. https://doi.org/10.1175/JAMC-D-17-0061.1.

Mann HB (1945) Nonparametric tests against trend. *Econometrica: Journal of the Econometric Society*, 13: 245-59. http://www.jstor.org/stable/1907187.

Massey Jr FJ (1951) The Kolmogorov-Smirnov test for goodness of fit. *Journal of the American statistical Association*, 46: 68-78. .

Meehl GA, Arblaster JM, Branstator G (2012) Mechanisms contributing to the warming hole and the consequent US east–west differential of heat extremes. *Journal of Climate*, 25: 6394-408. https://doi.org/10.1175/JCLI-D-11-00655.1.

Miralles DG, Teuling AJ, Van Heerwaarden CC, de Arellano JV (2014) Mega-heatwave temperatures due to combined soil desiccation and atmospheric heat accumulation. *Nature Geoscience*, 7: 345-9. https://doi.org/10.1038/ngeo2141.

Morrison SR (1983) Ruminant heat stress: effect on production and means of alleviation. *Journal of animal science*, 57: 1594-600. https://doi.org/10.2527/jas1983.5761594x.

Murage P, Hajat S, Kovats RS (2017) Effect of night-time temperatures on cause and age-specific mortality in London. *Environmental Epidemiology*, 1: e005. Http://www.doi.org/10.1097/EE9.0000000000000005.

Noji EK (1996) *The public health consequences of disasters.* Oxford University Press. New York, USA.

Obradovich N, Fowler JH (2017) Climate change may alter human physical activity patterns. *Nature Human Behaviour*, 1: 0097. https://doi.org/10.1038/s41562-017-0097.

Oswald EM (2018) An Analysis of the Prevalence of Heat Waves in the United States between 1948 and 2015. *Journal of Applied Meteorology and Climatology*, 57: 1535-49. https://doi.org/10.1175/JAMC-D-17-0274.1.

Pal JS, Eltahir EA (2016) Future temperature in southwest Asia projected to exceed a threshold for human adaptability. *Nature Climate Change*, 6: 197-200. https://doi.org/10.1038/nclimate2833.

Palecki MA, Changnon SA, Kunkel KE (2001) The nature and impacts of the July 1999 heat wave in the midwestern United States: learning from the lessons of 1995. *Bulletin of the American Meteorological Society*, 82: 1353-68. https://doi.org/10.1175/1520-0477(2001)0822.3.CO;2.

Pan Z, Arritt RW, Takle ES, Gutowski WJ, Anderson CJ, Segal M (2004) Altered hydrologic feedback in a warming climate introduces a "warming hole". *Geophysical Research Letters*, 31: L17109. https://doi.org/10.1029/2004GL020528.

Pandolf KB, Goldman RF (1977) The convergence of skin and rectal temperatures as a criterion for heat tolerance. *The convergence of skin and rectal temperatures as a criterion for heat tolerance*, 49: 1095–1101. http://www.dtic.mil/dtic/tr/fulltext/u2/a050260.pdf.

Perkins SE, Alexander LV, Nairn JR (2012) Increasing frequency, intensity and duration of observed global heatwaves and warm spells. *Geophysical Research Letters*, 39: n/a. https://doi.org/10.1029/2012GL053361.

Peterson TC, Willett KM, Thorne PW (2011) Observed changes in surface atmospheric energy over land. *Geophysical Research Letters*, 38: https://doi.org/10.1029/2011GL048442.

Pettitt AN (1979) A non-parametric approach to the change-point problem. *Journal of the Royal Statistical Society*, 28: 126-35. http://www.jstor.org/stable/2346729.

Pierece W (1922) Air-Conditioning, Longevity, and Health. *The Nation's Health*, 4: 563-6. https://books.google.com/books?id=EG0D3QSusxAC&pg=PA563&lpg=PA563&dq=%22+humidity%22++%2B+%22health+factor%22&source=bl&ots=INXKtpAEkr&sig=ACfU3U1AnBJvkP0mBD2KnOnU_L6-jgEARw&hl=en&sa=X&ved=2ahUKEwj3voj08qjkAhVOM6wKHWIMDgQQ6AEwDXoECAcQAg#v=onepage&q&f=false.

Rahmani V, Tavakol A (2019) Spatiotemporal Changes of Correlated Hot, Dry, and Windy Conditions in the Central United States. *AGU*. December 2019. San Francisco, CA, USA. https://agu.confex.com/agu/fm19/meetingapp.cgi/Paper/594147.

Rahmani V, Harrington Jr J (2018) Assessment of climate change for extreme precipitation indices: A case study from the central United States. *International Journal of Climatology*https://doi.org/10.1002/joc.5858.

Rahmani V, Hutchinson SL, Harrington Jr JA, Hutchinson JMS, Anandhi A (2015) Analysis of temporal and spatial distribution and change- points for annual precipitation in Kansas, USA. *International Journal of Climatology*, 35: 3879-87. https://doi.org/10.1002/joc.4252.

Rieck T (2014) Heat index climatology for the north-central United States. *http://www.crh.noaa.gov/crh/ssd/pdf/tsp_17.pdf and accessed on November*, 15: 2014. https://mrcc.illinois.edu/living_wx/heatwaves/HeatIndexClim-tsp17-Rieck.pdf.

Robinson PJ (2001) On the definition of a heat wave. *Journal of Applied Meteorology*, 40: 762-75. https://doi.org/10.1175/1520-0450(2001)0402.0.CO;2.

Robinson PJ (2000) Temporal trends in United States dew point temperatures. *International Journal of Climatology: A Journal of the Royal Meteorological Society*, 20: 985-1002. https://doi.org/10.1002/1097-0088(200007)20:93.0.CO;2-W.

Rothfusz LP (1990) The heat index equation (or, more than you ever wanted to know about heat index), 9023: 2. .

Russo S, Sillmann J, Sterl A (2017) Humid heat waves at different warming levels. *Scientific Reports*, 7: 7477. https://doi.org/10.1038/s41598-017-07536-7.

Santer BD, Mears C, Wentz FJ, Taylor KE, Gleckler PJ, Wigley T, Barnett TP, Boyle JS, Bruggemann W, Gillett NP (2007) Identification of human-induced changes in atmospheric moisture content. *Proceedings of the National Academy of Sciences*, 104: 15248-53. https://doi.org/10.1073/pnas.0702872104.

Scheuren JM, de Waroux, O le Polain, Below R, Guha-Sapir D, Ponserre S (2007) Annual disaster statistical review, The numbers and trends 2007. *Centre for Research on the Epidemiology of Disasters (CRED)*52. https://www.unisdr.org/files/2796_CREDAnnualStatisticalReview2007.pdf.

Schoof JT, Ford TW, Pryor SC (2017) Recent changes in US regional heat wave characteristics in observations and reanalyses. *Journal of Applied Meteorology and Climatology*, 56: 2621-36. https://doi.org/10.1175/JAMC-D-16-0393.1.

Seneviratne SI, Donat MG, Mueller B, Alexander LV (2014) No pause in the increase of hot temperature extremes. *Nature Climate Change*, 4: 161-2. https://doi.org/10.1038/nclimate2145.

Sharkey P, Killick R (2014) *Nonparametric methods for online changepoint detection.* Lancaster University. Lancaster, UK.

Sheridan SC, Lee CC (2018) Temporal trends in absolute and relative extreme temperature events across North America. *Journal of Geophysical Research: Atmospheres*, 123: 11,889,11,898. https://doi.org/10.1029/2018JD029150.

Sheridan SC, Lee CC, Allen MJ (2019) The mortality response to absolute and relative temperature extremes. *International journal of environmental research and public health*, 16: 1493. https://doi.org/10.3390/ijerph16091493.

Sherwood SC, Huber M (2010) An adaptability limit to climate change due to heat stress. *Proceedings of the National Academy of Sciences*, 107: 9552-5. https://doi.org/10.1073/pnas.0913352107.

Simmons AJ, Willett KM, Jones PD, Thorne PW, Dee DP (2010) Low-frequency variations in surface atmospheric humidity, temperature, and precipitation: Inferences from reanalyses and monthly gridded observational data sets. *Journal of Geophysical Research: Atmospheres*, 115: https://doi.org/10.1029/2009JD012442.

Smith TT, Zaitchik BF, Gohlke JM (2013) Heat waves in the United States: definitions, patterns and trends. *Climatic Change*, 118: 811-25. https://doi.org/10.1007/s10584-012-0659-2.

Steadman RG (1979) The assessment of sultriness. Part I: A temperature-humidity index based on human physiology and clothing science. *Journal of Applied Meteorology*, 18: 861-73. https://doi.org/10.1175/1520-0450(1979)0182.0.CO;2.

St-Pierre NR, Cobanov B, Schnitkey G (2003) Economic losses from heat stress by US livestock industries1. *Journal of dairy science*, 86: E52-77. https://doi.org/10.3168/jds.S0022-0302(03)74040-5.

Tavakol A, Rahmani V (2019a) Analysis of compound hot, dry winds using Copula. *AGU.* December 2019. San Francisco, CA, USA. https://agu.confex.com/agu/fm19/meetingapp.cgi/Paper/552421.

Tavakol A, Rahmani V (2019b) Changes in the frequency of hot, humid conditions in the Mississippi River Basin. *American Society of Agricultural and Biological Engineers.* July 2019. Boston, MA, USA. http://www.doi.org/10.13031/aim.201901502.

Tavakol A, Rahmani V (2018) Changes of heat wave duration in the Mississippi River Basin. *American Society of Agricultural and Biological Engineers.* July 2018. Detroit, MI, USA. https://doi.org/10.13031/aim.201801071.

Trenberth KE (2011) Changes in precipitation with climate change. *Climate Research*, 47: 123-38. https://doi.org/10.3354/cr00953.

Trenberth KE, Stepaniak DP (2001) Indices of el Niño evolution. *Journal of Climate*, 14: 1697-701. https://doi.org/10.1175/1520-0442(2001)0142.0.CO;2.

Trigo RM, Ramos AM, Nogueira PJ, Santos FD, Garcia-Herrera R, Gouveia C, Santo FE (2009) Evaluating the impact of extreme temperature based indices in the 2003 heatwave excessive mortality in Portugal. *Environmental Science & Policy*, 12: 844-54. https://doi.org/10.1016/j.envsci.2009.07.007.

Turner RE, Rabalais NN (2003) Linking landscape and water quality in the Mississippi River basin for 200 years. *Bioscience*, 53: 563-72. https://doi.org/10.1641/0006-3568(2003)053[0563:LLAWQI]2.0.CO;2.

Vining KC, Chase KJ, Loss GR (2013) General weather conditions and precipitation contributing to the 2011 flooding in the Mississippi River and Red River of the North Basins, December 2010 through July 2011: Chapter B in 2011 floods of the central United States. *General weather conditions and precipitation contributing to the 2011 flooding in the Mississippi River and Red River of the North Basins, December 2010 through July 2011: Chapter B in 2011 floods of the central United States*22. https://pubs.usgs.gov/pp/1798b/pp1798b.pdf.

Vose RS, Easterling DR, Gleason B (2005) Maximum and minimum temperature trends for the globe: An update through 2004. *Geophysical Research Letters*, 32: L23822. https://doi.org/10.1029/2005GL024379.

Willett KM, Sherwood S (2012) Exceedance of heat index thresholds for 15 regions under a warming climate using the wet-bulb globe temperature. *International Journal of Climatology*, 32: 161-77. https://doi.org/10.1002/joc.2257.

Willett KM, Jones PD, Gillett NP, Thorne PW (2008) Recent changes in surface humidity: Development of the HadCRUH dataset. *Journal of Climate*, 21: 5364-83. https://doi.org/10.1175/2008JCLI2274.1.

WMO (2016) Guidelines on the definition and monitoring of extreme weather and climate events62. https://www.wmo.int/pages/prog/wcp/ccl/opace/opace2/documents/DraftversionoftheGuidelinesontheDefinitionandMonitoringofExtremeWeatherandClimateEvents.pdf.

Wolkoff P (2018) Indoor air humidity, air quality, and health–An overview. *International journal of hygiene and environmental health*, 221: 376-90. https://doi.org/10.1016/j.ijheh.2018.01.015.

Yip FY, Flanders WD, Wolkin A, Engelthaler D, Humble W, Neri A, Lewis L, Backer L, Rubin C (2008) The impact of excess heat events in Maricopa County, Arizona: 2000–2005. *International journal of biometeorology*, 52: 765-72. https://doi.org/10.1007/s00484-008-0169-0.

Chapter 5 - **Temporal and spatial variation in the frequency of compound hot, dry winds in the central United States**

This chapter is in the final stage of preparation to submit to peer-reviewed journals.

Introduction

The World Meteorological Organization (WMO) has defined climate extremes as infrequent climatological and meteorological phenomena that surpass a stated threshold (Das et al., 2003). The Intergovernmental Panel on Climate Change (IPCC) reported an increase in the probability of extreme weather events (Hartmann et al., 2013) that corresponds with the rise in the average number of annual disasters in the United States from 10 to 35 in less than 50 years (Changnon & Changnon, 1998). Extreme events influence the environment and society resulting in the loss of habitat, property, and even life (NOAA NCEI, 2019a). Negative impacts from extreme events are more significant when events happen simultaneously. Compound extreme events are (1) two or more extreme events occurring successively or simultaneously, (2) combinations of extreme events that amplify the impact of the events on underlying conditions, or (3) combinations of events that are not extremes by themselves but lead to an extreme event when combined (Seneviratne et al., 2012).

A hot, dry, and windy event (HDW) is a compound extreme that merits further examination. While any single extreme of either high temperature, low humidity, or high wind speed could have negative influences, the combination of these three extremes can have a significant impact on crop yield (Leathers & Harrington, 2001; Lydolph, 1964; Lydolph & Williams, 1982; Wang et al., 2016; Yang & Wang, 1978; Rahmani & Tavakol, 2019). Desiccated corn acreage in southern Kansas in 1888 (Curtis, 1891) provides a historic example of the impact of HDWs on cropland. An extended and severe drought was reported in Kansas in

1887 and in the next year (1888) a series of hot winds destroyed 30% of the corn crop in south-central Kansas. Between 1883 and 1888 nearly 40 occurrences of HDWs were reported in the Great Plains including locations in Kansas, Nebraska, the Dakotas, Texas, and Arkansas (Curtis, 1891). The majority of the events were in June, July, and August. In September 1931 and following a month without rain, seven consecutive days of hot winds were reported at Ashland, Kansas, including a report of 49°C (120°F) for September 5th (Avery, 1931). Similar reports from observers in the Great Plains and other states documented crop damage from only a few days of HDWs.

Despite the belief that HDWs were an exclusive characteristic of the Great Plains, many reports in early 1890 showed that other areas of the United States also experienced these conditions (Curtis, 1891; Williams, 1916). For example, Leathers and Harrington (2001) provided a comprehensive summary of the occurrence of "furnace winds" in the United States. They analyzed the geography of HDWs from 1948 to 1993 in the Great Plains and the region between the Great Plains and the West Coast. A greater frequency of the hot and dry conditions (high temperature and low humidity) was observed in the Southwest including the deserts of Arizona and Nevada. However, the highest frequency of HDWs was captured in the southern Great Plains (Leathers & Harrington, 2001). While hot and dry summers in the western United States are common, the rare occurrence of moderate to strong winds limits the regional occurrence of HDWs (Leathers & Harrington, 2001).

An investigation of the occurrence of HDWs in the interior plains of North America showed a higher intensity compared to conditions in Russia (Lydolph & Williams, 1982). The study focused on an area from the eastern part of the Rocky Mountains to the East Coast. While almost the entire area was subject to the occurrence of HDWs, results demonstrated a lower

frequency toward the east with the highest frequency occurring in the southern Great Plains (Lydolph & Williams, 1982).

Generally, plant water demands for growth and evaporative cooling of tissues increase on sunny days with dry winds (Derrel et al., 1993). As the soil dries due to evaporation and plant transpiration, the soil water below the surface starts moving upward by capillary action. If evapotranspiration continues and the soil becomes drier, resistance in the rate of water flow in the soil can become limited (Derrel et al., 1993). Limiting evaporation changes the partitioning of solar energy (from latent to sensible heat), with a warming of the soil surface and the air above the soil (Derrel et al., 1993).

Transport of energy between the vegetative cover and the atmosphere depends on the nature of the plants, their immediate environment, and the physical characteristics of the atmosphere (Woodward & Sheehy, 1983). The amount of energy transferred by advection (horizontal transfer of a substance) depends on air temperature, humidity, and wind speed (Derrel et al., 1993). In hot, arid, and windy locations, advection can provide as much energy as net radiation to drive evapotranspiration (Derrel et al., 1993). When the rate of moisture transpired from the leaves is faster than the rate of moisture received from the roots, plant damage can begin and the amount of damage depends on the length of time plants are exposed to these conditions (Lydolph, 1964). However, in more humid regions with lower wind speeds, the contribution of advection to the rate of evapotranspiration is considerably less. Overall, HDWs can affect crop yield and cause significant economic impact. Lydolph (1964) explained the correlation between the distribution of HDWs and crop yields, with a higher destructive impact occurring in unirrigated croplands.

In addition to the impact of HDWs on croplands, these conditions can also play a critical role in the spread of wildfires. Winkler et al. (2005) examined the climatology of an atmospheric index that combines stability with dryness to estimate erratic wildfire behavior. Maps from the climatic analysis document areas of high risk for the southern Great Plains and these areas can have extended periods of consecutive days of high risk. The co-occurrence of HDW events may lead to more severe wildfires (Flannigan & Harrington, 1988; Jolly et al., 2015). Temperature, relative humidity, precipitation, and wind speed are weather variables that influence the intensity and speed of wildfires. An ability to forecast these variables has been used to develop a fire-weather prediction index to predict when the weather may make wildfires more difficult to manage (Srock et al., 2018).

An increase in global temperature (Easterling et al., 2000; Hartmann et al., 2013; Perkins et al., 2012) is expected to substantially increase the probability of multiple simultaneous extremes (Aghakouchak et al., 2014; Mazdiyasni & Aghakouchak, 2015; Wuebbles et al., 2014). The aim of this study is to understand the spatial patterns and temporal variation in HDWs in the central United States in two different periods. The study is organized as follows: Section 2 provides a comprehensive review on how HDWs are defined in different studies and then identifies the data and methods selected for this study; research results and related discussion are provided in Section 3; and concluding remarks are given in Section 4.

Definitions, Materials, and Methods

Hot, Dry, windy events (HDWs) Definition

HDWs are called “Sukhovey” in Russia (Lydolph, 1964) and were defined based on temperature, relative humidity, and vapor pressure deficit. Because of the lack of data for determining vapor pressure in the United States, Lydolph and Williams (1982) suggested

considering the co-occurrence of low relative humidity, high temperature, and stronger winds to define an hourly HDW event. They defined five different classes of HDWs based on relative humidity less than 30%, wind speed less than or greater than 7m/s, and temperature higher than 29°C (Table 1). Leathers and Harrington (2001) classified HDWs or "furnace winds" with a temperature higher than 35°C (a threshold considered critical for crop development), relative humidity lower than 30%, and wind speed equal to or greater than 7m/s. Previous studies documented a negative impact of temperatures higher than 34°C on crops in the United States (Schlenker et al., 2006). Table 1 shows several definitions and classifications of HDWs. In this study, hourly data observations were used to count the number of HDW events.

Table 5-1. Definition and categorization of hot, dry wind events based on different studies.

Classification	Temperature (°C)	Relative humidity (%)	Wind speed (m/s)	Reference
1	> 29	< 30	--	(Lydolph & Williams, 1982)
2	29-37	< 30	< 7	
3	29-37	< 30	≥ 7	
4	≥ 38	< 30	< 7	
5	≥ 38	< 30	≥ 7	
--	> 35	< 30	≥7	(Leathers & Harrington, 2001)
Slight	> 32	< 30	> 2	(Wang et al., 2016)
Severe	> 35	< 25	> 3	
--	> 30	< 30	> 2	(Chen et al., 2001; Liu & Kang, 2006)
Light	≥ 32	≤ 25	≥ 3	(Shi et al., 2016)
Heavy	≥ 35	≤ 30	≥ 3	

Seasonally, the majority of HDWs are reported in late spring and summer worldwide. In Siberia, they occur primarily in May and June, with very few in late summer (Lydolph, 1964). In

Russia, the occurrence of HDWs differs from west to the east. In western regions, the events mainly occur in July and August, simultaneous with the blooming stage of grains. In eastern Russia, they occur mainly in late spring when southerly winds blow out from the Gobi Desert of China (Lydolph, 1964). In the Great Plains, USA, HDWs mainly occur in mid-summer, however, the less-frequent HDWs of the southeastern United States occur mainly during less humid periods in September, June, or May (Lydolph & Williams, 1982). In China, most HDWs are reported in May and June (Wang et al., 2016). A study from a wind tower in Algeria documented a HDW event blowing from the deserts during the hot season with a wind speed of 4.7m/s in July (Bouchahm et al., 2011). Across Africa, the "Khamsin", "Sharav", and "Sirocco'' HDWs mostly occur in late spring and early summer. As HDWs are usually expected between May and September, the warm season in the Great Plains (May through September) was selected for this study.

The HDW definition advanced by Leathers and Harrington (2001) was used in this study (Table 1). After calculating the frequency of HDWs in each annual warm season, changes in the frequency of these events were analyzed spatially and temporally, considering frequency in different years and individual months. Then, the Mann-Kendall trend test (Kendall, 1975; Mann, 1945), which is widely used for climate variables (Ahiablame et al., 2017; Marofi et al., 2011; Oswald, 2018), was applied to determine the existence of any monotonic trend in the frequency of HDWs over time. In addition, the widely used Pearson and Spearman correlation test (Helsel & Hirsch, 2002; Kendall & Gibbons, 1990; Tavakol et al., 2019) was applied to look for associations between HDWs and extreme temperature, humidity, and wind speed. A two-sided significant level of 0.05 was used for all parameters.

Study Area

Previous studies (Leathers & Harrington, 2001; Lydolph & Williams, 1982) showed the greatest probability of HDWs in the central United States. The higher number of extreme HDWs in this region can be explained in part by the relatively high mean annual wind speed and a summer maximum in mean wind speeds (Klink, 1999b). The relative flatness of the Great Plains and a lack of tree cover are contributing factors. With an area of 2,898,107 km^2, the ten states that contain the Great Plains span from Texas in the south to Canada in the north, and from the Rocky Mountains eastward to Kansas. In this study, weather observing sites within 10 states of Montana, Wyoming, Colorado, New Mexico, North Dakota, South Dakota, Nebraska, Kansas, Oklahoma, and Texas, were analyzed.

Data

Sub-daily temperatures, relative humidity, and wind speed data were obtained from HadISD for 1949–2018 to analyze the long-term (70-year) changes of compound HDWs in the central United States. HadISD (version 3.0.1.201906p) is a station-based, sub-daily, quality-controlled dataset available from the Met Office website (http://www.metoffice.gov.uk/hadobs/hadisd). The dataset uses a subset of the Integrated Surface Database (ISD) (Smith et al., 2011) from the National Oceanic and Atmospheric Administration (NOAA) National Centre for Environmental Information (NCEI), which initially provided data with temporal coverage beginning in 1973 (Dunn et al., 2012). An update of the HadISD data added new stations and extended the temporal coverage back to 1931 (Dunn et al., 2016). The most recent version of HadISD data includes 7,677 stations with global coverage filtered by updated quality-control methods (Dunn et al., 2016). The new sets of HadISD data contain sub-daily humidity and heat-health measurements (e.g., heat index and apparent temperature).

Stations with less than 10% missing data were selected for this study. In addition, stations with an entire year missing were excluded from the study to prevent bias in the results of temporal trend analysis.

Results and Discussion

Frequency of HDWs

Two periods were selected to study the changes in HDWs. A 70-year period (1949–2018) was studied using 27 stations and a 50-year period (1969–2018) using 44 stations (Figure 4-1). The frequency of hourly HDW events was calculated at each station for each month in the warm season. Then the monthly values were summed to calculate an annual (warm season) total. No matter which time period was considered, the highest annual frequencies of HDWs occurred at stations in Kansas and Texas (Figure 4-1). Across all stations analyzed, the mean annual frequency of HDWs ranged from less than 1.0 to more than 60.0 hours, with the largest number occuring in southwest Kansas (Dodge City). This finding reinforces results from a previous study from 1948–1993 that identified Dodge City, Kansas, as the hotspot (Leathers & Harrington, 2001). This location coincides with a high-speed-wind region in the United States (Archer & Jacobson, 2003; DeHarpporte, 1984; Elliott et al., 1986; Klink, 1999a). Analysis of the geographic pattern of mean monthly wind speed for 1961–1990 showed the highest values in the Great Plains in the warm season, with the highest values in Kansas and Texas in June, July, August, and September (Klink, 1999a). Classification of wind-power density showed the highest classes of wind speed (greatr than 7m/s) in southwest Kansas, northwest Nebraska, and north Texas in the summer (Elliott et al., 1986).

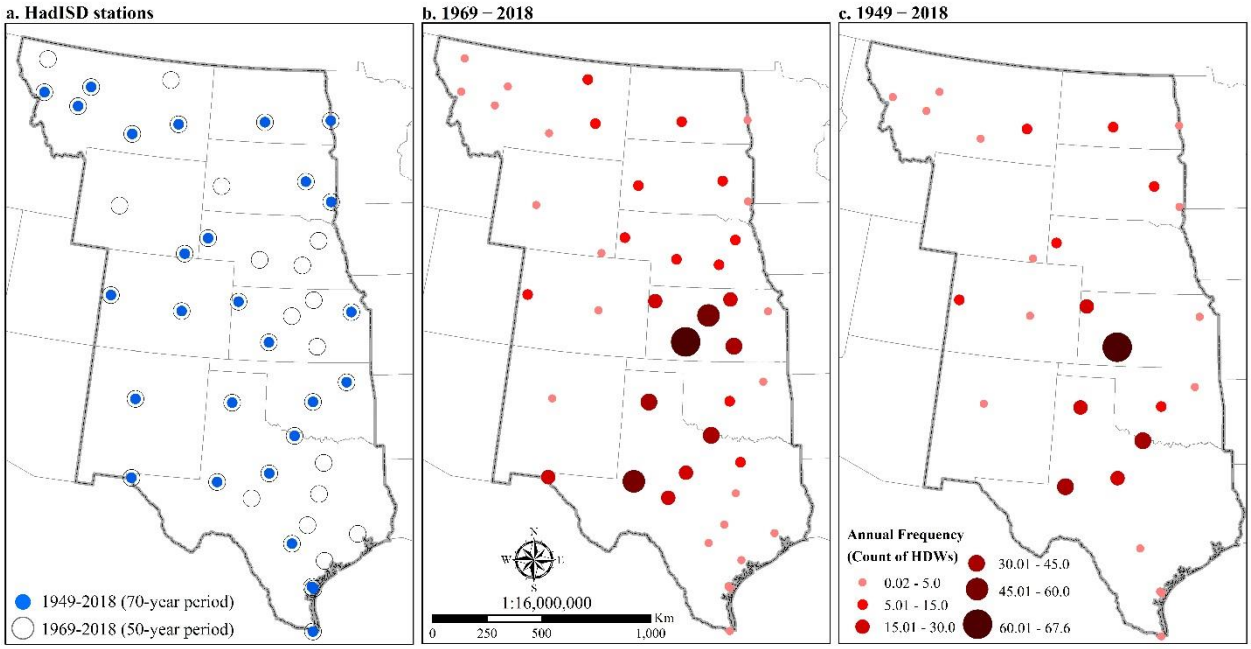

Figure 5-1. Location of stations analyzed in the central United States. The number of available stations increased from 27 to 44 when the study period decreased from 70 to 50 years (a). Annual mean frequency of hourly warm season HDWs in 50-year (b) and 70-year (c) periods. Highest values were determined for Dodge City, Kansas, for both periods.

Year-to-year variation in the occurrence of HDWs in the central United States was determined based on calculating the average occurrence of HDWs across all stations. Temporally, the highest average number of HDWs in the study area were reported during the droughts of 2011 and 1980 (Figure 4-2). For the 70-year period, the highest averages of annual HDWs were 45 and 31 in 2011 and 1980, respectively. For the 50-year period, the average frequency of HDWs was 41 and 35 in 2011 and 1980, respectively (Figure 4-2). In the summer of 1980, a major concurrent drought and heatwave caused severe agricultural damage and about 10,000 excess human deaths from the direct and indirect influences of heat stress (NOAA NCEI, 2019b). The summer was unusually dry and hot, especially in the southern and central Great Plains, with an estimated $16 billion in economic losses (Karl & Quayle, 1981). The hot and dry conditions started in June and continued until late November (NOAA NCEI, 2019b). The major heatwave and drought of 2011 began in March and continued to late August. The concurrent

drought and heatwave of 2011 caused about $13.9 billion in economic losses with major impacts in Kansas, Texas, Oklahoma, New Mexico, and Arizona (NOAA NCEI, 2019b). In the summer of 2011, Texas and Oklahoma recorded their hottest summer, based on long-term records dating back to 1895 (NOAA, 2013).

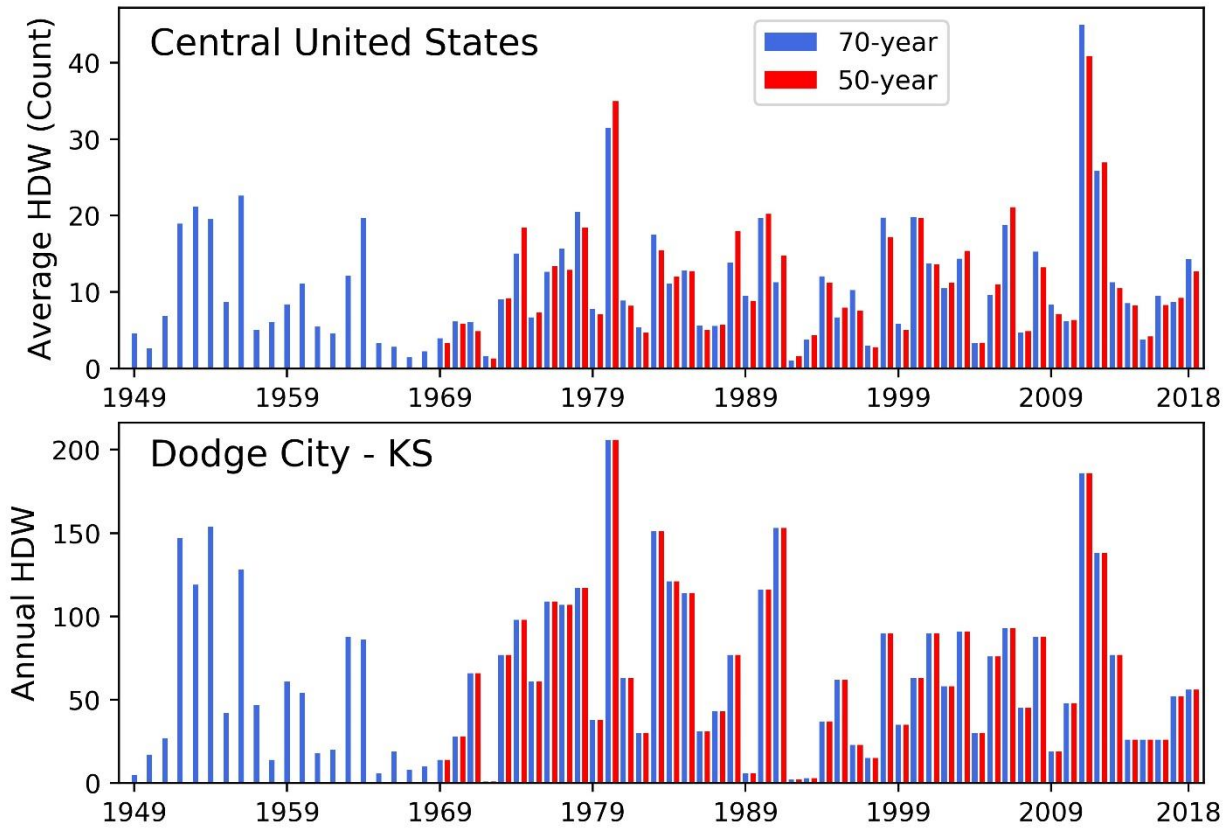

Figure 5-2. The annual multi-station average frequency of hourly HDWs in 50-year (red) and 70-year (blue) periods for all stations in the central United States (top) and for Dodge City (bottom). The highest frequencies occurred in 2011 and 1980. Dodge City, in southwest Kansas, recorded the highest frequency of HDWs among all stations. The difference between 50-year and 70-year average frequency values for the study area is due to the different number of stations analyzed for each period.

Monthly and Diurnal Changes

Monthly frequency of hourly HDWs showed the same pattern of occurrence for both periods (Figure 4-3). Analyzing the relationship between single variable extremes showed the

highest probability of extreme temperature (higher than 35°C) occurred in July and August. However, extreme wind events (higher than or equal to 7m/s) occurred mostly in May and June and the distribution was almost equal in all months for relative humidity extremes (less than 30%).

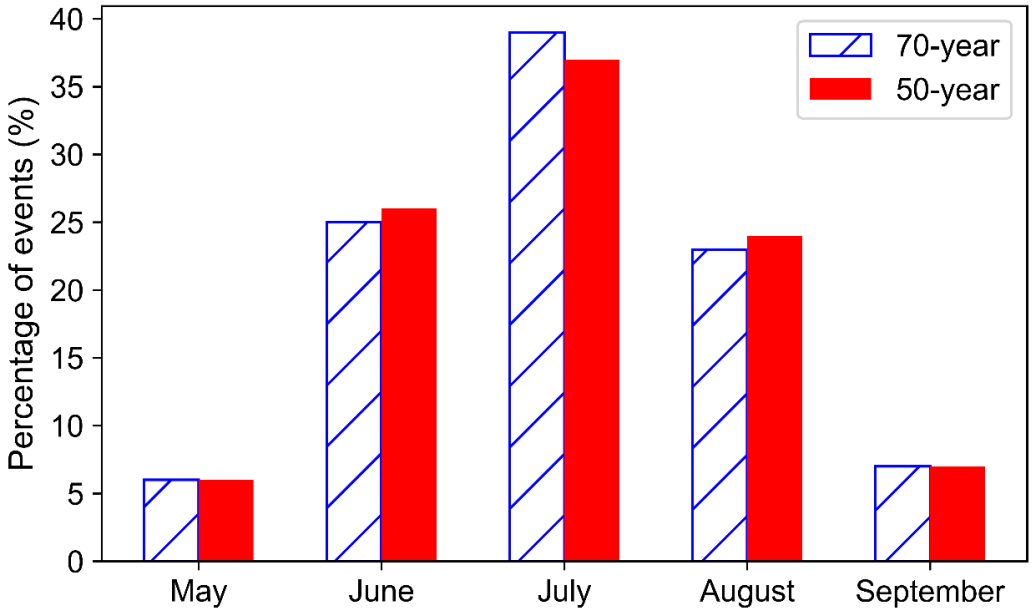

Figure 5-3. The annual multi-station average frequency of hourly HDWs in 50-year (red) and 70-year (blue) periods for all stations in the central United States (top) and for Dodge City (bottom). The highest frequencies occurred in 2011 and 1980. Dodge City, in southwest Kansas, recorded the highest frequency of HDWs among all stations. The difference between 50-year and 70-year average frequency values for the study area is due to the different number of stations analyzed for each period.

Extreme temperature events mostly occurred in Texas, Kansas, and Oklahoma (Figure 4-4). For relative humidity, the majority of extreme events took place in the western Great Plains. For wind, Texas and Kansas had the highest frequency of wind events greater than or equal to 7m/s. Correlation analysis, based on the Pearson and Spearman method, showed no significant relationship between the annual frequency of HDWs and the annual frequency of extreme relative humidity. However, a significant correlation was determined for both wind and temperature extremes with HDWs.

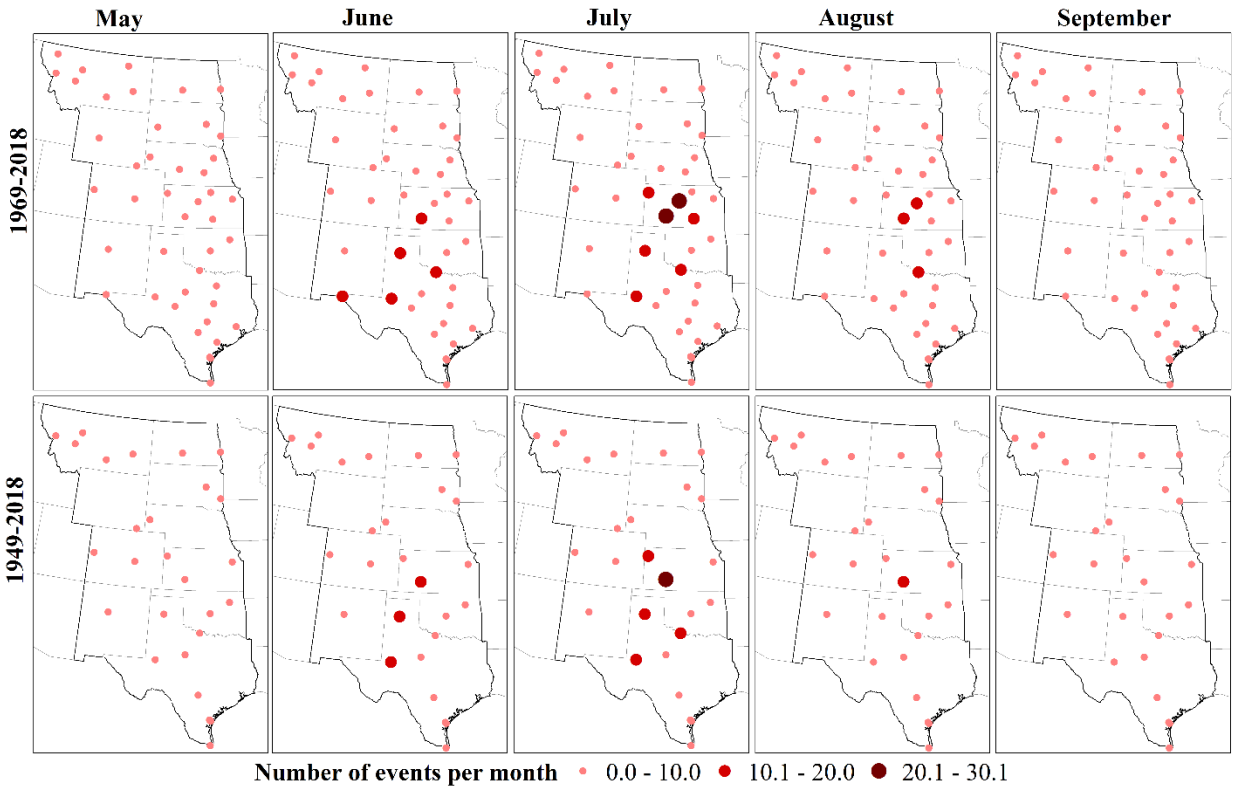

Figure 5-4. Spatial pattern of monthly frequency (average number of hourly events) of HDWs for 50-year (top) and 70-year (bottom) periods. Highest mean values were in July, June, and August, respectively. Stations in Kansas and Texas had the highest frequencies in summer months.

The afternoon maximum is a predominant characteristic of the diurnal pattern of HDW events (Figure 4-5). For HadISd data, all times are provided as coordinated universal time (UTC). However, the study area contains two different time zones, Mountain and Central. The stations were separated based on their time zone and then local time was calculated for each station. Hourly observation of HDWs occurred between 10 a.m. and 11 p.m. with a maximum frequency in the afternoon (4:00 p.m. and 5:00 p.m. local time).

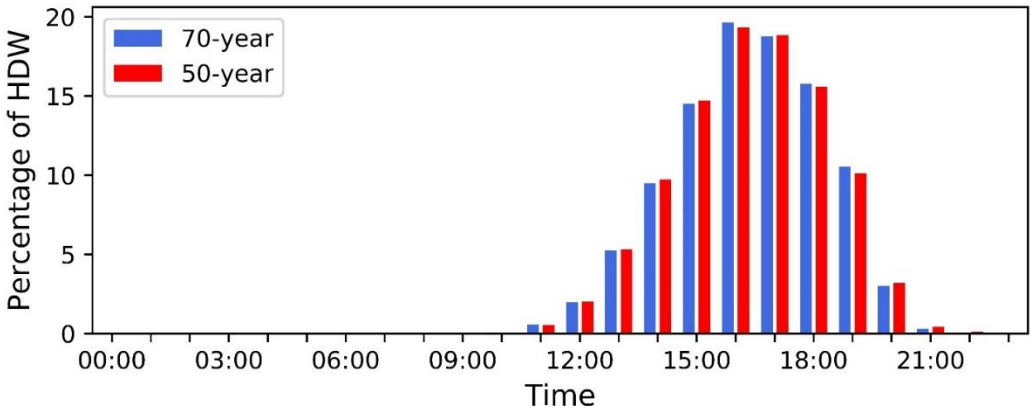

Figure 5-5. Diurnal pattern of hourly HDW occurrences in 50-year (red) and 70-year (blue) periods for all stations in the central United States. The greatest percentage of compound HDWs occurred in the afternoon at 4:00 and 5:00 p.m. A similar temporal pattern was determined for Dodge City, Kansas.

Temporal Trend

The Mann-Kendall trend test was used to analyze any station-based trend in the frequency of HDWs. From 1949–2018 and using annual totals, 30% (75% positive) of the stations showed significant trend (Figure 4-6). When analyzed on a monthly basis, August had the highest percentage of significant trends (18%; 11% positive). Negative trends in August occurred in eastern areas of South Dakota and North Dakota. Other months did not have stations with a decreasing trend. Positive monthly trends were mostly significant in Texas, Kansas, Colorado, and Montana.

From 1969–2018, 27% (67% positive) of all stations showed a significant trend on the annual total. For this analysis period, the majority of significant positive trends (87%) were in Texas. This finding can be linked to the higher number of HDW events associated with dry periods later in the time series (e.g., 2011). All statistically significant negative trends occurred in eastern portions of Nebraska, South Dakota, and North Dakota. The decrease was consistent with the decrease of extreme low humidity, high temperature, and wind speed. Analysis of monthly frequencies (Table 2) documented that May had increases in the occurrence of HDWs

(18% stations) with no downward trends. Trend analysis for the September frequency values showed no significant trend in the occurrence of HDWs in either time periods. Dodge City with the highest frequency of HDWs showed a nonsignificant positive trend over the 70-year period and a nonsignificant negative trend over the 50-year period. The different pattern of trends at stations over the periods 1949–2018 and 1969–2018 demonstrates the importance of data period on the results. It is interesting to note that when the data are summarized for the entire warm season (compared to individual monthly results), a larger number of stations have a statistically significant trend. Figure 4-6 shows the temporal changes of HDWs at stations that experience at least one HDW in each warm season. Station location is identified in Figure 4-7.

Table 5-2. Two-tailed Mann-Kendall trend test results indicate the temporal changes of HDW events in the central United States. The values indicate the percentage of stations with a significant positive or negative trend with α=0.05 in 50-year (1969–2018) and 70-year (1949–2018) periods.

Time	1969–2018			1949–2018		
	Significant	Positive	Negative	Significant	Positive	Negative
Warm season	27.3	18.2	9.1	29.6	22.2	7.4
May	18.2	18.2	0.0	11.1	11.1	0.0
June	9.1	9.1	0.0	7.4	7.4	0.0
July	11.4	4.5	6.8	11.1	11.1	0.0
August	11.4	9.1	2.3	18.5	11.1	7.4
September	0.0	0.0	0.0	0.0	0.0	0.0

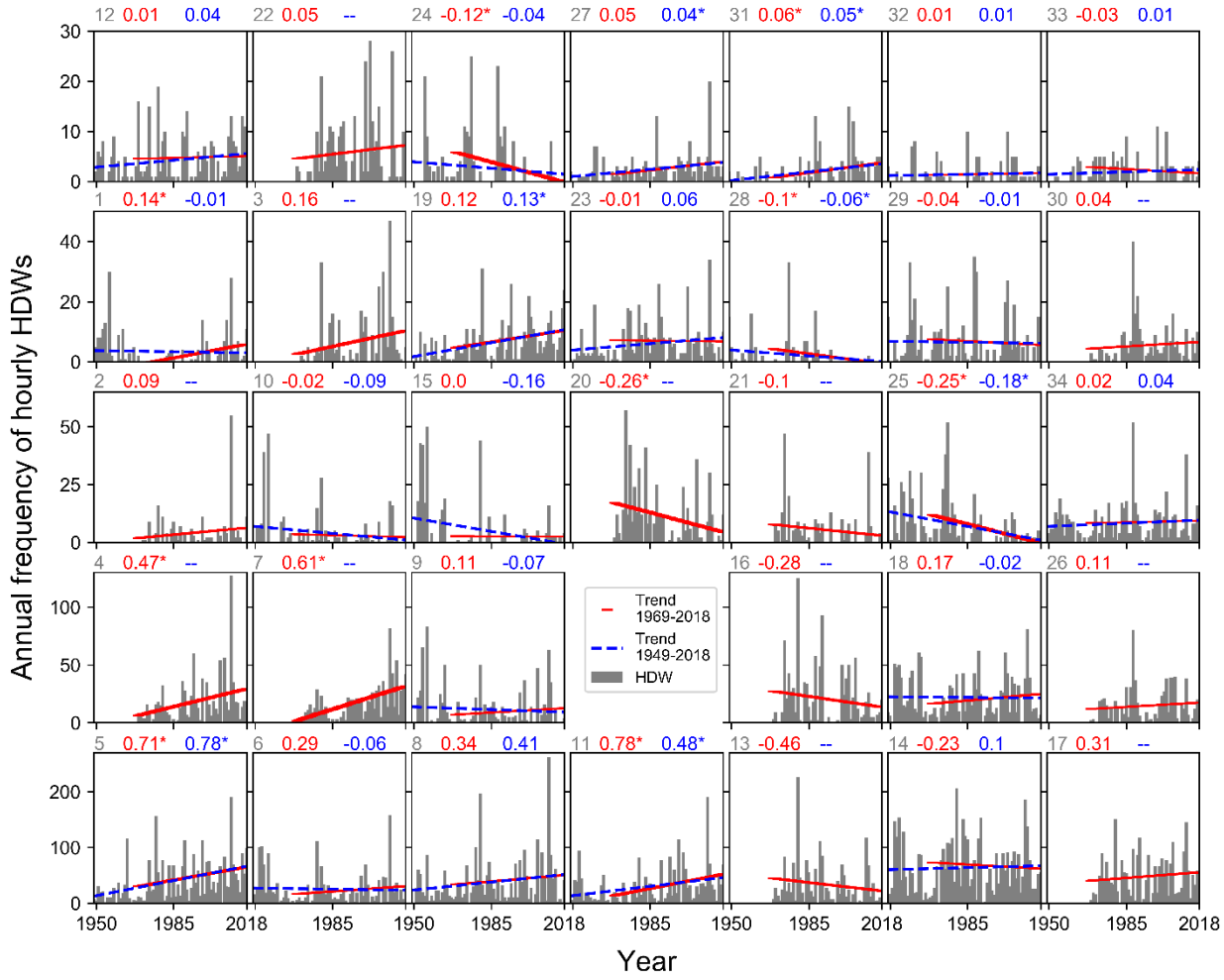

Figure 5-6. The annual frequency of hourly HDWs at stations that experience at least one HDW in each warm season. Each plot shows results for one station. The geographical location of stations is indicated by the first number on the top of each plot and the associated number locations shown in Figure 4-7. Plots are sorted based on the maximum number of HDWs. The dashed blue line shows the trend for HDWs from 1949–2018 and the solid red line shows the trend from 1969–2018. Plots with no blue line do not include data for the 70-year period. The slope of the trend for 1949–2018 (blue) and 1969–2018 (red) are indicated on top of the plots. Significant trends are specified with a star next to the trend slope.

Trends in extremes of temperature, wind speed, and relative humidity were also analyzed to understand the influence of each variable on temporal changes in HWDs (Figure 4-7). For the 50-year period, 45% of stations had a significant trend for extreme temperature (41% positive) and relative humidity (43% positive) events. Among stations that had a significant trend for high wind speed in the 50-year period (36%), there was a similar number of stations with positive and

negative trends (18%). For the 70-year period, 59% of stations had a significant trend in extreme temperature events that were mostly positive (52%). The changes in extreme low relative humidity were less significant (19%; 11% positive) over the longer period. However, high wind speed had a significant negative trend for a majority (52%) of stations. Only one station located in Texas had a significant positive trend for high wind speed in the 70-year period (Figure 4-7).

The changes in extreme temperature events are consistent with global climate change (Easterling et al., 2000; Hartmann et al., 2013; Perkins et al., 2012). Only two stations located in the north-eastern part of the study area had a significant negative trend for both time periods. This area might be considered as part of the "warming hole" in the United States where temperature and extreme temperature events have a downward trend (Meehl et al., 2012; Pan et al., 2004; Tavakol et al., 2020).

Although water vapor is increasing in the atmosphere (Hartmann et al., 2013; Tavakol et al., 2020; Willett et al., 2008), the frequency of extreme low humidity events has also been increasing in western Great Plains. At 57% of the stations, the upward trend in extreme temperature events corresponds with an upward trend in the frequency of low relative humidity events in the 50-year period. When the time series does not include the southern Great Plains drought of the 1950s, the upward trends in extreme temperature and low relative humidity are statistically significant across Texas. The downward trend of extreme wind events was consistent with Pryor et al. (2009) in which a decline was discovered in the 90^{th} percentile and annual mean wind speed in the United States. Here, a decrease in HDWs was discovered at the stations with either a decline in all three single extremes (Figure 4-7). The increase of HDWs may affect water resource management challenges associated with the greater evapotranspiration (Derrel et al., 1993).

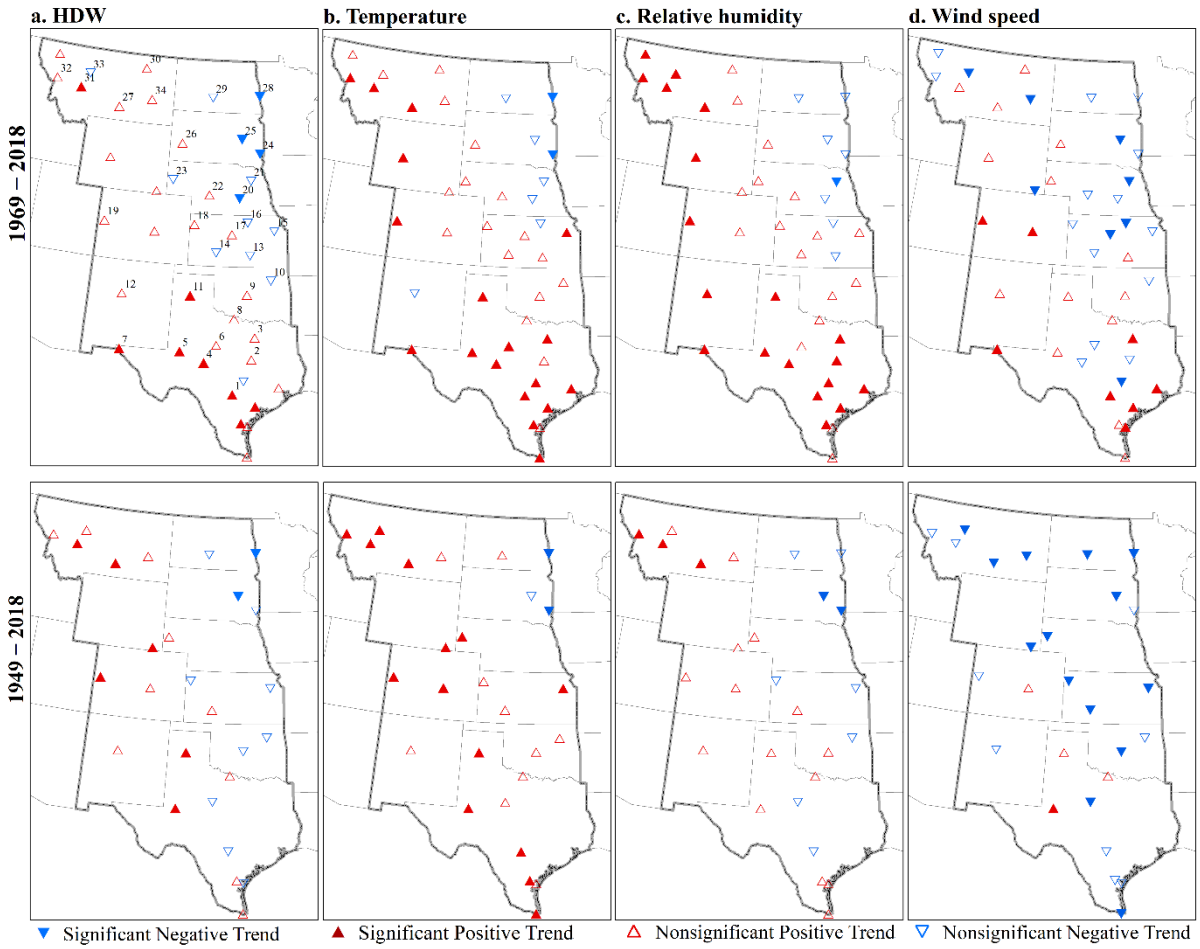

Figure 5-7. Trends of the frequency of HDWs (a), extreme high temperature (b), extreme low relative humidity (c), and extreme high wind speed (d) at each station in 50-year (top) and 70-year (bottom) periods.

Summary and Conclusions

Spatial and temporal variations of HDWs were analyzed for the central United States (including the Great Plains) over two different periods of 1969–2018 (50-year) and 1949–2018 (70-year). For the 50-year period, there were more stations (44 stations) compared to the 70-year period (27 stations) that helped lead to a better understanding of spatial patterns. HDWs were defined as compound hourly events with high wind speeds (higher than or equal to 7m/s), high temperature (higher than 35°C), and low relative humidity (lower than 30%). Frequency analysis

showed a greater occurrence of HDWs in western Kansas southward into Texas. This was consistent with the spatial pattern of extreme wind (wind speeds higher than 7m/s) and extreme temperature (temperatures higher than 35°C) events. Monthly analysis showed the greater probability of HDWs in summer, with fewer occurrences in May and September. Compound HDW events were mainly observed in the afternoon with the highest frequencies at 4:00 and 5:00 p.m.

Results document the influence of the data period on the trend analysis. However, most stations located in Texas and the western Great Plains showed an upward trend in the HDWs. A downward trend in HDWs was found in the northeastern portion of the study region, consistent with the decrease in the extreme temperature, humidity, and wind speed events over time. Temporally, central United States experienced large numbers of HDWs in 1980 and 2011. Two major, concurrent drought and heatwaves in the summers of 1980 and 2011 coincided with the higher frequency of HDWs. The higher temperatures associated with climate change may increase the frequency of extreme HDWs. HDW events have implications not only for those involved in crop production. Wind-driven wildfires and increased evapotranspiration effects on water management systems are potential impacts of these compound extreme meteorological events. Adaptation and mitigation strategies may need to be adjusted to cope with the negative impacts of these events.

References

Aghakouchak, A., Cheng, L., Mazdiyasni, O., & Farahmand, A., 2014. Global warming and changes in risk of concurrent climate extremes: Insights from the 2014 California drought. *Geophysical Research Letters.* 41: 8847-8852. http://doi.org/10.1002/2014GL062308

Ahiablame, L., Sheshukov, A. Y., Rahmani, V., & Moriasi, D., 2017. Annual baseflow variations as influenced by climate variability and agricultural land use change in the Missouri River Basin. *Journal of Hydrology.* 551: 188-202. https://doi.org/10.1016/j.jhydrol.2017.05.055

Archer, C. L.& Jacobson, M. Z., 2003. Spatial and temporal distributions of US winds and wind power at 80 m derived from measurements. *Journal of Geophysical Research: Atmospheres.* 108: http://www.doi.org/10.1029/2002JD002076

Avery, C. 1931. HOT WINDS IN WESTERN KANSAS. *Bulletin of the American Meteorological Society.* 12: 202-203. https://doi.org/10.1175/1520-0477-12.12.202a

Bouchahm, Y., Bourbia, F., & Belhamri, A., 2011. Performance analysis and improvement of the use of wind tower in hot dry climate. *Renewable Energy.* 36: 898-906. https://doi.org/10.1016/j.renene.2010.08.030

Changnon, S. A.& Changnon, D., 1998. Record-high losses for weather disasters in the United States during the 1990s: How excessive and why? *Natural Hazards.* 18: 287-300. https://doi.org/10.1023/A:1026475006301

Chen, H. L., Zou, C. H., Fu, X. J., & Guan, W. Y., 2001. The EOF analysis on wheat dry-hot-wind in Henan province. *Journal of Natural Resources.* 16: 59-64.

Curtis, G. E. 1891. The hot winds of the plains. *Seventh Biennial Report, Kansas Department of Agriculture.* 7: 162-183. https://www.kansasmemory.org/item/225333

Das, H. P., Adamenko, T. I., Anaman, K. I., Gommes, R. G., & Johnson, G., 2003. Agrometeorology related to extreme events. *World Meteorological Organization.* Geneva, Switzerland. 152p.

DeHarpporte, D. 1984. West and southwest wind atlas. *Van Nostrand Reinhold Company.* New York, USA. 120p.

Derrel, M. L., Gilley, J. R., & Baumer, O. W., 1993. Irrigation Handbooks and Manuals (Part 623, Chapter 2) Irrigation Water Requirements. *United States Department of Agriculture.* Washington, DC, USA. https://www.nrcs.usda.gov/wps/portal/nrcs/detailfull/national/water/manage/irrigation/?cid=stelprdb1045075

Dunn, R. J., Willett, K. M., Parker, D. E., & Mitchell, L., 2016. Expanding HadISD: quality-controlled, sub-daily station data from 1931. *Geoscientific Instrumentation, Methods and Data Systems.* 5: 473-491. http://www.doi.org/10.5194/gi-5-473-2016

Dunn, R. J., Willett, K. M., Thorne, P. W., Woolley, E. V., Durre, I., Dai, A., ..., and Vose, R. E., 2012. HadISD: a quality-controlled global synoptic report database for selected variables at long-term stations from 1973--2011. *arXiv Preprint arXiv:1210.7191*. htpp://www.doi.org/10.5194/cp-8-1649-2012

Easterling, G., Meehl, C., Parmesan, S. A., Changnon, T., Karl, L., & Mearns, L., 2000. Climate extremes: Observations, modeling, and impacts. *Science (Washington).* 289: 2068-2074. http://science.sciencemag.org/content/289/5487/2068

Elliott, D. L., Holladay, C. G., Barchet, W. R., Foote, H. P., & Sandusky, W. F., 1986. Wind energy resource atlas of the United States. *U.S. Department of Energy.* Colorado, USA. https://rredc.nrel.gov/Wind/pubs/atlas/

Flannigan, M. D.& Harrington, J. B., 1988. A study of the relation of meteorological variables to monthly provincial area burned by wildfire in Canada (1953–80). *Journal of Applied Meteorology.* 27: 441-452. https://doi.org/10.1175/1520-0450(1988)0272.0.CO;2

Hartmann, D. L., Tank, A. M. K., Rusticucci, M., Alexander, L. V., Brnnimann, S., Charabi, Y. A. R., ..., and Kaplan, A., 2013. Observations: Atmosphere and surface. *In: Climate change 2013 the physical science basis: Working group I contribution to the fifth assessment report of the intergovernmental panel on climate change.* (pp. 159-254). Cambridge University Press. Cambridge, United Kingdom and New York, NY, USA.

Helsel, D. R., & Hirsch, R. M., 2002. Statistical methods in water resources. Techniques of Water Resources Investigations of the United States Geological Survey (2002). 522p.

Jolly, W. M., Cochrane, M. A., Freeborn, P. H., Holden, Z. A., Brown, T. J., Williamson, G. J., & Bowman, D. M., 2015. Climate-induced variations in global wildfire danger from 1979 to 2013. *Nature Communications.* 6: 7537. https://doi.org/10.1038/ncomms8537

Karl, T. R.& Quayle, R. G., 1981. The 1980 summer heat wave and drought in historical perspective. *Monthly Weather Review.* 109: 2055-2073. https://doi.org/10.1175/1520-0493(1981)1092.0.CO;2

Kendall, M. G. 1975. Rank Correlation Measures. *Charles Griffin.* London, UK. 202p.

Kendall, M., & Gibbons, J., 1990. Rank correlation methods. Oxford University Press. Oxford, UK. 260p.

Klink, K. 1999a. Climatological mean and interannual variance of United States surface wind speed, direction and velocity 1. *International Journal of Climatology: A Journal of the Royal Meteorological Society.* 19: 471-488. https://doi.org/10.1002/(SICI)1097-0088(199904)19:53.0.CO;2-X

Klink, K. 1999b. Trends in mean monthly maximum and minimum surface wind speeds in the coterminous United States, 1961 to 1990. *Climate Research.* 13: 193-205. www.doi.org/10.3354/cr013193

Leathers, N.& Harrington, J., 2001. Furnace winds of the West. *Journal of the West.* 40: 48-57.

Liu, H.& Kang, Y., 2006. Regulating field microclimate using sprinkler misting under hot-dry windy conditions. *Biosystems Engineering.* 95: 349-358. https://doi.org/10.1016/j.biosystemseng.2006.07.010

Lydolph, P. E. 1964. The russian sukhovey. *Annals of the Association of American Geographers.* 54: 291-309. https://doi.org/10.1111/j.1467-8306.1964.tb00490.x

Lydolph, P. E.& Williams, T. B., 1982. The North American Sukhovey. *Annals of the Association of American Geographers.* 72: 224-236. https://doi.org/10.1111/j.1467-8306.1982.tb01821.x

Mann, H. B. 1945. Nonparametric tests against trend. *Econometrica: Journal of the Econometric Society.* 13: 245-259. http://www.jstor.org/stable/1907187

Marofi, S., Sohrabi, M. M., Mohammadi, K., Sabziparvar, A. A., & Abyaneh, H. Z., 2011. Investigation of meteorological extreme events over coastal regions of Iran. Theoretical and Applied Climatology. 103: 401-412. https://doi.org/10.1007/s00704-010-0298-3

Mazdiyasni, O., & Aghakouchak, A., 2015. Substantial increase in concurrent droughts and heatwaves in the United States. *Proceedings of the National Academy of Sciences.* 112: 11484-11489. https://doi.org/10.1073/pnas.1422945112

Meehl, G. A., Arblaster, J. M., & Branstator, G., 2012. Mechanisms contributing to the warming hole and the consequent US east–west differential of heat extremes. *Journal of Climate.* 25: 6394-6408. https://doi.org/10.1175/JCLI-D-11-00655.1

NOAA.2013. Regional climate trends and scenarios for the US climate assessment, Part 4: climate of the US Great Plains. *NOAA technical report NESDIS 142-4.* Washington, D.C. USA. https://www.nesdis.noaa.gov/sites/default/files/asset/document/NOAA_NESDIS_Tech_Report_142-4-Climate_of_the_US_Great_Plains.pdf.

NOAA NCEI. (2019a). Billion-dollar weather and climate disasters. Retrieved from https://www.ncdc.noaa.gov/billions; 3/9/2019.

NOAA NCEI. (2019b). Billion-dollar weather and climate disasters: Table of events. Retrieved from https://www.ncdc.noaa.gov/billions/events; 7/1/2019.

Oswald, E. M. 2018. An Analysis of the Prevalence of Heat Waves in the United States between 1948 and 2015. Journal of Applied Meteorology and Climatology. 57: 1535-1549. https://doi.org/10.1175/JAMC-D-17-0274.1

Pan, Z., Arritt, R. W., Takle, E. S., Gutowski, W. J., Anderson, C. J., & Segal, M., 2004. Altered hydrologic feedback in a warming climate introduces a “warming hole”. *Geophysical Research Letters.* 31: L17109. https://doi.org/10.1029/2004GL020528

Perkins, S. E., Alexander, L. V., & Nairn, J. R., 2012. Increasing frequency, intensity and duration of observed global heatwaves and warm spells. *Geophysical Research Letters.* 39: n/a. https://doi.org/10.1029/2012GL053361

Pryor, S. C., Barthelmie, R. J., Young, D. T., Takle, E. S., Arritt, R. W., Flory, D., ..., and Roads, J., 2009. Wind speed trends over the contiguous United States. *Journal of Geophysical Research: Atmospheres.* 114: http://www.doi.org/10.1029/2008JD011416

Rahmani, V., & Tavakol, A., 2019. Spatiotemporal Changes of Correlated Hot, Dry, and Windy Conditions in the Central United States. In: *AGU Fall Meeting 2019,* https://agu.confex.com/agu/fm19/meetingapp.cgi/Paper/594147.

Schlenker, W., Hanemann, W. M., & Fisher, A. C., 2006. The impact of global warming on US agriculture: an econometric analysis of optimal growing conditions. *Review of Economics and Statistics.* 88: 113-125. https://doi.org/10.1162/rest.2006.88.1.113

Seneviratne, S. I., Nicholls, N., Easterling, D., Goodess, C. M., Kanae, S., Kossin, J., ..., and Zwiers, F. W., 2012. Changes in climate extremes and their impacts on the natural physical environment: An overview of the IPCC SREX report. *Cambridge University Press. Cambridge.* New York, NY, USA. 109-230p.

Shi, B., Zhu, X., Li, H., Hu, Y., & Zhang, Y., 2016. Analysis of how dry-hot wind hazard has changed for winter wheat in the Huang-huai-hai plain. *Natural Hazards and Earth System Sciences.* 2016: 1. https://www.researchgate.net/publication/292186761_Analysis_of_how_dry-hot_wind_hazard_has_changed_for_winter_wheat_in_the_Huang-huai-hai_plain

Smith, A., Lott, N., & Vose, R., 2011. The integrated surface database: Recent developments and partnerships. *Bulletin of the American Meteorological Society.* 92: 704-708. http://doi.org/10.1175/2011BAMS3015.1

Srock, A., Charney, J., Potter, B., & Goodrick, S., 2018. The Hot-Dry-Windy Index: A New Fire Weather Index. *Atmosphere.* 9: 279. https://doi.org/10.3390/atmos9070279

Tavakol, A., Rahmani, V., & Harrington, J., 2020. Changes in the frequency of hot, humid days and nights in the Mississippi River Basin. *Int J Climatol.* 1-16. https://doi.org/10. 1002/joc.6484

Tavakol, A., Rahmani, V., Quiring, S., & Kumar, S., 2019. Evaluation analysis of NASA SMAP L3 and L4 and SPoRT-LIS soil moisture data in the United States. *Remote Sensing of Environment.* 229: 234-246. https://doi.org/10.1016/j.rse.2019.05.006

Wang, S., Zheng, H., Liu, S., Miao, Y., & Li, J., 2016. Numerical study on the stomatal responses to dry-hot wind episodes and its effects on land-atmosphere interactions. *PloS One.* 11: e0162852. https://doi.org/10.1371/journal.pone.0162852

Willett, K. M., Jones, P. D., Gillett, N. P., & Thorne, P. W., 2008. Recent changes in surface humidity: Development of the HadCRUH dataset. *Journal of Climate.* 21: 5364-5383. https://doi.org/10.1175/2008JCLI2274.1

Williams, H. E. 1916. Fire-weather warnings. Monthly Weather Review. 44: 133-135. https://doi.org/10.1175/1520-0493(1916)442.0.CO;2

Winkler, J. A., Potter, B., Wilhelm, D., Shadbolt, R., Bian, X., & Piromsopa, K., 2005. A cimatology of the Haines Index for North America derived from NCEP/NCAR reanalysis fields. In: *Sixth Fire and Forest Meteorology Symposium, American Meteorological Society,* https://ams.confex.com/ams/6FireJoint/techprogram/paper_97645.htm.

Woodward, F. I., & Sheehy, J. E., 1983. Principles and measurements in environmental biology. *Butterworths.* London, UK. 274p.

Wuebbles, D. J., Kunkel, K., Wehner, M., & Zobel, Z., 2014. Severe weather in United States under a changing climate. *Eos, Transactions American Geophysical Union.* 95: 149-150. https://doi.org/10.1002/2014EO180001

Yang, Z.& Wang, S., 1978. The climatal analysis and forecast on Dry-hot wind at Guangzhong, Shaanxi. *Meterology Shaanxi.* 3: 6-13.

Chapter 6 - **The Probability of compound climate extremes in a changing climate: A copula-based study of hot, dry, and windy events in the central United States**

This chapter is in the final stage of preparation to submit to peer-reviewed journals.

Introduction

In September 1882, Kansas and Missouri suffered from several consecutive days with severe hot, dry, and windy events (HDWs) from the southwest with a temperature higher than 38°C and the relative humidity lower than 17%. The "furnace winds" withered and burned up the vegetation and suspended outdoor labor (Curtis, 1891). In another sever condition, after the prolonged, severe drought in 1887, the HDWs during July and August in Kansas damaged 30% of the promising crop worth of seven million dollars (Curtis, 1891). These historic examples of extreme weather/climate events with more than one weather variable involved are called the compound extremes. Compound extreme events are defined by IPCC as "(1) two or more extreme events occurring simultaneously or successively, (2) combinations of extreme events with underlying conditions that amplify the impact of the events, or (3) combinations of events that are not themselves extremes but lead to an extreme event or impact when combined" (Seneviratne et al., 2012). Leonard et al., (2014) also defined a compound extreme as "an extreme impact that depends on multiple statistically dependent variables or events".

Compound extremes are typically classified into three categories (Hao et al., 2018). First, when all the variables involved are lower than specific thresholds such as precipitation and soil moisture deficit (Kao & Govindaraju, 2010). Second, when all variables exceed a specific

threshold such as extreme precipitation or river discharge compound with storm surges or sea-level rise (Bevacqua et al., 2017; Paprotny et al., 2018; van den Hurk et al., 2015; Wahl et al., 2015). These first two categories are similar in that an established threshold is exceeded. A third category occurs when one or more of the variables exceeds a threshold while the other variables are lower than a threshold; this third type has been called an exceedance/non-exceedance compound extreme, with examples involving drought and heatwave events (Mazdiyasni & Aghakouchak, 2015; Sharma & Mujumdar, 2017). HDWs are exceedance/non-exceedance compound extremes when high temperature and moderately high wind speeds are accompanied by low relative humidity.

HDW events have been observed to cause a suite of severe impacts on croplands around the world (Curtis, 1891; Leathers & Harrington, 2001; Lydolph, 1964; Lydolph & Williams, 1982; Wang et al., 2016; Yang & Wang, 1978). Increased evapotranspiration (Derrel et al., 1993) and damage to plant tissues, when the rate of plant respiration is higher than the rate of water received from the root system, are characteristic of HDWs (Lydolph, 1964). A recent study on the flash droughts (Otkin et al., 2018) suggests that HDWs can be a factor in the rapid onset of a drought. In addition, HDWs can influence the initiation of and the intensification of wildfires (Flannigan & Harrington, 1988; Jolly et al., 2015; Srock et al., 2018). Based on our review of published literature, just two studies have analyzed the spatial frequency of HDWs in the United States. Lydolph and Williams (1982) analyzed the spatial distribution of HDWs in the eastern half of the contiguous United States (CONUS) including the Great Plains. Analyzing data during 1951–1960 along with case-studies from 1961–1963 and 1980, they found a higher occurrence of HDWs in the Great Plains. Analyzing both the Great Plains and western half of CONUS, Leathers and Harrington (2001) found the greatest occurrence of hot and dry conditions in the

southwest deserts over the period of 1948–1993. However, the rare occurrence of high-speed winds in the southwest shifted the higher probability of HDWs toward the southern Great Plains (Leathers & Harrington, 2001). There is substantial evidence that Northern Hemisphere HDWs are usually observed between mid-May and mid-September for the United States and in mid-summer in the Great Plains (Lydolph & Williams, 1982).

Lydolph and Williams (1982) classified HDWs or "sukhovey" into five classes, with the temperature threshold varying across a range of 29°C-38°C, the humidity threshold lower than 30%, and with wind speeds higher or lower than 7m/s. Leathers and Harrington (2001) defined a HDW or "furnace wind" event with a temperature higher than 35°C, relative humidity lower than 30%, and wind speed equal to or higher than 7m/s. The 35°C threshold for temperature was considered a critical temperature for crop development in the United States (Leathers & Harrington, 2001). The critical temperature threshold may be adjusted for different crop types. For example, a temperature higher than 29°C, 30°C, and 32°C would be harmful to corn, soybean, and cotton, respectively and reduces the productivity of these crops by 30–82% when the temperature is higher than the identified thresholds (Schlenker & Roberts, 2009). Analysis of the influence of global warming on United States crop agriculture revealed the harmfulness of temperatures above 34°C (Schlenker et al., 2006). Here, the fixed thresholds (35°C for temperature, 7m/s for wind speed, and 30% for relative humidity) were used to analyze the co-occurrence of HDWs.

Previous studies analyzed only the spatial pattern of HDWs across the United States. Here, we modeled the joint behavior of the three elements that combine to create HDWs as well as the temporal and spatial changes of HDWs over a 70-year period in the central United States. Copula families have recently been used to characterize compound hydrologic and climatic

extremes. A copula is a function that links or joins a multivariate distribution function to its single dimension marginal distribution functions (Nelson 2003). Diverse copula families characterize the scale-free dependence between/among random variables. Based on the knowledge available now, there is no study that has analyzed the trivariate co-occurrence of HDWs applying copula. The focus of the analysis is restricted to the application of copula to analyze the HDWs in the warm-season (from May through September). In addition, the influence of dependence structure on the frequency of HDWs over the period of 1949–2018 was assessed. Finally, changes in the univariate extreme temperature, humidity, and wind speed were analyzed over time to assess the influence of each individual variable on the occurrence of HDWs.

Materials and methods

Data

A long-term dataset extending from 1949 through 2018 with an hourly time-step was obtained from the HadISD (https://www.metoffice.gov.uk/hadobs/hadisd/). HadISD is a global, station-based, sub-daily, and quality-controlled dataset developed based on the Integrated Surface Database (ISD) at the National Oceanic and Atmospheric Administration's National Centre for Environmental Information (NOAA/NCEI, formerly the National Climatic Data Center – NCDC; (Dunn et al., 2012; Dunn et al., 2016)). The dataset has been extended to cover from 1931 to the present and is designed to study the long-term changes of extreme temperature, pressure, and humidity (Dunn et al., 2016). The advantage of using this dataset is the availability of all three variables (temperature, relative humidity, and wind speed) for all stations. The data from 1931–1948 were excluded to include stations with minimal missing data. Stations with less than 10% missing data in temperature, relative humidity, and wind speed for the warm season were selected to study the changes of compound HDWs in the central United States. Missing

data at a station was identified when at least one of the three climate variables was not available. Stations that had less than 10% missing data but had no data for the entire year were also excluded to reduce bias in the trend analysis results. Twenty-seven stations are available for this study of HDW events during the period 1949–2018 for the 10 states in the United States that comprise the central United States (Figure 5-1).

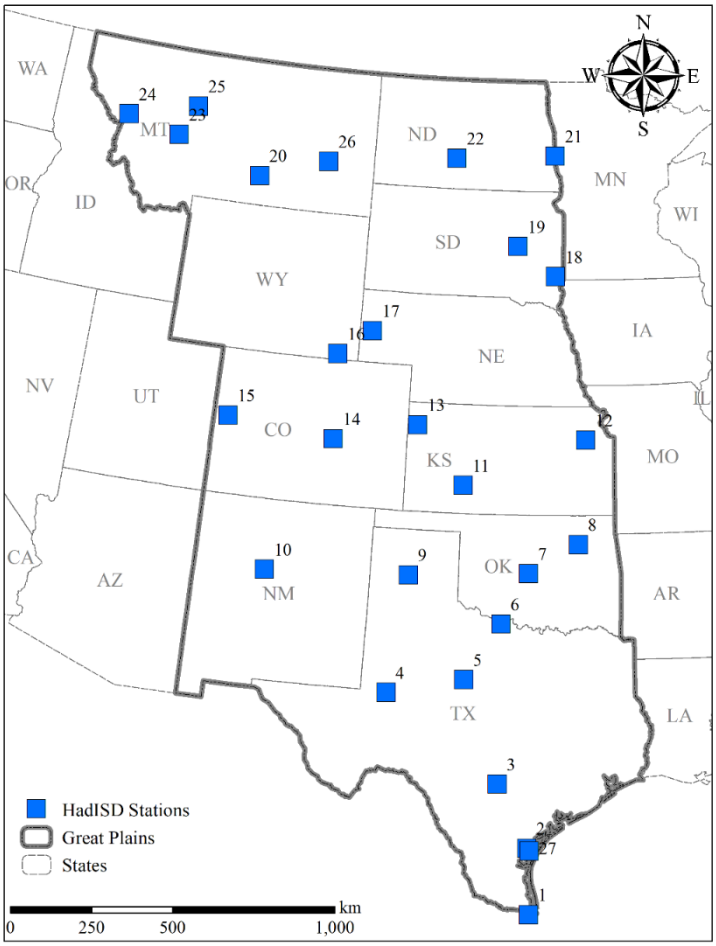

Figure 6-1. Location of analyzed stations in the central United States from 1949–2018. Data was retrived from HadISD.

Methods

Two different approaches were used to investigate the compound extremes of HDWs. An empirical method, a simple annual count of the hours with compound exceedances of temperature and wind speed above 35°C and 7m/s respectively, and relative humidity below 30%, was used. The second approach develops copula families to model the trivariate dependence of temperature, relative humidity, and wind speed. For the three random variables of *X* (e.g., relative humidity), *Y* (e.g., temperature), and *Z* (e.g., wind speed) with cumulative distribution functions $F_X(x) = \Pr(X \leq x)$, $F_Y(y) = \Pr(Y \leq y)$, and $F_Z(z) = \Pr(Z \leq z)$, the trivariate joint distribution function or copula *(C)* can be written as:

$$F(x, y, z) = \Pr(X \leq x, Y \leq y, Z \leq z) = C(u, v, z) \quad (1)$$

Where three variables are less than a stablished threshold and u, v, and z are the uniformly distributed marginals on [0,1]. However, there is an obvious difference between non-exceedance (F) and exceedance probabilities (P). The probability of hours in each warm season when temperature and wind speed exceed the 90th percentile and the relative humidity is at the same time below the 10th percentile is called the exceedance/non-exceedance probability. The exceedance/non-exceedance probability can be written as:

$$P = \Pr(X \leq x, Y > y, Z > z) = C(u, v', z') \quad (2)$$

Where $v' = 1 - v$, and $z' = 1 - z$ are the exceedance probabilities of temperature and wind speed, respectively, and u is the exceedance probability of relative humidity below the threshold. Therefore, the equation can be solved as (Liu et al., 2018; Nelsen, 2006):

$$P = u - C(u, v') - C(u, z') + C(u, v', z') \quad (3)$$

Then, the trivariate extremes would be defined as the area in three-dimensional space where temperature and wind speed exceed the established threshold, while relative humidity is lower than a threshold. If considering the 90th and 10th percentile thresholds as it is done in the literature of extremes and climate change; hence, $v' = z' = 0.9$ and $u = 0.1$. When considering the fixed thresholds, the value of u, v', and z' are not necessarily equal.

Copula Families

Six copula functions were used from Archimedean and Elliptical copulas that have been widely used in hydrological and climate studies (Aghakouchak et al., 2014; Hao et al., 2018; Liu et al., 2018; Zhou & Liu, 2018; Zscheischler & Seneviratne, 2017). Clayton, Gumbel, Frank and Joe copulas with different patterns of dependence structure were selected among several Archimedean copulas (Figure 5-2). Frank copula is a symmetric copula with no tail dependence. However, the Clayton copula has a greater lower tail dependence and Joe and Gumbel copulas have a greater upper tail dependence (Nelsen, 2006). Gaussian and Student-t are Elliptical and radially symmetric copulas with no tail dependence for the Gaussian copula (Figure 5-2). For the Student-t copula, tail dependence depends on the correlation and the degree of freedom (Nelsen, 2006). Sadegh et al., (2017) provides a complete list of copula families and their related functions as well as the range of parameters for each copula.

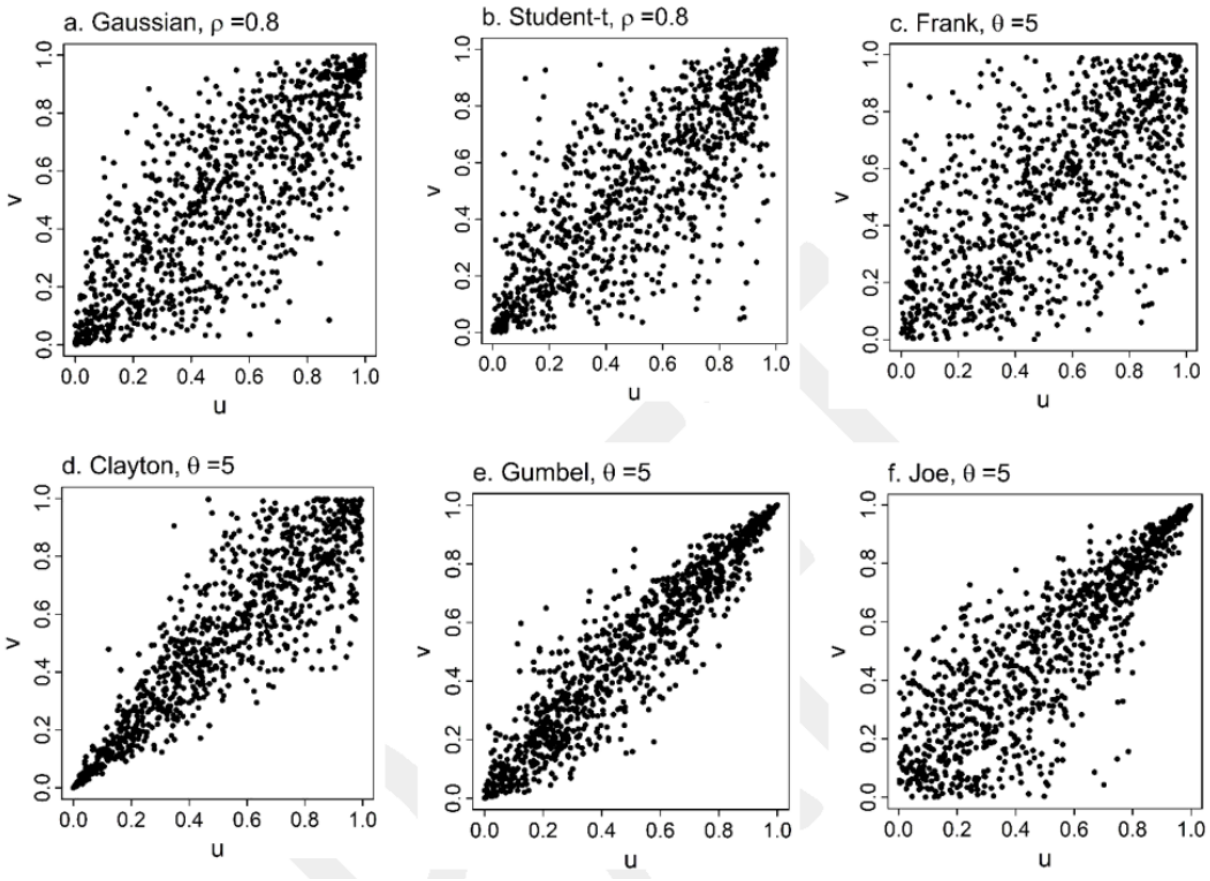

Figure 6-2. Random samples of Elliptical and Archimedean copulas. Plots show 1000 random samples from a Gaussian (a), Student-t (b), Frank (c), Clayton (d), Gumbel (e), and Joe (f) copulas. The Elliptical and Archimedean copulas were created using $\rho = 0.8$ and $\theta = 5$, respectively.

Fitting the copula

Before modeling the joint probability distribution, it is necessary to transform random variables (i.e., temperature, relative humidity, and wind speed) to uniformly distributed marginals [0,1] through calculating the normalized ranks, which is a common process for copula analysis (Hofert et al., 2018; Salvadori et al., 2011; Serinaldi, 2016; Zscheischler & Seneviratne, 2017). After calculating the marginal distribution, the best-fitted copulas (e.g., Frank copula; Figure 5-3) were selected based on the smallest Akaike Information Criterion (AIC) and Bayesian Information Criterion (BIC) statistics (Miao et al., 2016; Tosunoglu & Singh, 2018).

The largest log-likelihood statistics were then used to confirm the selection of copulas (Nelsen, 2006).

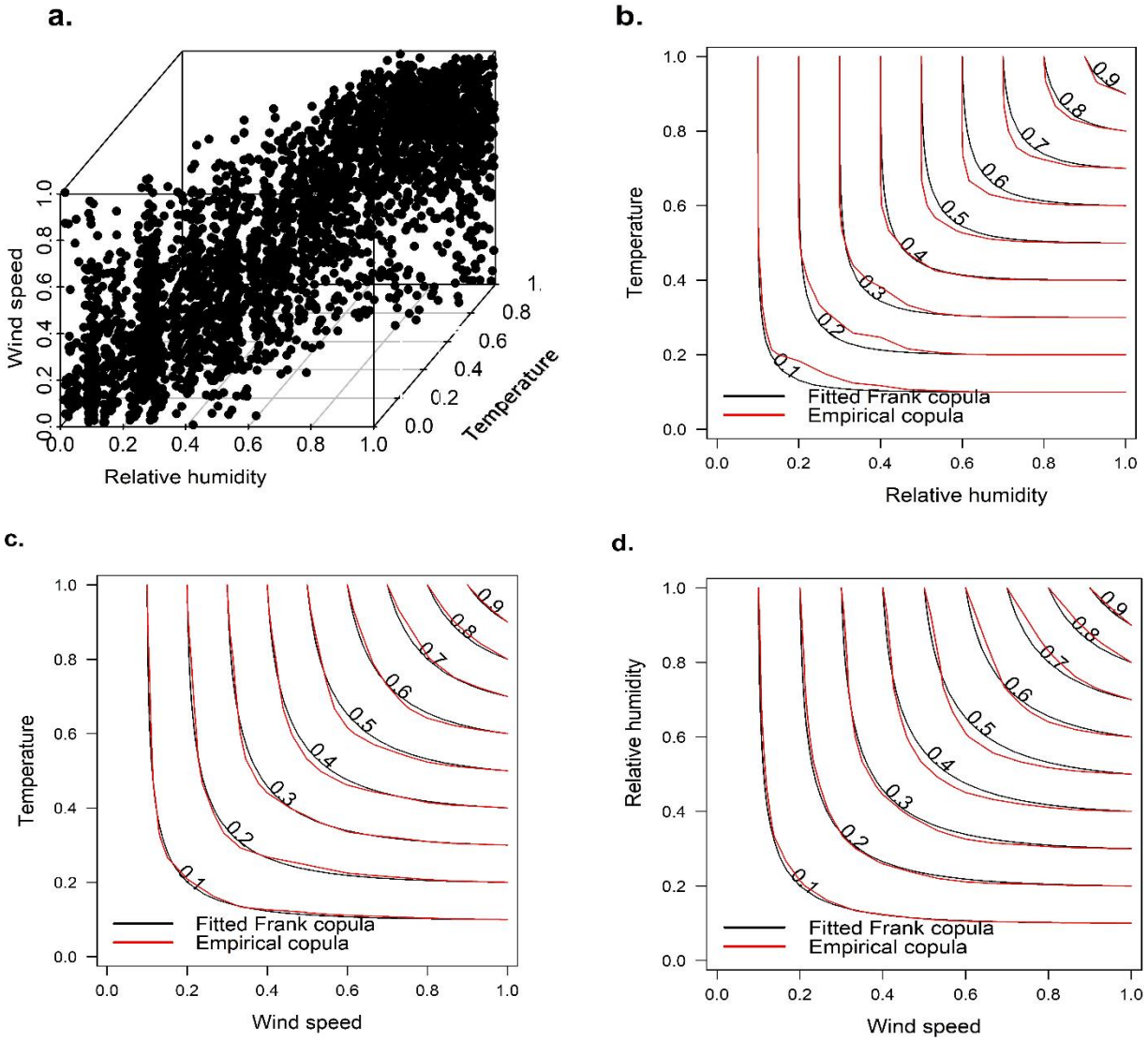

Figure 6-3. The 3-dimensional distribution of normally transformed temperature, relative humidity, and wind speed (a) and the contour plots of fitted and empirical copula for temperature and relative humidity (b), temperature and wind speed (c), and relative humidity and wind speed (d) for the station located at Brownsville in Texas at 97.4°W and 25.9°N. Frank copula was the best-fitted copula for all three bivariate random variable combinations (b-d) and the trivariate random variables.

After fitting the best copula for each year and each station, the exceedance probability was given by Eq.3. The frequency of extreme HDWs was calculated using both empirical (counting) and copula methods. The limitations of the empirical approach are that it needs a long period of data and cannot describe the compound interaction among the contributing variables (Hao et al., 2018). Compared to copula, an empirical method has a higher uncertainty when calculating the probability of extreme events (Hao et al., 2018; Zscheischler & Seneviratne, 2017).

This research compares the probability of extreme events calculated from both the empirical method and the copula model. In addition, the dependence between variables was calculated. Regular correlation methods (e.g., Pearson, Spearman, and Kendall) indicate the dependence on a full range of data (Helsel & Hirsch, 2002; Maritz, 1995) and does not consider the influence of variable distribution function on correlation (Hofert et al., 2018). However, the measure of association, developed for each copula family, can calculate the dependence among variables after transforming the data variables to a standard uniform distribution (Hofert et al., 2018). In this study, both regular correlation methods and the measure of associations (Spearman and Kendall; http://copula.r-forge.r-project.org/) were calculated and the impact of dependence on the probability of compound extremes was analyzed. For trivariate cases, when all three variables are considered together, the measure of associations (τ_{XYZ}) was calculated as the average of corresponding pairwise coefficients (Genest et al., 2011; Nelsen, 1996).

$$\tau_{XYZ} = \frac{1}{3}(\tau_{XY} + \tau_{XZ} + \tau_{YZ}) \qquad (4)$$

where for example the τ_{XY}, τ_{XY}, and τ_{XY} denote Kendall's tau for a bivariate measure of associations between pairwise variables (e.g., temperature and wind speed).

The Mann-Kendall test (Kendall, 1975; Mann, 1945), was used to identify any monotonic trends in the time series. In addition, the two-sample Kolmogorov-Smirnov (K-S) test (Massey Jr, 1951) was used to recognize the differences between the cumulative distribution functions (CDFs) of single and compound extreme events values for the two 35-year sub-periods: 1949–1983 and 1984–2018.

Results

Empirical vs copula

An important step in employing copulas to model the dependence between stochastic variables is the selection of a copula that best fits the data. Trivariate copulas were selected based on the lowest AIC and BIC and the greatest log-likelihood for the entire period (70-year data) and each year, separately. Considering the entire period (1949–2018), Student-t copula was the best fit for the majority of stations (89%). When analyzing each year separately, Student-t copula (74%) and Frank copula (20%) were the best-fitted trivariate families.

Counting the number of events when wind speed and temperature are both higher than their 90^{th} percentile and relative humidity is simultaneously less than its 10^{th} percentile threshold, is a relatively straightforward approach to calculate the probability of HDWs. This empirical approach (Hao et al., 2018) has been used to analyze the co-occurrence of compound or consecutive multiple extremes (Beniston, 2009; Fischer & Knutti, 2013; Hao et al., 2013; Morán-Tejeda et al., 2013). The limitations with the empirical method include the shortcoming of data because the empirical approach requires a long dataset to assess the change of HDWs and its disability to model the dependence among variables (Hao et al., 2018). For example, if relative humidity, temperature, and wind speed are independent, for 3672 data pairs (hourly data for one warm-season) there would be an average of only 4 compound HDWs each year based on

the 90th and 10th percentile thresholds (0.1*0.1*0.1*3672=3.7). Relative humidity, temperature, and wind speed could be considered independent in stations with less than annual 3.7 HDWs per warm season. In this study, the simple empirical approach was not done due to how HDWs were defined in previous research. The expected number of HDW events per year based on the 90th and 10th percentiles (3.7) should be different than what was determined using fixed thresholds that seem to matter given plant physiology.

After fitting the best trivariate copula on the data, the probability of compound HDWs was calculated for each station. Given that the fixed thresholds of 35°C for temperature, 30% for relative humidity, and 7m/s for wind speed matter for agricultural crops, the probability of HDWs was calculated using the fixed thresholds. To test the robustness of the fitted copulas, the co-occurrence of HDWs was also calculated based on the empirical method. Both of the approaches lead to a similar spatial pattern in the results with the highest probability of HDWs in the region extending from southwest Kansas into northwest Texas (Figure 5-4). The copula approach documented a higher risk of annual HDWs for the majority of stations (96%). For the central United States and particularly for the stations with the highest probability of HDWs located from Texas into Kansas (Figure 5-4, hotspots: surrounded by the dashed line), higher numbers of HDWs were determined during the drought years in 2011 and 1980 based on both statistical approaches. Data from the weather station located at Dodge City, in southwest Kansas, showed the highest probability of HDWs using both approaches (Figure 5-4).

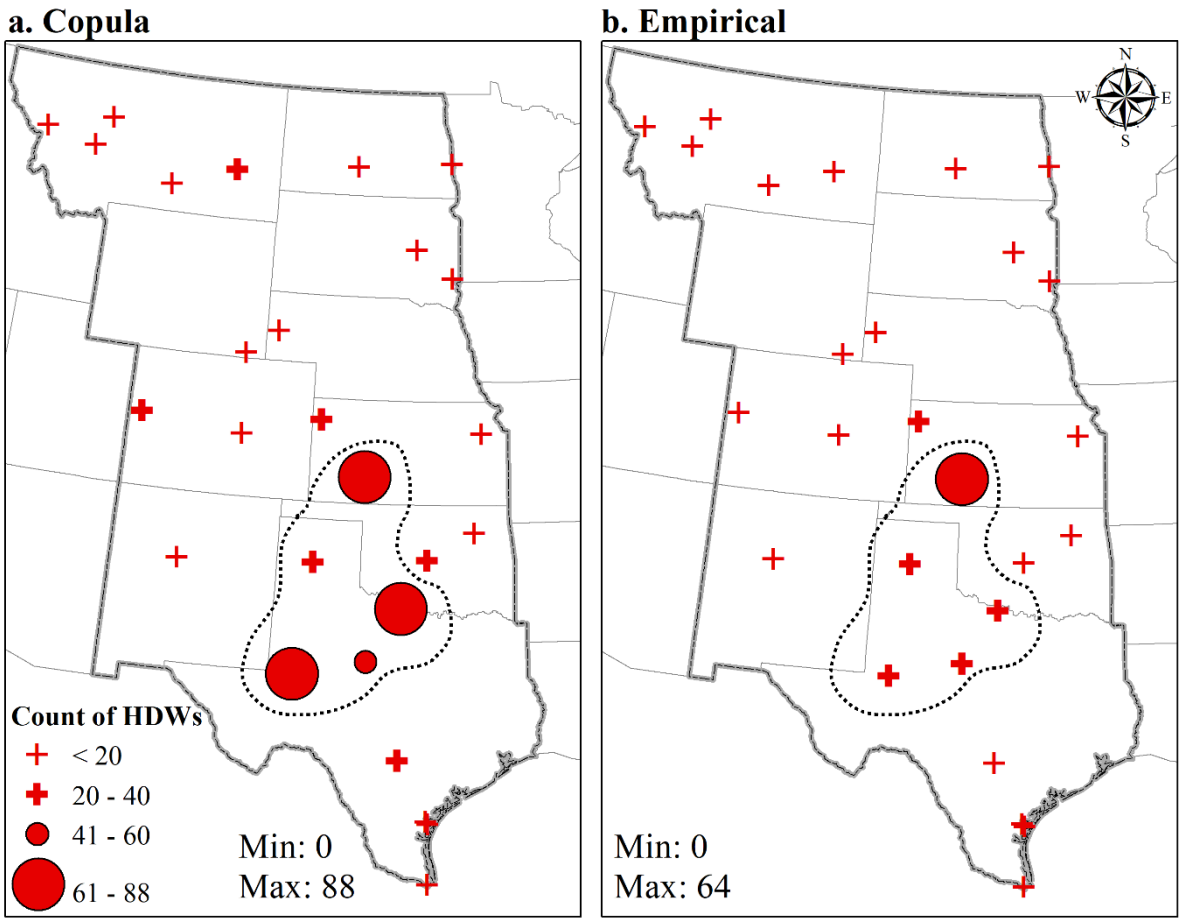

Figure 6-4. The annual co-occurrence of HDWs in the central United States based on copula (a) and empirical (b) methods. Percentiles used in the copula analysis correspond to the same fixed thresholds that were applied for the empirical method. Stations surrounded by the dashed line are the ones with the highest probability of HDWs (the southern Great Plains hotspot).

Variability of percentiles corresponding to the fixed thresholds

The spatial variability of the computed percentiles corresponding to the fixed thresholds of 35°C for temperature, 30% for relative humidity, and 7m/s for wind speed was analyzed. The values of the percentiles have different spatial patterns. For temperature, the spatial pattern of differences in the value of percentiles corresponding to 35°C is very small with a minimum of 91st percentile in the North Texas and a maximum of 100th in the northeast (North Dakota and South Dakota) and to the east of the Rocky Mountains in Colorado and Montana (Figure 5-5a).

In these regions, 35°C is considerably higher than the local 90th percentile of temperature and the overall comparatively low temperatures limit the occurrence of HDWs. For relative humidity, the lowest percentile values are located in the western half of the Great Plains (Figure 5-5b). The percentile corresponding to 30% relative humidity is very close to zero in coastal south Texas that limits the frequency of HDWs. For wind (Figure 5-5c), the percentiles ranged from 68th percentile in southwest Kansas to the 93rd percentile in Montana. The 68th percentile for wind speed at the southwest Kansas station demonstrates the relatively high probability of wind speed exceeding 7m/s. Temperature is the variable that is most limiting for the co-occurrence of these compound events across the central United States (Figure 5-5a). Hypothetically, in stations where the temperature percentile is lower, then more HDWs are expected. However, along the Texas coast, only wind speed and temperature meet the criteria for HDWs, since humid air from the Gulf of Mexico increases atmospheric water vapor in the Great Plains (Durán-Quesada et al., 2010) and limits the probability occurrence of HDWs.

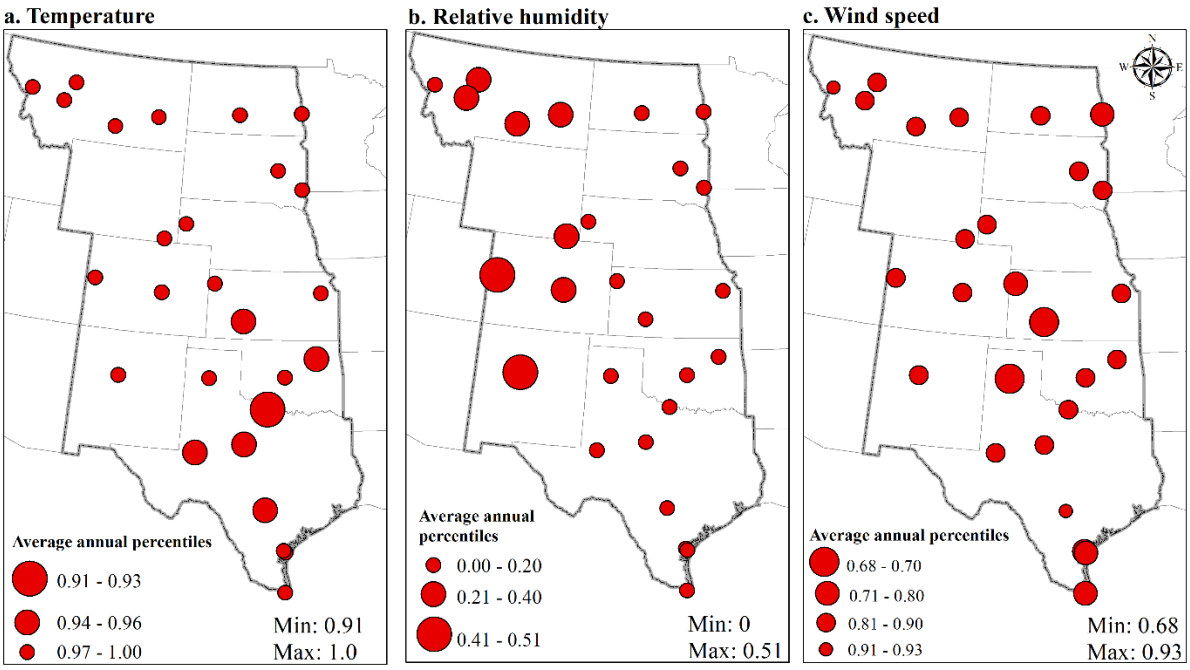

Figure 6-5. Annual averages of the percentiles corresponding to a temperature of 35°C (a), a relative humidity of 30% (b), and a wind speed of 7m/s (c).

Dependence among variables

Pearson and Mann-Kendall tests were used to calculate the association between variables and analyze the influence of correlation on the probability of HDW events. The strongest and weakest linear correlation values were discovered between temperature and relative humidity (the inverse correlation values ranged from 0.48 to 0.82), and temperature and wind (the positive correlation values ranged from 0.0 to 0.57), respectively. To eliminate the influence of climate change on the long-term trends of variables used in this study, all three variables were de-trended linearly and correlations were re-calculated for the de-trended data. The Student-*t* test results indicated no statistically significant difference between the correlation values calculated based on the original and de-trended data. Calculated Mann-Kendall correlation values (Figure 5-6) indicate a strong association between temperature and relative humidity (the inverse correlation values ranged from 0.33 to 0.66), especially in the south (Texas) and northwest (Montana). The

correlation between temperature and wind (the positive correlation values ranged from 0.0 to 0.45) and wind and relative humidity (the inverse correlation values ranged from 0.05 to 0.44) was stronger in south Texas and northeast Kansas (Figure 5-6). Calculating the measure of association based on fitted copula showed the same relationship between pairwise variables. The Student-*t* test results showed no statistically significant difference between the correlation values and the measure of association values.

Considering the percentile thresholds, the highest probability of HDWs was found for stations with higher correlation values among the three sets of bivariate random variables in southern Texas (Figure 5-6). Although the highest correlation will increase the probability of events (Zhou & Liu, 2018; Zscheischler & Seneviratne, 2017), generally higher humidity near the Gulf of Mexico would limit the prospect of experiencing a HDW event defined based on fixed thresholds in southern Texas. Results demonstrate no influence of correlation on the probability of compound HWDs when using the fixed thresholds. Calculating the trivariate Kendall dependence among variables (applying equation 4) and based on the best-fitted copula for each station in each year, the lowest dependency between variables was observed in western New Mexico and Colorado. The highest trivariate dependence was found in southern Texas. Again, no relationship was found between the dependence among variables and the highest frequency of HDWs.

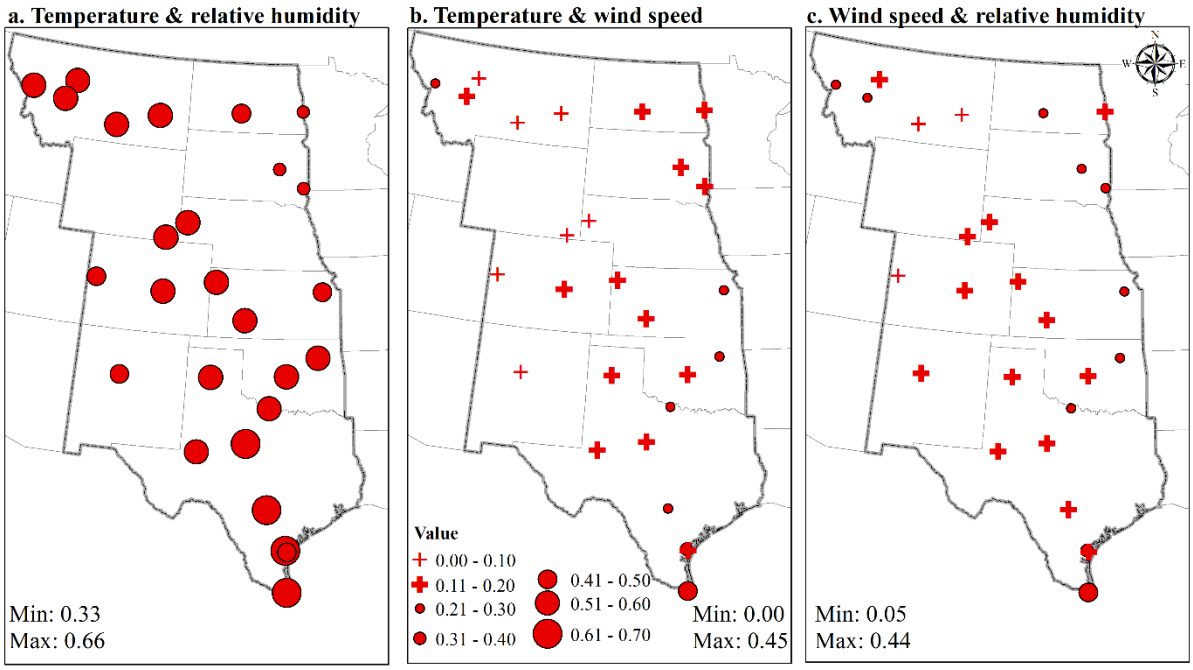

Figure 6-6. Mann-Kendall correlation values between temperature, wind speed, and relative humidity. The correlation values are negative between temperature and relative humidity, and wind speed and relative humidity. The highest and lowest correlation was discovered between temperature and relative humidity (a) and temperature and wind speed (b), respectively.

Pairwise probability between variables

The copula approach was also used to model the bivariate relationship between randomly distributed variables. Among all six analyzed families, Frank copula was the best-fitted family for a majority (69%) of stations for all these pairs. First, the dependence was calculated based on the best-fitted bivariate copula. Then, the fixed thresholds were used to calculate the bivariate co-occurrence probability of variables. The highest probability of compound high temperature and low humidity was discovered in a region that extends from northwest Texas into southwestern Kansas (Figure 5-7a). The probability decreased toward the northwest and northeast. A similar pattern of change in the bivariate co-occurrence probability was found for temperature and wind speed (Figure 5-7b).

Although the occurrence probability of simultaneous moderate-speed winds and low humidity is higher in western Great Plains (Borchert, 1950), however, low temperature in northern sections of these regions (Fig 7a-b) limits the occurrence of HDWs. Comparing the calculated bivariate probabilities (Figure 5-7) with correlations (Figure 5-6) suggests no relationship between the variable inter-dependence and the probability of compound events. In principle, although variables, especially temperature and relative humidity, were well correlated, the extremes of the variables may not co-occur since there was no tail dependence (Nelsen, 2006). Unlike previous studies that showed the effect of the high correlation between precipitation and temperature on the co-occurrence of extreme events (Zhou & Liu, 2018; Zscheischler & Seneviratne, 2017), here no influence of correlation among variables on the frequency of compound HDWs was discovered. This finding likely relates to the lack of dependence as exhibited by using the percentiles corresponding to the fixed thresholds. In addition, previous studies (Zhou & Liu, 2018; Zscheischler & Seneviratne, 2017) assessed the concurrency of other combinations of variables, such as low precipitation and high temperature. However, in this study of HDWs, the diverse nature of wind speed and humidity influence the results.

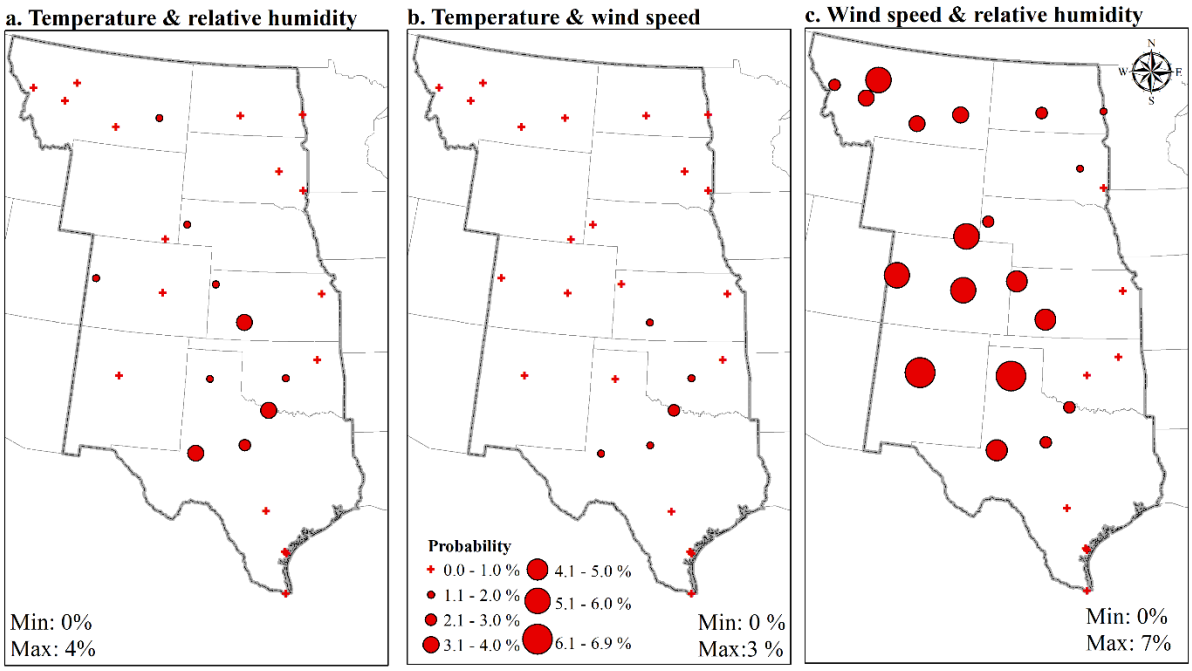

Figure 6-7. The annual co-occurrence probability of extreme temperature and relative humidity (a), temperature and wind (b), and wind and relative humidity (c) in the central United States. The threshold was defined based on the temperature higher than 35 ℃, relative humidity less than 30%, and the wind speed higher than 7m/s.

Temporal changes of HDWs

The changes in the probability of HDWs were analyzed over the two 35-year sub-periods individually. K-S test results revealed no difference in the distribution of HDWs over two periods for a majority of stations. Except for five stations (18.5%) that had a statistically significant different distribution in the second 35-year period (Table 1), most stations had no significant change over time. Mann-Kendall trend test results indicate a significant trend in the frequency of HDWs in 44% (33% positive) of stations (Table 1). Stations with the highest frequency of HDWs (hotspots; Figure 5-4) had a nonsignificant, but upward trend.

To better understand the effects of individual variables on the variability of HWDs, the number of extreme hot (temperature higher than 35°C), dry (relative humidity less than 30%), and windy (wind speed higher than 7m/s) events were calculated for each station. The frequency

of occurrence of events varied across the stations, with between 1-28, 2-171, and 237-1109 hourly events per warm season for HDWs, respectively. Hot extremes with the lowest number of events were considered as the primary limiting parameter for HWD in the central United States. The highest frequency of both hot or windy events was found at stations in Texas and Kansas. For dry events, the greatest frequency was observed in the western half of the study area, in Colorado, New Mexico, and Montana.

Mann-Kendall trend test results indicate an upward trend in extreme hot events in the majority (89%, 52% significant) of stations mainly over the western Great Plains (Figure 5-8, Table 5-1). Two stations (7%) in the eastern Dakotas had significant downward trends for hot events. The majority of stations (67%, 11% significant) had an upward trend in the frequency of dry events. In the east and northeast, the trend of dry events was mostly decreasing. Windy events indicated a downward trend in a majority of the study area (85%, 52% significant; Figure 5-8, Table 5-1).

Table 6-1. Two-sample K-S test for changes in extreme HWD events in the central United States between 1949–1983 and 1984–2018. P-values smaller than 0.05 indicate that the two distributions are significantly different. The plus and minus signs in the D Statistics column indicate if the period 1984–2018 had higher or lower frequency of HDWs compared to 1949–1983. The Mann-Kendall trend test indicates the temporal changes of compound (HDW) and single (hot, dry, or windy) extreme events. Values show the slope of the linear fit on data. The bold values indicate a significant trend with α=0.05. The location of stations is indicated by station ID in Figures 1 and 8.

Station ID	K-S test		The Mann-Kendall trend tests for extreme events			
	D Statistics	*P*-value	HDWs	Hot events	Dry events	Windy events
1	0.26	0.20	**0.01**	**0.87**	0.05	**-5.42**
2	0.29	0.11	**0.06**	**1.32**	0.17	-1.23
3	0.26	0.20	0.08	**1.50**	-0.06	-0.99
4	**0.43**$^{+}$	**0.00**	**0.90**	**2.51**	3.49	**4.17**
5	0.11	0.98	0.05	0.78	-0.09	**-2.60**
6	0.20	0.49	0.08	0.23	0.64	2.34
7	0.09	1.00	0.07	1.08	0.35	**-4.70**
8	0.11	0.98	-0.02	0.72	-0.18	-1.43
9	0.20	0.49	0.40	**0.89**	2.34	1.95
10	0.20	0.49	-0.02	0.04	1.19	-0.19
11	0.17	0.69	0.15	0.84	0.09	**-3.09**
12	0.17	0.68	-0.17	**0.35**	-0.48	**-8.67**
13	0.14	0.87	-0.04	0.16	-0.87	**-2.12**
14	0.17	0.68	0.03	**0.05**	1.19	0.13
15	0.26	0.20	**0.26**	**1.15**	4.64	-1.38
16	0.23	0.32	**0.01**	**0.01**	1.48	**-4.51**
17	0.29	0.11	**0.20**	**0.64**	1.97	**-2.42**
18	**0.40**$^{-}$	**0.01**	**-0.07**	**-0.14**	**-1.50**	-1.02
19	**0.43**$^{-}$	**0.00**	**-0.17**	-0.30	**-1.62**	**-5.64**
20	0.29	0.11	0.07	**0.26**	**4.37**	**-2.57**
21	**0.34**$^{-}$	**0.03**	**-0.03**	**-0.11**	-0.29	**-5.20**
22	0.17	0.68	-0.02	0.02	-0.91	**-4.72**
23	**0.54**$^{+}$	**0.00**	**0.15**	**0.31**	**5.87**	-0.68
24	0.31	0.06	**0.09**	**0.22**	**4.07**	-0.61
25	0.23	0.32	**0.07**	**0.18**	0.25	**-4.47**
26	0.26	0.20	0.08	0.30	2.01	**-1.03**
27	0.14	0.87	0.00	0.05	0.02	-7.02

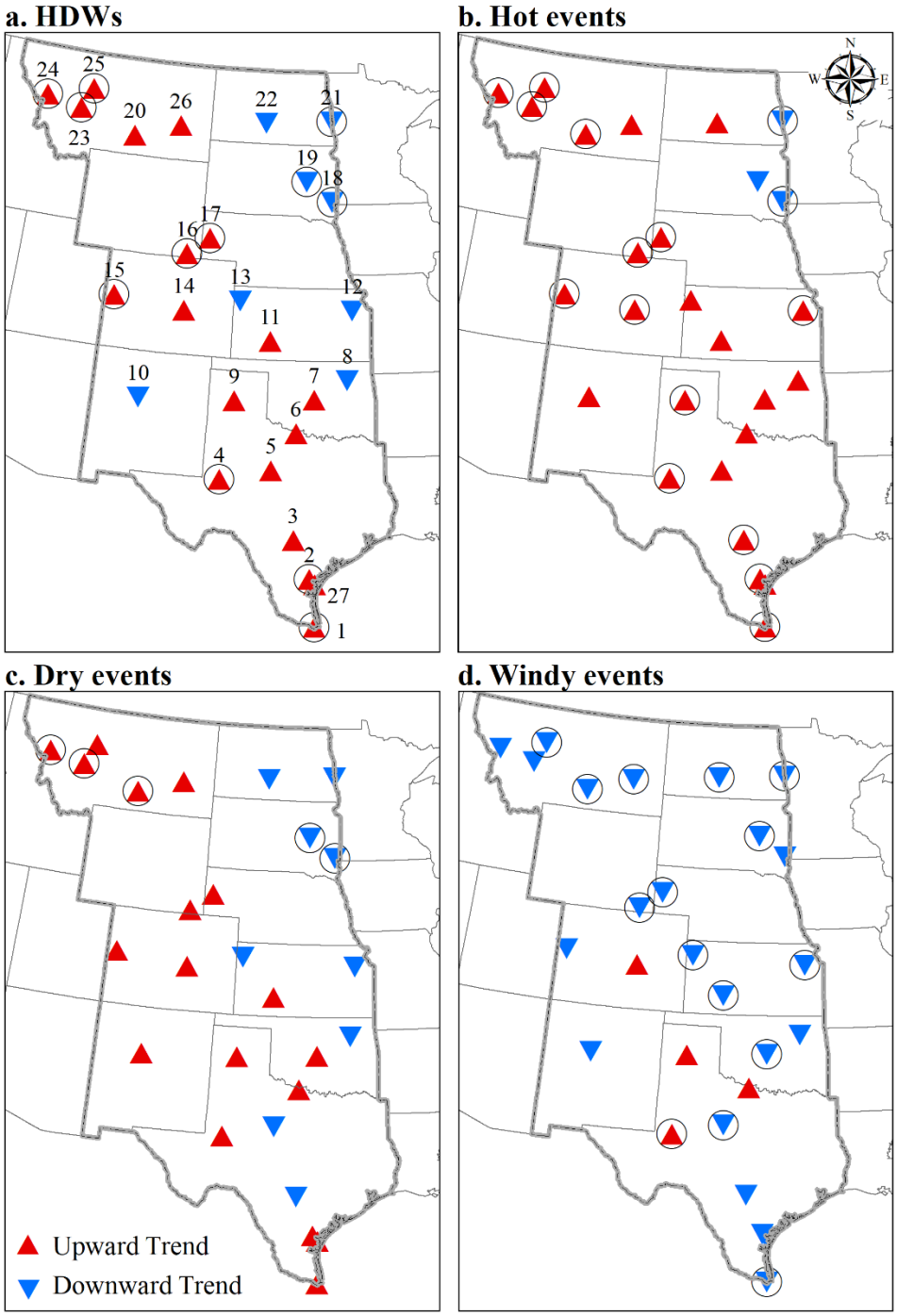

Figure 6-8. Spatial patterns of 70-year temporal trends for extreme HDWs (a), hot events (b), dry events (c), and windy events (d) in the central United States. Circled symbols indicate a significant trend (α=0.05).

Discussion

A warmer world (Easterling et al., 2000; Hartmann et al., 2013; Perkins et al., 2012) might naturally lead to an increase in the probability of compound extremes (Aghakouchak et al., 2014) or intensify the severity of other extreme events that involve temperature such as drought (MacDonald et al., 2016; Trenberth et al., 2013). Warmer temperatures initially increase evapotranspiration rates; but as soils dry, there is a reduction in evaporative cooling (Seneviratne et al., 2010). The greener vegetated lands in higher latitudes with longer growing seasons and higher transpiration rates (Wolf et al., 2016) are expected to see a rise in temperature related to a decrease in soil moisture and a change in the partitioning of energy between latent and sensible heat fluxes (Alexander, 2011). Accompanying with the hotter and drier conditions, moderate winds are expected to increase evapotranspiration (Derrel et al., 1993), increase plant damage (Curtis, 1891; Wang et al., 2016; Yang & Wang, 1978), and create environments more favorable for the spread of wildfire (Flannigan & Harrington, 1988; Jolly et al., 2015; Srock et al., 2018).

The highest risk of HDWs mirrors the highest risk of the extremely hot and windy conditions. Strengthening of the dependence between variables did not influence the co-occurrence of HDWs in the central United States (Figures 5-4 and 5-6). The region extending from southwest Kansas into northwest Texas was identified as a hotspot (Figure 5-4) where a higher occurrence of HDWs is expected, coinciding with a region of faster speeds (Archer & Jacobson, 2003; DeHarpporte, 1984; Elliott et al., 1986; Klink, 1999). Temperature and wind are respectively the most and the least limiting variables that control the occurrence of HDWs in the central United States (Figure 5-5). HDWs occurred more frequently in 1980 and 2011, with the co-occurrence of drought and a heatwave (Hoerling et al., 2013; Karl & Quayle, 1981; NOAA NCEI, 2019). Despite not finding a significant trend in droughts, Mazdiyasni and AghaKouchak

(2015) found a substantial increase in concurrent heatwave and drought during 1960–2010 in the United States. This increase may trigger more HDWs when moderate-speed winds occur simultaneously with compound hot and dry conditions.

Results from this study demonstrate that, although wind speeds at the 90^{th} and 50^{th} percentile thresholds are decreasing in the Great Plains (Pryor et al., 2009), the increase of hot and dry events (Figure 5-8, Table 5-1) can potentially increase the risk of HDWs. The increase is more significant in the west, northwest, and the southern Great Plains portions of the study area (Figure 5-8). In the east and northeast, the temperature decrease corresponding to the "warming hole" (Meehl et al., 2012; Pan et al., 2004; Tavakol et al., 2020), along with a lower occurrence of windy and dry events, drops the risk of HDWs (Figure 5-8).

This study suggests that traditional empirical methods fall short in communicating the risk of compound HDWs in the central United States. Copula families with flexible dependence modeling are a better alternative for the analysis of climate extremes, since more than one variable is typically responsible for the extreme impacts (Leonard et al., 2014). However, the concept of copula has been defined based on the independent and identically distributed random variables with continuous univariate margins, with no expected ties to occur (Hofert et al., 2018; Nelsen, 2006). Yet, because of the lack of precise measurements and rounding, it is common to observe ties in data in practice. This study acknowledges the crucial influence of ties in distinguishing copula families (Hofert et al., 2018).

References

Aghakouchak, A., Cheng, L., Mazdiyasni, O., & Farahmand, A., 2014. Global warming and changes in risk of concurrent climate extremes: Insights from the 2014 California drought. *Geophysical Research Letters.* 41: 8847-8852. http://doi.org/10.1002/2014GL062308

Alexander, L. 2011. Climate science: Extreme heat rooted in dry soils. *Nature Geoscience.* 4: 12-13. https://doi.org/10.1038/ngeo1045

Archer, C. L.& Jacobson, M. Z., 2003. Spatial and temporal distributions of US winds and wind power at 80 m derived from measurements. *Journal of Geophysical Research: Atmospheres.* 108: http://www.doi.org/10.1029/2002JD002076

Beniston, M. 2009. Trends in joint quantiles of temperature and precipitation in Europe since 1901 and projected for 2100. *Geophysical Research Letters.* 36: n/a.

Bevacqua, E., Maraun, D., Hobæk Haff, I., Widmann, M., & Vrac, M., 2017. Multivariate statistical modelling of compound events via pair-copula constructions: analysis of floods in Ravenna (Italy). *Hydrology and Earth System Sciences.* 21: 2701-2723. https://doi.org/10.5194/hess-21-2701-2017

Borchert, J. R. 1950. The climate of the central North American grassland. *Annals of the Association of American Geographers.* 40: 1-39. http://www.doi.org/10.1080/00045605009352020

Curtis, G. E. 1891. The hot winds of the plains. *Seventh Biennial Report, Kansas Department of Agriculture.* 7: 162-183. https://www.kansasmemory.org/item/225333

DeHarpporte, D. 1984. West and southwest wind atlas. *Van Nostrand Reinhold Company.* New York, USA. 120p.

Derrel, M. L., Gilley, J. R., & Baumer, O. W., 1993. Irrigation Handbooks and Manuals (Part 623, Chapter 2) Irrigation Water Requirements. *United States Department of Agriculture.* Washington, DC, USA. https://www.nrcs.usda.gov/wps/portal/nrcs/detailfull/national/water/manage/irrigation/?cid=stelprdb1045075.

Dunn, R. J., Willett, K. M., Parker, D. E., & Mitchell, L., 2016. Expanding HadISD: quality-controlled, sub-daily station data from 1931. *Geoscientific Instrumentation, Methods and Data Systems.* 5: 473-491. http://www.doi.org/10.5194/gi-5-473-2016

Dunn, R. J., Willett, K. M., Thorne, P. W., Woolley, E. V., Durre, I., Dai, A., ..., and Vose, R. E., 2012. HadISD: a quality-controlled global synoptic report database for selected variables at long-term stations from 1973--2011. *arXiv Preprint arXiv:1210.7191.* htpp://www.doi.org/10.5194/cp-8-1649-2012

Durán-Quesada, A. M., Gimeno, L., Amador, J. A., & Nieto, R., 2010. Moisture sources for Central America: Identification of moisture sources using a Lagrangian analysis technique. *Journal of Geophysical Research: Atmospheres.* 115: https://doi.org/10.1029/2009JD012455

Easterling, G., Meehl, C., Parmesan, S. A., Changnon, T., Karl, L., & Mearns, L., 2000. Climate extremes: Observations, modeling, and impacts. *Science (Washington).* 289: 2068-2074. http://science.sciencemag.org/content/289/5487/2068

Elliott, D. L., Holladay, C. G., Barchet, W. R., Foote, H. P., & Sandusky, W. F., 1986. Wind energy resource atlas of the United States. *U.S. Department of Energy.* Colorado, USA. https://rredc.nrel.gov/Wind/pubs/atlas/.

Fischer, E. M.& Knutti, R., 2013. Robust projections of combined humidity and temperature extremes. *Nature Climate Change.* 3: 126. https://doi.org/10.1038/nclimate1682

Flannigan, M. D.& Harrington, J. B., 1988. A study of the relation of meteorological variables to monthly provincial area burned by wildfire in Canada (1953–80). *Journal of Applied Meteorology.* 27: 441-452. https://doi.org/10.1175/1520-0450(1988)0272.0.CO;2

Genest, C., Nešlehová, J., & Ben Ghorbal, N., 2011. Estimators based on Kendall's tau in multivariate copula models. *Australian & New Zealand Journal of Statistics.* 53: 157-177. https://doi.org/10.1111/j.1467-842X.2011.00622.x

Hao, Z., AghaKouchak, A., & Phillips, T. J., 2013. Changes in concurrent monthly precipitation and temperature extremes. *Environmental Research Letters.* 8: 034014. http://www.doi.org/10.1088/1748-9326/8/3/034014

Hao, Z., Singh, V., & Hao, F., 2018. Compound extremes in hydroclimatology: a review. *Water.* 10: 718. https://doi.org/10.3390/w10060718

Hartmann, D. L., Tank, A. M. K., Rusticucci, M., Alexander, L. V., Brnnimann, S., Charabi, Y. A. R., ..., and Kaplan, A., 2013. Observations: Atmosphere and surface. *In: Climate change 2013 the physical science basis: Working group I contribution to the fifth assessment report of the intergovernmental panel on climate change.* (pp. 159-254). Cambridge University Press. Cambridge, United Kingdom and New York, NY, USA.

Helsel, D. R., & Hirsch, R. M., 2002. Statistical methods in water resources. *Techniques of Water Resources Investigations of the United States Geological Survey (2002).* 522p.

Hoerling, M., Kumar, A., Dole, R., Nielsen-Gammon, J. W., Eischeid, J., Perlwitz, J., ..., and Chen, M., 2013. Anatomy of an extreme event. *Journal of Climate.* 26: 2811-2832. https://doi.org/10.1175/JCLI-D-12-00270.1

Hofert, M., Kojadinovic, I., Machler, M., & Yan, J., 2018. Elements of copula modeling with R. *Springer.* Berlin, Germany. 267p.

Jolly, W. M., Cochrane, M. A., Freeborn, P. H., Holden, Z. A., Brown, T. J., Williamson, G. J., & Bowman, D. M., 2015. Climate-induced variations in global wildfire danger from 1979 to 2013. *Nature Communications.* 6: 7537. https://doi.org/10.1038/ncomms8537

Kao, S.& Govindaraju, R. S., 2010. A copula-based joint deficit index for droughts. *Journal of Hydrology.* 380: 121-134. https://doi.org/10.1016/j.jhydrol.2009.10.029

Karl, T. R.& Quayle, R. G., 1981. The 1980 summer heat wave and drought in historical perspective. *Monthly Weather Review.* 109: 2055-2073. https://doi.org/10.1175/1520-0493(1981)1092.0.CO;2

Kendall, M. G. 1975. Rank Correlation Measures. *Charles Griffin.* London, UK. 202p.

Klink, K. 1999. Climatological mean and interannual variance of United States surface wind speed, direction and velocity 1. *International Journal of Climatology: A Journal of the Royal Meteorological Society.* 19: 471-488. https://doi.org/10.1002/(SICI)1097-0088(199904)19:53.0.CO;2-X

Leathers, N.& Harrington, J., 2001. Furnace winds of the West. *Journal of the West.* 40: 48-57.

Leonard, M., Westra, S., Phatak, A., Lambert, M., van den Hurk, B., McInnes, K., ..., and Stafford-Smith, M., 2014. A compound event framework for understanding extreme impacts. *Wiley Interdisciplinary Reviews: Climate Change.* 5: 113-128. https://doi.org/10.1002/wcc.252

Liu, Y., Cheng, Y., Zhang, X., Li, X., & Cao, S., 2018. Combined Exceedance Probability Assessment of Water Quality Indicators Based on Multivariate Joint Probability Distribution in Urban Rivers. *Water.* 10: 971. https://doi.org/10.3390/w10080971

Lydolph, P. E. 1964. The russian sukhovey. *Annals of the Association of American Geographers.* 54: 291-309. https://doi.org/10.1111/j.1467-8306.1964.tb00490.x

Lydolph, P. E.& Williams, T. B., 1982. The North American Sukhovey. *Annals of the Association of American Geographers.* 72: 224-236. https://doi.org/10.1111/j.1467-8306.1982.tb01821.x

MacDonald, G. M., Moser, K. A., Bloom, A. M., Potito, A. P., Porinchu, D. F., Holmquist, J. R., ..., and Kremenetski, K. V., 2016. Prolonged California aridity linked to climate warming and Pacific sea surface temperature. *Scientific Reports.* 6: 33325. https://doi.org/10.1038/srep33325

Mann, H. B. 1945. Nonparametric tests against trend. *Econometrica: Journal of the Econometric Society.* 13: 245-259. http://www.jstor.org/stable/1907187

Maritz, J. S. 1995. Distribution-free statistical methods. *Chapman and Hall.* London, UK. 276p.

Massey Jr, F. J. 1951. The Kolmogorov-Smirnov test for goodness of fit. *Journal of the American Statistical Association.* 46: 68-78.

Mazdiyasni, O., & Aghakouchak, A., 2015. Substantial increase in concurrent droughts and heatwaves in the United States. *Proceedings of the National Academy of Sciences.* 112: 11484-11489. https://doi.org/10.1073/pnas.1422945112

Meehl, G. A., Arblaster, J. M., & Branstator, G., 2012. Mechanisms contributing to the warming hole and the consequent US east–west differential of heat extremes. *Journal of Climate.* 25: 6394-6408. https://doi.org/10.1175/JCLI-D-11-00655.1

Miao, C., Sun, Q., Duan, Q., & Wang, Y., 2016. Joint analysis of changes in temperature and precipitation on the Loess Plateau during the period 1961– 2011. *Climate Dynamics; Observational, Theoretical and Computational Research on the Climate System.* 47: 3221-3234. http://doi.org/10.1007/s00382-016-3022-x

Morán-Tejeda, E., Herrera, S., López-Moreno, J. I., Revuelto, J., Lehmann, A., & Beniston, M., 2013. Evolution and frequency (1970–2007) of combined temperature–precipitation modes in the Spanish mountains and sensitivity of snow cover. *Regional Environmental Change.* 13: 873-885. https://doi.org/10.1007/s10113-012-0380-8

Nelsen, R. B.1996. Nonparametric measures of multivariate association. *In: Distributions with fixed marginals and related topics.* (pp. 223– 232). Inst. Math. Statist. Hayward , CA.

Nelsen, R. B. 2006. An introduction to copulas (Springer series in statistics). *Springer New York.* Portland, OR, USA. 275p.

NOAA NCEI. (2019). Billion-dollar weather and climate disasters. Retrieved from https://www.ncdc.noaa.gov/billions; 3/9/2019.

Otkin, J. A., Svoboda, M., Hunt, E. D., Ford, T. W., Anderson, M. C., Hain, C., & Basara, J. B., 2018. Flash droughts: A review and assessment of the challenges imposed by rapid-onset droughts in the United States. *Bulletin of the American Meteorological Society.* 99: 911-919. https://doi.org/10.1175/BAMS-D-17-0149.1

Pan, Z., Arritt, R. W., Takle, E. S., Gutowski, W. J., Anderson, C. J., & Segal, M., 2004. Altered hydrologic feedback in a warming climate introduces a "warming hole". *Geophysical Research Letters.* 31: L17109. https://doi.org/10.1029/2004GL020528

Paprotny, D., Vousdoukas, M. I., Morales-Nápoles, O., Jonkman, S. N., & Feyen, L., 2018. Compound flood potential in Europe. *Hydrol.Earth Syst.Sci.Discuss.* 2018: 1-34. https://doi.org/10.5194/hess-2018-132

Perkins, S. E., Alexander, L. V., & Nairn, J. R., 2012. Increasing frequency, intensity and duration of observed global heatwaves and warm spells. *Geophysical Research Letters.* 39: n/a. https://doi.org/10.1029/2012GL053361

Pryor, S. C., Barthelmie, R. J., Young, D. T., Takle, E. S., Arritt, R. W., Flory, D., ..., and Roads, J., 2009. Wind speed trends over the contiguous United States. *Journal of Geophysical Research: Atmospheres.* 114: http://www.doi.org/10.1029/2008JD011416

Sadegh, M., Ragno, E., & AghaKouchak, A., 2017. Multivariate C opula A nalysis T oolbox (MvCAT): Describing dependence and underlying uncertainty using a B ayesian framework. *Water Resources Research.* 53: 5166-5183. https://doi.org/10.1002/2016WR020242

Salvadori, G., Durante, F., & De Michele, C., 2011. On the return period and design in a multivariate framework. http://dx.doi.org/10.5194/hess-15-3293-2011

Schlenker, W., Hanemann, W. M., & Fisher, A. C., 2006. The impact of global warming on US agriculture: an econometric analysis of optimal growing conditions. *Review of Economics and Statistics.* 88: 113-125. https://doi.org/10.1162/rest.2006.88.1.113

Schlenker, W.& Roberts, M. J., 2009. Nonlinear temperature effects indicate severe damages to US crop yields under climate change. *Proceedings of the National Academy of Sciences.* 106: 15594-15598. https://doi.org/10.1073/pnas.0906865106

Seneviratne, S. I., Corti, T., Davin, E. L., Hirschi, M., Jaeger, E. B., Lehner, I., ..., and Teuling, A. J., 2010. Investigating soil moisture–climate interactions in a changing climate: A review. *Earth-Science Reviews.* 99: 125-161. https://doi.org/10.1016/j.earscirev.2010.02.004

Seneviratne, S. I., Nicholls, N., Easterling, D., Goodess, C. M., Kanae, S., Kossin, J., ..., and Zwiers, F. W., 2012. Changes in climate extremes and their impacts on the natural physical environment: An overview of the IPCC SREX report. *Cambridge University Press. Cambridge.* New York, NY, USA. 109-230p.

Serinaldi, F. 2016. Can we tell more than we can know? The limits of bivariate drought analyses in the United States. *Stochastic Environmental Research and Risk Assessment.* 30: 1691-1704. https://doi.org/10.1007/s00477-015-1124-3

Sharma, S.& Mujumdar, P., 2017. Increasing frequency and spatial extent of concurrent meteorological droughts and heatwaves in India. *Scientific Reports.* 7: 15582. https://doi.org/10.1038/s41598-017-15896-3

Srock, A., Charney, J., Potter, B., & Goodrick, S., 2018. The Hot-Dry-Windy Index: A New Fire Weather Index. *Atmosphere.* 9: 279. https://doi.org/10.3390/atmos9070279

Tavakol, A., Rahmani, V., & Harrington, J., 2020. Changes in the frequency of hot, humid days and nights in the Mississippi River Basin. *Int J Climatol.* 1-16. https://doi.org/10. 1002/joc.6484

Tosunoglu, F.& Singh, V. P., 2018. Multivariate modeling of annual instantaneous maximum flows using copulas. *Journal of Hydrologic Engineering.* 23: 04018003. https://doi.org/10.1061/(ASCE)HE.1943-5584.0001644

Trenberth, K. E., Dai, A., Gerard Van, D. S., Jones, P. D., Barichivich, J., Briffa, K. R., & Sheffield, J., 2013. Global warming and changes in drought. *Nature Climate Change.* 4: 17-22. https://doi.org/10.1038/nclimate2067

van den Hurk, B., van Meijgaard, E., de Valk, P., van Heeringen, K., & Gooijer, J., 2015. Analysis of a compounding surge and precipitation event in the Netherlands. *Environmental Research Letters.* 10: 035001. http://www.doi.org/10.1088/1748-9326/10/3/035001

Wahl, T., Jain, S., Bender, J., Meyers, S. D., & Luther, M. E., 2015. Increasing risk of compound flooding from storm surge and rainfall for major US cities. *Nature Climate Change.* 5: 1093. https://doi.org/10.1038/nclimate2736

Wang, S., Zheng, H., Liu, S., Miao, Y., & Li, J., 2016. Numerical study on the stomatal responses to dry-hot wind episodes and its effects on land-atmosphere interactions. *PloS One.* 11: e0162852. https://doi.org/10.1371/journal.pone.0162852

Wolf, S., Keenan, T. F., Fisher, J. B., Baldocchi, D. D., Desai, A. R., Richardson, A. D., ..., and Brunsell, N. A., 2016. Warm spring reduced carbon cycle impact of the 2012 US summer drought. *Proceedings of the National Academy of Sciences.* 113: 5880-5885. https://doi.org/10.1073/pnas.1519620113

Yang, Z.& Wang, S., 1978. The climatal analysis and forecast on Dry-hot wind at Guangzhong, Shaanxi. *Meterology Shaanxi.* 3: 6-13.

Zhou, P.& Liu, Z., 2018. Likelihood of concurrent climate extremes and variations over China. *Environmental Research Letters.* 13: 094023. https://doi.org/10.1088/1748-9326/aade9e

Zscheischler, J.& Seneviratne, S. I., 2017. Dependence of drivers affects risks associated with compound events. *Science Advances.* 3: e1700263. http://doi.org/10.1126/sciadv.1700263

Chapter 7 - **Summary and Conclusion**

United States is home to a wide variety of climates that are supposed to change in association with global warming. Scientific studies specify that climate change is causing extreme climate events to become more frequent, more intense, and longer-lasting (Easterling et al., 2000; Hartmann et al., 2013; Meehl & Tebaldi, 2004). Changes in the frequency and severity of extreme events have recently received much attention because of the exponential rise of related economic losses (Mora et al., 2018; NOAA NCEI, 2019a) and excess deaths (Dematte et al., 1998; Huang et al., 2010; Mora et al., 2018). Considerable efforts have been made to understand the nature and changes of climate extreme events in the past decades. However, this is still an emerging science that requires more research to improve the reliability of results considering the lack of long-term, high-quality data. Considering the profound impacts of climate extremes on key socio-economic sectors (e.g., agriculture), both human and natural systems might be vulnerable and exposed to concurrent extreme events more frequently (Mora et al., 2018). The overarching goal of this study was to address the research gaps outlined in Chapter 1 including the spatial and temporal changes in single and compound extreme events including length and frequency of heatwaves, extremely hot-humid days and nights, and hot, dry, and windy events. The following sections would help understanding single and compound extreme events in the central United States.

Based on the IPCC, in a changing climate, it is expected that the extremes will increase more than the average values (Hartmann et al., 2013). Extreme climate events merit further research to improve strategies and decision making processes for adapting to climate change. For example, although heatwaves have been studied in the United States (e.g., DeGaetano & Allen, 2002; Lyon & Barnston, 2017; Oswald & Rood, 2014; Oswald, 2018), limited work has studied

the changes in heatwave maximum duration. In the 21st century, longer-lasting heatwaves are expected (Meehl & Tebaldi, 2004) that may cause an increase in human mortality (Anderson, B. G. & Bell, 2009; Hajat et al., 2002). Heatwaves are among the top 10 deadliest natural disasters (Guha-Sapir et al., 2012; Scheuren et al., 2007) with profound influence on human health (Anderson, G. B. & Bell, 2011; Basu & Samet, 2002; Patz et al., 2005), crop loss (Deryng et al., 2014), animal health (Thornton et al., 2009), and water scarcity (Seneviratne et al., 2006). A limited number of studies analyzed the trend in the average duration of heatwaves considering a long-term (1930–2010) period (e.g., Oswald & Rood, 2014). Here, the spatial and temporal changes in the frequency and the maximum length of heatwaves in each year were analyzed using reanalysis data (1948–2018). In addition, a change-point analysis was applied to find any sudden change in the frequency and duration of the heatwaves. Correlation analysis helped address the relationship between abrupt changes and major events such as El Niño Southern Oscillation (ENSO).

Two major regions of the United States were the focus of study: the Mississippi River Basin (MRB) and the central United States (including Great Plains). MRB covers about 41% of the contiguous United States (Turner & Rabalais, 2003) and is one of the world's major river systems. The MRB is characterized by a diversity of land cover types and biological productivities. Its diverse climate conditions, land use variability, and a population of 100 million people made it a strong candidate to study climate extreme events due to the possible need for adaptation.

For studying a trivariate extreme, HDWs were of interest. The highest probability of these extreme events was reported in the Great Plains (Leathers & Harrington, 2001; Lydolph & Williams, 1982). Therefore, the focus of chapters 4 (empirical analysis) and 5 (copula approach)

was to study spatial and temporal changes of HDWs in the central United States including the Great Plains.

The results presented in Chapter 2 revealed an increase in the frequency and duration of heatwaves in southern Louisiana, and the western, and north-western areas of the MRB. Results for eastern sections support the existence of a "warming hole" (Meehl et al., 2012; Pan et al., 2004) with a lower frequency of hot extremes and a decreasing trend from 1948 through 2017. No statistically significant influence of ENSO was found on heatwave event frequency. Since 1994, the percentage of area with a heatwave longer than 10 consecutive days increased. Results suggest that adaptation plans for the future should changes in these hot climate extremes associated with ongoing global climate change (Hartmann et al., 2013; Trenberth et al., 2013).

In Chapter 3, the spatial and temporal changes of hot-humid conditions were analyzed in the MRB by analysis of heat index data (HI, Rothfusz, 1990). The human-induced increase of global temperature as a result of a changed energy balance has warmed ocean temperatures and increased the atmospheric near-surface moisture (Santer et al., 2007). The increase in humidity has an influence on human health (Arundel et al., 1986; Barreca, 2012; Sherwood & Huber, 2010), livestock (Fuquay, 1981; Morrison, 1983), and crops (Ford & Thorne, 1974; Wlnneberger, 1958). The global rise in specific humidity (Gaffen & Ross, 1999; Hartmann et al., 2013; Willett et al., 2008) may intensify the compound extreme associated with hot-humid conditions. Daytime and nighttime HI were calculated based on temperature and relative humidity. Calculated HI mirrors the spatial pattern of temperature. The daytime and nighttime HI higher than 40.6℃ (105°F) and 26.7℃ (80°F) (respectively) are considered extremes due to the National Weather Services (NWS) definition. Extreme humidity and temperature were defined as specific humidity and temperature higher than the 90th percentile threshold. Extreme daytime

and nighttime specific humidity had significant upward trends over 97% and 93% of the MRB, respectively. The extreme daytime temperature had a significant decrease in 12% of MRB, especially in eastern sections of the MRB. An upward trend in extreme daytime temperature was only significant in 4% of the MRB. A majority of MRB (72%) had a significant upward trend in nighttime extreme temperature. Trends of daytime HI were mainly upward (63%), except for eastern regions of MRB. The increase in the frequency and intensity of HI values may adversely affect human health and livestock production (including dairy cattle).

In chapter 4, the spatial and temporal changes of hot, dry, and windy events (HDWs) were analyzed for two time periods, 1949 to 2018 (70-years) and 1969 to 2018 (50-years). The HDWs were defined with a temperature higher than 35°C, wind speed higher than 7m/s, and relative humidity lower than 30% (Leathers & Harrington, 2001). The highest frequency of HDWs were observed in western Kansas and Texas for both time series. The major drought and heatwave of 1980 and 2011 (Karl & Quayle, 1981; NOAA NCEI, 2019b) triggered a higher probability of HDWs. The monthly and diurnal analysis showed the highest occurrence of HDWs in July and June, and 4:00 p.m. and 5:00 p.m. local time. Trend analysis of HDWs was done along with the changes in high temperature extremes (higher than 35°C), low humidity extremes (relative humidity lower than 30%), and extreme high wind speeds (wind speed higher than 7m/s). HDWs had a significant upward trend in 18% and 22% of stations for 50-year and 70-year periods, respectively. A downward trend in HDWs was found in the northeastern portion of the central Unites States, consistent with the decrease in the extreme temperature, humidity, and wind speed events over time. The increases in HDWs would accelerate evapotranspiration and plant water use, surface and groundwater loss, and the spread of wildfire, and negatively impact plant, human, and livestock health.

In chapter 5, after fitting the best copula family on the data, the probability of compound HDWs was assessed in the central United States. The same fixed thresholds used in chapter 4 were applied to define HDWs. For copula, each fixed threshold transformed to the corresponding percentile for each year in every station. Bivariate copulas were used to model the dependence between pairwise variables. The highest probability of compound high temperature and low humidity, and high temperature and high wind speed were discovered in northern Texas and western Kansas. Bivariate analysis of high-speed winds and low humidity showed the highest probability of these extremes in the western Great Plains. However, the lower temperatures in these regions limited the occurrence of HDWs. Same as with the empirical method (chapter 4), the highest frequency of HDWs was discovered in Kansas and Texas. Temporally, 1980 and 2011 were the years with a high risk of HDWs because of the concurrent drought and heatwaves. However, a higher risk of HDWs was calculated based on copula in a majority (96%) of stations compared to the empirical method. Although applying the copula model showed almost the same spatial distribution of HDWs in 1949–2018 as the empirical model, results showed the shortcoming of the empirical method in communicating the risk of HDWs. Unlike previous studies (Zhou & Liu, 2018; Zscheischler & Seneviratne, 2017) that reported the effect of high correlation between variables on the probability of extreme events, no relationship was discovered for HDWs. Results revealed that, although wind speed is decreasing in the Great Plains (Pryor et al., 2009), the increase in high temperature and low relative humidity extremes, potentially increase the risk of HDWs. The increase of HDWs would accelerate evapotranspiration (Derrel et al., 1993), and damage plants (Curtis, 1891; Wang et al., 2016; Yang & Wang, 1978). Knowing the HDWs hotspots help to schedule an irrigation system to keep soil moisture depletion less than the plants' damage threshold, provide soil water, and cool

the air temperature. In addition, HDWs influence the birth or intensifying of the wildfires (Flannigan & Harrington, 1988; Jolly et al., 2015; Srock et al., 2018) and can be used as a warning index in hotspots for the onset of droughts.

Recommendations and limitations

In this study, the spatial and temporal changes in single and compound (bivariate and trivariate) extreme events were analyzed in the central United States. Both observational and reanalysis data were used. Working with each set of data has its own benefits and challenges. NCEP-NCAR reanalysis data perform well in estimating the observational temperature data but the performance is less for relative humidity. Station-based observations have large numbers of missing data resulting in a decrease in the number of stations to 27 for a long period of record (1949–2018). Access to longer high-quality data sets may enhance the quality of results. Repeating the same analysis on HDWs using gridded data (e.g., reanalysis) would extend the spatial coverage and decrease the uncertainty in identifying hotspot regions. Finding hotspots is important for agriculture and irrigation management to decrease the economic risk of HDWs.

Compared to empirical methods, copula is a powerful method to communicate the risk of the concurrent extreme events. Considering the number of ties in observation (explained in chapter 5), the copula approach is suggested for studies that focus on annual or monthly average values (e.g., concurrent drought and heatwave), or when the focus is on single events (e.g., 2018 flash flood in Manhattan, Kansas or 2014 drought in California, USA).

References

Anderson, B. G.& Bell, M. L., 2009. Weather-related mortality: how heat, cold, and heat waves affect mortality in the United States. *Epidemiology (Cambridge, Mass.).* 20: 205.

Anderson, G. B.& Bell, M. L., 2011. Heat waves in the United States: mortality risk during heat waves and effect modification by heat wave characteristics in 43 US communities. *Environmental Health Perspectives.* 119: 210-218. http://doi.org/10.1289/ehp.1002313

Arundel, A. V., Sterling, E. M., Biggin, J. H., & Sterling, T. D., 1986. Indirect health effects of relative humidity in indoor environments. *Environmental Health Perspectives.* 65: 351-361. www.doi.org/10.1289/ehp.8665351

Barreca, A. I. 2012. Climate change, humidity, and mortality in the United States. *Journal of Environmental Economics and Management.* 63: 19-34. https://doi.org/10.1016/j.jeem.2011.07.004

Basu, R.& Samet, J. M., 2002. Relation between elevated ambient temperature and mortality: a review of the epidemiologic evidence. *Epidemiologic Reviews.* 24: 190-202. https://doi.org/10.1093/epirev/mxf007

Curtis, G. E. 1891. The hot winds of the plains. *Seventh Biennial Report, Kansas Department of Agriculture.* 7: 162-183. https://www.kansasmemory.org/item/225333

DeGaetano, A. T., & Allen, R. J., 2002. Trends in twentieth-century temperature extremes across the United States. *Journal of Climate.* 15: 3188-3205. https://doi.org/10.1175/1520-0442(2002)0152.0.CO;2

Dematte, J. E., O'mara, K., Buescher, J., Whitney, C. G., Forsythe, S., McNamee, T., ..., and Ndukwu, I. M., 1998. Near-fatal heat stroke during the 1995 heat wave in Chicago. *Annals of Internal Medicine.* 129: 173-181.

Derrel, M. L., Gilley, J. R., & Baumer, O. W., 1993. Irrigation Handbooks and Manuals (Part 623, Chapter 2) Irrigation Water Requirements. *United States Department of Agriculture.* Washington, DC, USA. https://www.nrcs.usda.gov/wps/portal/nrcs/detailfull/national/water/manage/irrigation/?cid=stelprdb1045075.

Deryng, D., Conway, D., Ramankutty, N., Price, J., & Warren, R., 2014. Global crop yield response to extreme heat stress under multiple climate change futures. *Environmental Research Letters.* 9: 034011. https://doi.org/10.1088/1748-9326/9/3/034011

Easterling, D. R., Evans, J. L., Groisman, P. Y., Karl, T. R., Kunkel, K. E., & Ambenje, P., 2000. Observed variability and trends in extreme climate events: a brief review. *Bulletin of the American Meteorological Society.* 81: 417-426. https://doi.org/10.1175/1520-0477(2000)0812.3.CO;2

Flannigan, M. D.& Harrington, J. B., 1988. A study of the relation of meteorological variables to monthly provincial area burned by wildfire in Canada (1953–80). *Journal of Applied Meteorology*. 27: 441-452. https://doi.org/10.1175/1520-0450(1988)0272.0.CO;2

FORD, M. A.& Thorne, G. N., 1974. Effects of atmospheric humidity on plant growth. *Annals of Botany.* 38: 441-452. https://doi.org/10.1093/oxfordjournals.aob.a084827

Fuquay, J. W. 1981. Heat Stress as it Affects Animal Production. *Journal of Animal Science.* 52: 164-174. https://doi.org/10.2527/jas1981.521164x

Gaffen, D. J.& Ross, R. J., 1999. Climatology and trends of US surface humidity and temperature. *Journal of Climate.* 12: 811-828. https://doi.org/10.1175/1520-0442(1999)0122.0.CO;2

Guha-Sapir, D., Vos, F., Below, R., & Ponserre, S., 2012. Annual disaster statistical review 2011: the numbers and trends. *Centre for Research on the Epidemiology of Disasters.* Brussels, Belgium. http://www.cred.be/sites/default/files/ADSR_2011.pdf.

Hajat, S., Kovats, R. S., Atkinson, R. W., & Haines, A., 2002. Impact of hot temperatures on death in London: a time series approach. *Journal of Epidemiology & Community Health.* 56: 367-372. http://dx.doi.org/10.1136/jech.56.5.367

Hartmann, D. L., Tank, A. M. K., Rusticucci, M., Alexander, L. V., Brnnimann, S., Charabi, Y. A. R., ..., and Kaplan, A., 2013. Observations: Atmosphere and surface. *In: Climate change 2013 the physical science basis: Working group I contribution to the fifth assessment report of the intergovernmental panel on climate change.* (pp. 159-254). Cambridge University Press. Cambridge, United Kingdom and New York, NY, USA.

Huang, W., Kan, H., & Kovats, S., 2010. The impact of the 2003 heat wave on mortality in Shanghai, China. *Science of the Total Environment.* 408: 2418-2420. https://doi.org/10.1016/j.scitotenv.2010.02.009

Jolly, W. M., Cochrane, M. A., Freeborn, P. H., Holden, Z. A., Brown, T. J., Williamson, G. J., & Bowman, D. M., 2015. Climate-induced variations in global wildfire danger from 1979 to 2013. *Nature Communications.* 6: 7537. https://doi.org/10.1038/ncomms8537

Karl, T. R.& Quayle, R. G., 1981. The 1980 summer heat wave and drought in historical perspective. *Monthly Weather Review.* 109: 2055-2073. https://doi.org/10.1175/1520-0493(1981)1092.0.CO;2

Leathers, N.& Harrington, J., 2001. Furnace winds of the West. *Journal of the West.* 40: 48-57.

Lyon, B.& Barnston, A. G., 2017. Diverse Characteristics of US Summer Heat Waves. *Journal of Climate.* 30: 7827-7845. https://doi.org/10.1175/JCLI-D-17-0098.1

Meehl, G. A., Arblaster, J. M., & Branstator, G., 2012. Mechanisms contributing to the warming hole and the consequent US east–west differential of heat extremes. *Journal of Climate.* 25: 6394-6408.

Meehl, G. A.& Tebaldi, C., 2004. More intense, more frequent, and longer lasting heat waves in the 21st century. *Science.* 305: 994-997. http://science.sciencemag.org/content/305/5686/994

Mora, C., Spirandelli, D., Franklin, E. C., Lynham, J., Kantar, M. B., Miles, W., ..., and Louis, L. V., 2018. Broad threat to humanity from cumulative climate hazards intensified by greenhouse gas emissions. *Nature Climate Change.* 8: 1062. https://doi.org/10.1038/s41558-018-0315-6

Morrison, S. R. 1983. Ruminant heat stress: effect on production and means of alleviation. *Journal of Animal Science.* 57: 1594-1600. https://doi.org/10.2527/jas1983.5761594x

NOAA NCEI. (2019a). Billion-dollar weather and climate disasters. Retrieved from https://www.ncdc.noaa.gov/billions; 3/9/2019.

NOAA NCEI. (2019b). Billion-dollar weather and climate disasters: Table of events. Retrieved from https://www.ncdc.noaa.gov/billions/events; 7/1/2019.

Oswald, E. M. 2018. An Analysis of the Prevalence of Heat Waves in the United States between 1948 and 2015. *Journal of Applied Meteorology and Climatology.* 57: 1535-1549. https://doi.org/10.1175/JAMC-D-17-0274.1

Oswald, E. M.& Rood, R. B., 2014. A trend analysis of the 1930–2010 extreme heat events in the continental United States. *Journal of Applied Meteorology and Climatology*. 53: 565-582. https://doi.org/10.1175/JAMC-D-13-071.1

Pan, Z., Arritt, R. W., Takle, E. S., Gutowski, W. J., Anderson, C. J., & Segal, M., 2004. Altered hydrologic feedback in a warming climate introduces a "warming hole". *Geophysical Research Letters.* 31: L17109. https://doi.org/10.1029/2004GL020528

Patz, J. A., Campbell-Lendrum, D., Holloway, T., & Foley, J. A., 2005. Impact of regional climate change on human health. *Nature.* 438: 310-317. https://doi.org/10.1038/nature04188

Pryor, S. C., Barthelmie, R. J., Young, D. T., Takle, E. S., Arritt, R. W., Flory, D., ..., and Roads, J., 2009. Wind speed trends over the contiguous United States. *Journal of Geophysical Research: Atmospheres.* 114: http://www.doi.org/10.1029/2008JD011416

Rothfusz, L. P.1990. The heat index equation (or, more than you ever wanted to know about heat index). *National Oceanic and Atmospheric Administration, National Weather Service, Office of Meteorology.* Forth Worth, TX.

Santer, B. D., Mears, C., Wentz, F. J., Taylor, K. E., Gleckler, P. J., Wigley, T., ..., and Gillett, N. P., 2007. Identification of human-induced changes in atmospheric moisture content. *Proceedings of the National Academy of Sciences.* 104: 15248-15253. https://doi.org/10.1073/pnas.0702872104

Scheuren, J. M., de Waroux, O le Polain., Below, R., Guha-Sapir, D., & Ponserre, S., 2007. Annual disaster statistical review, The numbers and trends 2007. *Center for Research on*

the Epidemiology of Disasters (CRED). https://www.unisdr.org/files/2796_CREDAnnualStatisticalReview2007.pdf.

Seneviratne, S. I., Lthi, D., Litschi, M., & Schr, C., 2006. Land-atmosphere coupling and climate change in Europe. *Nature.* 443: 205-209. https://doi.org/10.1038/nature05095

Sherwood, S. C.& Huber, M., 2010. An adaptability limit to climate change due to heat stress. *Proceedings of the National Academy of Sciences.* 107: 9552-9555. https://doi.org/10.1073/pnas.0913352107

Srock, A., Charney, J., Potter, B., & Goodrick, S., 2018. The Hot-Dry-Windy Index: A New Fire Weather Index. *Atmosphere.* 9: 279. https://doi.org/10.3390/atmos9070279

Thornton, P. K., van de Steeg, J., Notenbaert, A., & Herrero, M., 2009. The impacts of climate change on livestock and livestock systems in developing countries: A review of what we know and what we need to know. *Agricultural Systems.* 101: 113-127. https://doi.org/10.1016/j.agsy.2009.05.002

Trenberth, K. E., Dai, A., Gerard Van, D. S., Jones, P. D., Barichivich, J., Briffa, K. R., & Sheffield, J., 2013. Global warming and changes in drought. *Nature Climate Change.* 4: 17-22. https://doi.org/10.1038/nclimate2067

Turner, R. E.& Rabalais, N. N., 2003. Linking landscape and water quality in the Mississippi River basin for 200 years. *Bioscience.* 53: 563-572. https://doi.org/10.1641/0006-3568(2003)053[0563:LLAWQI]2.0.CO;2

Wang, S., Zheng, H., Liu, S., Miao, Y., & Li, J., 2016. Numerical study on the stomatal responses to dry-hot wind episodes and its effects on land-atmosphere interactions. *PloS One.* 11: e0162852. https://doi.org/10.1371/journal.pone.0162852

Willett, K. M., Jones, P. D., Gillett, N. P., & Thorne, P. W., 2008. Recent changes in surface humidity: Development of the HadCRUH dataset. *Journal of Climate.* 21: 5364-5383. https://doi.org/10.1175/2008JCLI2274.1

Wlnneberger, J. H. 1958. Transpiration as a requirement for growth of land plants. *Physiologia Plantarum.* 11: 56-61. https://doi.org/10.1111/j.1399-3054.1958.tb08425.x

Yang, Z.& Wang, S., 1978. The climatal analysis and forecast on Dry-hot wind at Guangzhong, Shaanxi. *Meterology Shaanxi.* 3: 6-13.

Zhou, P.& Liu, Z., 2018. Likelihood of concurrent climate extremes and variations over China. *Environmental Research Letters.* 13: 094023. https://doi.org/10.1088/1748-9326/aade9e

Zscheischler, J.& Seneviratne, S. I., 2017. Dependence of drivers affects risks associated with compound events. *Science Advances.* 3: e1700263. http://doi.org/10.1126/sciadv.1700263